Midwest States' Regional Pooled Fund Research Program
Fiscal Year 1999-2000 (Year 10)
Research Project Number SPR-3(017)
NDOR Sponsoring Agency Code RPFP-00-06

EVALUATION OF ALTERNATE CABLE ANCHOR DESIGNS AND THREE-CABLE GUARDRAIL ADJACENT TO STEEP SLOPE

Submitted by

Ryan M. Nelson, M.S.C.E.
Former Graduate Research Assistant

Dean L. Sicking, Ph.D., P.E.
Professor and MwRSF Director

Ronald K. Faller, Ph.D., P.E.
Research Assistant Professor

John D. Reid, Ph.D.
Professor

John R. Rohde, Ph.D., P.E.
Associate Professor

Karla A. Polivka, M.S.M.E., E.I.T.
Research Associate Engineer

Jason A. Hascall, B.S.C.E., E.I.T.
Graduate Research Assistant

MIDWEST ROADSIDE SAFETY FACILITY
University of Nebraska-Lincoln
527 Nebraska Hall
Lincoln, Nebraska 68588-0529
(402) 472-6864

Submitted to

MIDWEST STATES' REGIONAL POOLED FUND PROGRAM
Nebraska Department of Roads
1500 Nebraska Highway 2
Lincoln, Nebraska 68502

MwRSF Research Report No. TRP-03-155-05

February 3, 2005

TECHNICAL REPORT DOCUMENTATION PAGE

1. Report No.	2.	3. Recipient's Accession No.
TRP-03-155-05		

4. Title and Subtitle	5. Report Date
Evaluation of Alternate Cable Anchor Designs and Three-Cable Guardrail Adjacent to Steep Slope	February 3, 2005
	6.

7. Author(s)	8. Performing Organization Report No.
Nelson, R.M., Sicking, D.L., Faller, R.K., Reid, J.D., Rohde, J.R., Polivka, K.A., and Hascall, J.A.	TRP-03-155-05

9. Performing Organization Name and Address	10. Project/Task/Work Unit No.
Midwest Roadside Safety Facility (MwRSF) University of Nebraska-Lincoln 527 Nebraska Hall Lincoln, Nebraska 68588-0529	11. Contract © or Grant (G) No. SPR-3(017)

12. Sponsoring Organization Name and Address	13. Type of Report and Period Covered
Midwest States' Regional Pooled Fund Program Nebraska Department of Roads 1500 Nebraska Highway 2 Lincoln, Nebraska 68502	Final Report 1999-2005
	14. Sponsoring Agency Code RPFP-00-06

15. Supplementary Notes

Prepared in cooperation with U.S. Department of Transportation, Federal Highway Administration

16. Abstract (Limit: 200 words)

The three-cable guardrail system is most commonly used to protect motorists from roadside slopes. Due to the fact that the system is limited to sites where relatively large barrier displacement is acceptable, concern arises when the barrier system must be placed close to steep roadside slopes. An additional concern with regard to the use of cable guardrail is that there only exists one approved non-proprietary end terminal which utilizes a large, cast-in-place, reinforced concrete anchor block. The current terminal and anchor design has proven to be quite costly when compared to the entire system.

The objectives of the study were: (1) to evaluate three cable anchor designs in order to develop a more cost-effective anchor alternative and (2) to evaluate South Dakota's three-cable barrier system placed adjacent to 1.5H:1V slopes. Dynamic bogie testing of various anchor alternatives determined the capacity of each anchor. Subsequent, computer simulation modeling with BARRIER VII analyzed and predicted dynamic barrier performance with each anchor alternative.

One full-scale crash test, 2,034-kg (4,484-lb) pickup truck impacting at a speed of 98.1 km/h (61.0 mph) and at an angle of 26.2 degrees, was conducted and reported in accordance with the requirements specified in the National Cooperative Highway Research Program (NCHRP) Report No. 350, *Recommended Procedures for the Safety Performance Evaluation of Highway Features*. The full-scale crash test was conducted to verify that the cable guardrail adjacent to a steep slope performs adequately with the weakest anchor alternative, the driven steel post as shown through computer modeling, but was determined to be unacceptable according to the Test Level 3 (TL-3) evaluation criteria specified in NCHRP Report No. 350 due to vehicle vaulting and rollover.

The poor performance observed in the full-scale crash test warranted design modifications. Consequently, additional computer simulation with BARRIER VII predicted that increasing the cable guardrail stiffness with reduced post spacing and increasing the offset from the slope breakpoint significantly improved the barrier's performance. Therefore, it is recommended that a full-scale crash test be conducted on the modified cable barrier to verify its safety performance.

Furthermore, the steel post anchor design performed as intended and provided adequate cable tension for the barrier system. However, since the impacting vehicle was not contained nor smoothly redirected, it is recommended that the new anchor alternatives continue to be evaluated in the future.

17. Document Analysis/Descriptors	18. Availability Statement
Highway Safety, Roadside Appurtenances, Cable, Cable Guardrail, Slope, Anchor, Cable Anchor, Crash Testing, Compliance Testing	No restrictions. Document available from: National Technical Information Services, Springfield, Virginia 22161

19. Security Class (this report)	20. Security Class (this page)	21. No. of Pages	22. Price
Unclassified	Unclassified	126	

DISCLAIMER STATEMENT

The contents of this report reflect the views of the authors who are responsible for the facts and the accuracy of the data presented herein. The contents do not necessarily reflect the official views nor policies of the State Highway Departments participating in the Midwest States' Regional Pooled Fund Research Program nor the Federal Highway Administration. This report does not constitute a standard, specification, or regulation.

ACKNOWLEDGMENTS

The authors wish to acknowledge several sources that made a contribution to this project: (1) the Midwest States' Regional Pooled Fund Program funded by the Connecticut Department of Transportation, Illinois Department of Transportation, Iowa Department of Transportation, Kansas Department of Transportation, Minnesota Department of Transportation, Missouri Department of Transportation, Nebraska Department of Roads, Ohio Department of Transportation, South Dakota Department of Transportation, Texas Department of Transportation, and Wisconsin Department of Transportation for sponsoring this project; (2) Richard Butler and Florida Wire and Cable for donating the cable materials; and (3) MwRSF personnel for constructing the barriers and conducting the crash tests.

Acknowledgment is also given to the following individuals who made a contribution to the completion of this research project.

Midwest Roadside Safety Facility

J.C. Holloway, M.S.C.E., E.I.T., Research Manager
B.A. Coon, Ph.D., P.E., former Graduate Research Assistant
R.W. Bielenberg, M.S.M.E., E.I.T., Research Associate Engineer
A.T. Russell, B.S.B.A., Laboratory Mechanic II
Undergraduate and Graduate Assistants

Connecticut Department of Transportation

Dionysia Oliveira, Transportation Engineer 3

Illinois Department of Transportation

David Piper, P.E., Highway Policy Engineer

Iowa Department of Transportation

David Little, P.E., Assistant District Engineer
Will Stein, P.E., Design Methods Engineer

Kansas Department of Transportation

Ron Seitz, P.E., Assistant Bureau Chief
Rod Lacy, P.E., Road Design Leader

Minnesota Department of Transportation

Jim Klessig, Implementation Liaison
Mohammad Dehdashti, P.E., Design Standards Engineer
Ron Cassellius, former Research Program Coordinator
Andrew Halverson, P.E., former Assistant Design Standards Engineer

Missouri Department of Transportation

Daniel Smith, P.E., Research and Development Engineer

Montana Department of Transportation

Susan Sillick, Research Bureau Chief

Nebraska Department of Roads

Amy Starr, Research Engineer
Phil Tenhulzen, P.E., Design Standards Engineer
Leona Kolbet, former Research Coordinator
David Luhring, former Research Coordinator
Jodi Gibson, Research Coordinator

Ohio Department of Transportation

Monique Evans, P.E., Administrator
Dean Focke, P.E., Standards Engineer

South Dakota Department of Transportation

David Huft, Research Engineer
Bernie Clocksin, Lead Project Engineer

Texas Department of Transportation

Mark Bloschock, P.E., Supervising Design Engineer
Mark Marek, P.E., Design Engineer

Wisconsin Department of Transportation

Peter Amakobe, Standards Development Engineer
Beth Cannestra, P.E., Chief in Roadway Development

Federal Highway Administration

John Perry, P.E., Nebraska Division Office
Danny Briggs, Nebraska Division Office

Dunlap Photography

James Dunlap, President and Owner

TABLE OF CONTENTS

Page

List of Figures

Page

List of Tables

Page

1 INTRODUCTION

1.1 Problem Statement

Three-cable guardrail was one of the first roadside barrier systems to be developed. The design incorporates strong, steel cables mounted on widely spaced posts. The steel cables are designed to crease into the side of an impacting vehicle. As a vehicle penetrates into the barrier, the cables are stretched to produce tension forces that act as re-directive forces, pushing the vehicle back toward the traveled way. The barrier posts are designed to bend under moderate lateral loading, which limits the accelerations applied to impacting vehicles. Further, cable tension diminishes as an impacting vehicle begins to move out of the system, thereby minimizing the risk of vehicles being projected back into the traffic stream in an uncontrolled manner potentially causing serious secondary impacts. Cable guardrail's excellent accident record is normally attributed to the low lateral stiffness of the system and its ability to limit secondary collisions (1-2).

Cable barrier is very economical to install. Materials used in a cable barrier system are significantly less costly than most other barriers. The use of a wide-post spacing makes it even more inexpensive to construct. Furthermore, the low cross-sectional area of the cable barrier eliminates problems with snow drifting that plague W-beam guardrail and shaped concrete barriers.

The limitations and disadvantages of the three-cable guardrail are highlighted by the same concepts that identify its advantages. The flexibility of the system permits large lateral displacements, which limits the use of the barrier to shield motorists from fixed objects placed near the traveled way. In addition, barrier flexibility leads to long damaged sections during even

moderate collisions. Finally, many highway agencies have reported that slack often develops in the barrier cables, which generates a need for periodic maintenance.

The three-cable guardrail is most commonly used to protect motorists from roadside slopes, and a survey of field installations revealed that cable barriers are sometimes used to shield traffic from slopes as steep as 1.5H:1V. However, concern arises when the barrier must be placed close to a steep slope. Full-scale crash tests conducted by the New York State Department of Transportation (NYDOT) have shown that the cable guardrail can provide adequate safety performance for large sedans when placed near 2H:1V roadside slopes (3-4). However, the light truck impact performance of cable guardrails placed near roadside slopes has never been adequately investigated.

Another concern regarding the use of cable guardrail is that there is only one approved non-proprietary terminal for this barrier, and it incorporates a 1,220-mm (48-in.) flare with an extremely large concrete dead-man anchor. When guardrails are placed adjacent to roadside slopes, this flared terminal requires significant grading to provide a relatively flat area around and behind the terminal. Furthermore, the concrete anchor weighs more than 3,628 kg (8,000 lbs). Costs associated with providing the additional grading and the large concrete dead-man anchor can exceed the cost of the rest of the cable guardrail system. If the flared configuration can be eliminated and/or the size and cost of the concrete anchor can be reduced, cable guardrail would become even more economical. Therefore, in recognition of the issues summarized previously, the Midwest States' Pooled Fund Program undertook the three-cable guardrail study described herein.

1.2 Objective

The objectives of this research project were to: (1) evaluate alternate end terminal anchor designs that would reduce installation and maintenance costs and (2) evaluate the safety performance of standard cable guardrail for light truck impacts when the barrier is installed adjacent to a 1.5H:1V roadside slope. The three-cable guardrail system was to be evaluated according to the Test Level 3 (TL-3) safety performance criteria set forth in the National Cooperative Highway Research Program (NCHRP) Report No. 350, *Recommended Procedures for the Safety of Performance Evaluation of Highway Features* (5).

1.3 Scope

The research objectives were achieved by performing several tasks. First, a detailed literature review on cable systems and components was conducted. Next, component testing of guardrail posts and anchor systems was undertaken. Following the component testing, computer modeling with BARRIER VII was used to predict the efficiency of various design alternatives. After the final design was completed, the cable guardrail system was fabricated and constructed at the Midwest Roadside Safety Facility's (MwRSF's) outdoor test facility. Following the fabrication of the cable system, a full-scale vehicle crash test was performed using a ¾-ton pickup truck, weighing approximately 2,000 kg (4,409 lbs), with a target impact speed and angle of 100.0 km/h (62.1 mph) and 25 degrees, respectively. Next, the test results were analyzed, evaluated, and documented. Finally, additional computer modeling was conducted to identify additional design changes that could improve the impact performance of cable guardrails installed adjacent to steep roadside slopes. Conclusions and recommendations were made that pertain to the safety performance of the cable guardrail system.

2 LITERATURE REVIEW

Cable barriers, one of the first roadside barrier systems developed, have and continue to be subject to a multitude of research studies. The purpose of these research studies resides in two distinct areas: (1) theory and design and (2) compliance testing. A similar review, compiled by Coon, provides a general description of these studies (6). The review discussed herein is an extension of Coon's work as it provides further elaboration on these studies.

2.1 Theory and Design

In the early 1960's, Graham et al., with the New York State (NY) Department of Public Works Bureau of Physical Research, undertook a six-year study to revise the standard barrier designs for roadsides, medians, and bridges specified by the NY Department of Public Works (3). Until the 1960's, cable barrier designs included that of a single cable mounted to a series of heavy wooden posts. The older designs also incorporated a strong, exposed end post that could cause both snagging and/or spearing of an impacting vehicle. The new system incorporated the strong rail, weak post concept as well as a buried end at the rail's terminal. Utilizing a standard S76x8.5 (S3x5.7) post and three 19-mm (¾-in.) steel cables, the post was allowed to release from the rail when impacted, reducing the snag potential. Several crash tests were conducted on both flat terrain and adjacent to a 2H:1V slope. From the results, it was determined that a 762-mm (30-in.) barrier height with a 76-mm (3-in.) incremental cable spacing and a 4,877-mm (16-ft) post spacing could successfully contain an impacting vehicle. With the utilization of spring tension compensators and the implementation of 152-mm x 152-mm (6-in. x 6-in.) soil plates, this design was adopted as the NYDOT standard.

Whitmore et al. continued the NY based studies into the early 1970's (4). From this study, a relationship between post spacing and lateral barrier deflection was obtained. Systems with post spacing ranging from 1,219 mm (4 ft) to 4,877 mm (16 ft) were evaluated. It was concluded that a reduction in post spacing produced a reduction in barrier deflection. Although the 4,877-mm (16-ft) spacing provides acceptable results, some design applications may warrant reduced lateral deflections which are achieved through reduced post spacing.

Between 1967 and 1968, a series of impact tests were performed on cable rail systems for rural highways by the Ontario Department of Highways (7). The primary focus was concentrated on three main elements: (1) cable size, quantity, and spacing; (2) post stiffness; and (3) anchor design. When installed adjacent to a 3H:1V slope, it was determined that cable spacing was important in order to minimize snagging. It was noted that barrier deflection was also a function of post stiffness. When compared to the performance of the New Standard Concrete Block Anchor, an expanded steel anchorage system only warranted satisfactory results.

In 1990, the NYDOT examined the design performance of the cable barrier end terminal (8). Preliminary testing showed that the long cable turndown utilized in the existing design standard could snag and overturn small vehicles during departure impacts. The cause of snagging was attributed to the unsuccessful cable release from the anchor. Based on this assessment, a new terminal concept was developed. The adopted design incorporated a 45-degree cable turndown and a slip-base end post.

In 1985, Kenyon undertook a study to investigate the causes of tension loss in cable guardrail and formulated corrective measures in order to increase performance (9). In 1992, Yang et al. later continued this study (10). The study was initiated by defining possible causes of tension loss in existing and new installations, which included: anchor movement, post settlement,

permanent cable stretch, post tipping, spring-compensator failure, accident impacts, barrier maintenance, installation procedures, and turnbuckle movement. Results of the study identified anchor movement and permanent cable stretch as the major causes of tension loss and adversely affected barrier performance. Frictional drag, causing non-uniform tension throughout the barrier, was also sited as a means of tension loss due to lowering the average tension in the system. Pro-rating the existing tensioning tables for smaller temperature-spring compression intervals and maintaining proper adjustment cycles were two recommendations for reducing tension loss in the cable barrier.

In 1998, Bateman et al. developed a FORTRAN based computer simulation program for the effective modeling of wire-rope safety fences (WRSF) containing ropes that are constrained by friction (11-12). The simulation efforts combined a dynamic vehicle model with a quasi-static fence model. Detailed results of eight Motor Industry Research Association (MIRA) full-scale tests served as the means for validation of the computer-simulated models. Simulation studies indicated that the performance of a WRSF was particularly sensitive to the impact conditions of vehicle speed and angle and the design parameters of cable mounting height, rope pre-tension, post spacing, and post strength. Studies also reinforced the benefits gained by utilizing computer simulation to effectively model complex engineering systems. The availability of this simulation program was not sought because of the utilization of readily available software and the confidence that existed in its predictions of roadside barrier performance.

In 1996, Sposito et al. from the Oregon Department of Transportation conducted a review of cable median barriers following three fatalities from crossover accidents (2). The weak-post three-cable median barrier was evaluated for performance and cost effectiveness. Results of the Oregon study were compared with similar cost studies and accident records of three additional

states. All studies and records shared similar results, each producing low fatality accident rates and low annual costs when compared to a concrete system.

2.2 Compliance Testing

In 1987, the Southwest Research Institute (SwRI) performed NCHRP Report No. 230 compliance testing on a series of modified G1 cable barrier systems transitioning into standard 1,219-mm (48-in) flare BCT (W-beam) terminals incorporating an 11,430-mm (450-in.) parabolic curve (13-15). The first of a three part test series involved a 2,126-kg (4,690-lb) sedan impacting the transition from the cable barrier to the BCT at a speed of 94.8 km/h (58.9 mph) and at an angle of 27.3 degrees. The test failed to meet the evaluation criteria of NCHRP Report No. 230. Thus, the system was retested with a revised impact angle of 24.4 degrees and subsequently met the NCHRP Report No. 230 guidelines. The last test was performed along the length-of-need (LON) with a 2,150-kg (4,740-lb) sedan impacting at a speed of 94.3 km/h (58.6 mph) and at an angle of 25 degrees. This test was successful according to NCHRP Report No. 230 safety performance guidelines.

NCHRP Report No. 230 compliance testing on a series of standard G1 cable barrier systems configured with 6 kg/m (4 lb/ft) Franklin posts was continued by SwRI (16-18). Originally detailed by the South Dakota Department of Transportation (SDDOT), the barrier design incorporated trapezoidal soil plates mounted to the Franklin steel post. For the initial test, a 2,040-kg (4,500-lb) vehicle impacted the system at a speed and angle of 100 km/h (60 mph) and 25 degrees, respectively. Structural adequacy concluded that the system's performance was successful. Identical testing repeated 2,438-mm (96-in) downstream from the previous impact point successfully met the performance criteria set forth in NCHRP Report No. 230. A

subsequent test with an 895-kg (1,974-lb) vehicle impacting at a speed and angle of 98.8 km/h (61.4 mph) and 21.1 degrees, respectively, was also successful.

In 1994, Mak et al. conducted NCHRP Report No. 350 compliance testing on the standard cable (G1) guardrail system with a 2,000-kg (4,405-lb) pickup truck (19). The G1 cable system was found to satisfy the TL-3 evaluation criteria presented in the NCHRP Report No. 350.

In 1996, the Washington State Department of Transportation (WSDOT) and Texas Transportation Institute's (TTI) Bullard et al. initiated a crash-test program to evaluate the safety performance of the WSDOT three-strand cable barrier system when impacted on the single-cable side of the installation (20). Constructed on level terrain, the WSDOT three-strand cable barrier system met all evaluation criteria set forth for Test Designation 3-10 of the NCHRP Report No. 350.

In 1998, NCRHP Report No. 350 Test Designation 3-34 compliance testing was performed on the NY three-cable barrier terminal constructed on a 6H:1V slope (21). Test Designation 3-34 required that an 820-kg (1,808-lb) passenger car impact the terminal at the midpoint between the end of the terminal and the beginning of the LON at a nominal impact speed and angle of 100 km/h (62.14 mph) and 15 degrees, respectively. The vehicle sustained minimal damage as it was allowed to gate through the end of the NY Terminal. Therefore, this system performed successfully according to the evaluation criteria of NCHRP Report No. 350.

The study of the WSDOT's three-strand cable barrier was continued by TTI's Bullard et al. to complete the LON testing (22). NCHRP Report No. 350 Test Designation 3-11 required that a 2000-kg (4,409-lb) pickup truck impact the LON section of the barrier at a nominal speed and angle of 100 km/h (62.14 mph) and 25 degrees, respectively. The WSDOT three-strand

cable barrier with NY cable terminals satisfied the Test Designation 3-11 performance criteria set forth in NCHRP Report No. 350.

3 INTRODUCTION TO CABLE GUARDRAIL SYSTEM

3.1 Cable Guardrail Description

The three-cable guardrail system consists of four major components: (1) wire rope; (2) posts; (3) spring compensating cable end assemblies; and (4) anchor assemblies.

3.1.1 Wire Rope

The three-cable guardrail system utilizes 19-mm (¾-in.) high-strength galvanized wire rope. Each cable is composed of three 9.5-mm (3/8-in.) diameter stands. Each strand is made up of seven individual wires. Although the rated strength for an individual cable is specified at 111 kN (25 kips) (23), tests show an average breaking strength greater than 178 kN (40 kips) (24). The top cable is typically mounted at a height of 686 to 762 mm (27 to 30 in.), and the lower cables are incrementally spaced at 76 to 152 mm (3 to 6 in.).

3.1.2 Posts

Line posts are S76x8.5 (S3x5.7) rolled steel sections. The post geometry includes an overall height and an embedment depth of 1,600 mm (63 in.) and 762 mm (30 in.), respectively. A 203-mm x 305-mm x 6-mm (8-in. x 12-in. x ¼-in.) bearing plate is welded to the post in order to increase lateral soil bearing capacity. The S76x8.5 (S3x5.7) post provides low weak-axis bending strength to allow the post to be deflected easily during an impact. Cable hook bolts are implemented to secure the cable to the posts, while permitting relatively free longitudinal cable movement along the system. The hook bolts are also designed to allow the cable to be released when the posts are bent down during an impact.

3.1.3 Cable End Compensators

Spring-type compensating devices and turnbuckles accommodate the cable's thermal expansion and contraction. When applied, the spring compensator is initially compressed to allow for temperature increases. Additional compressive stroke is available to allow extension when the temperature decreases. If the temperature decreases sufficiently to compress the compensator to its limit, excessive tensioning of the cable can cause yielding, consequently creating slack when the temperature rises again. Furthermore, a large increase in temperature can also produce slack in the system. Cable slack creates sag and reduces the barrier's ability to engage an impacting vehicle.

3.1.4 Anchors

The primary purpose of the anchor is to resist the cable tension loads encountered. The current anchor design relies on a massive concrete block to provide the required resisting forces. These designs typically specify cast-in-place or precast concrete, cast as either one or two units. The anchor base also serves as the mounting pad for the anchor plate and bracket assembly, which serves as a cable release mechanism during reverse direction impacts near the terminal end. The concrete anchor's volume ranges from 1.3 to 1.9 m^3 (1.75 to 2.5 yd^3) as shown in Figure 1. Consequently, the anchor weighs between 3,175 and 4,535 kg (3.5 and 5.0 tons) and requires little reinforcing steel. The corresponding English-unit drawing is shown in Appendix A.

3.2 Limitations

3.2.1 Slope

Cable guardrail installed adjacent to a slope creates numerous safety concerns. An impacting vehicle can traverse too far onto the slope, thus allowing the vehicle to become

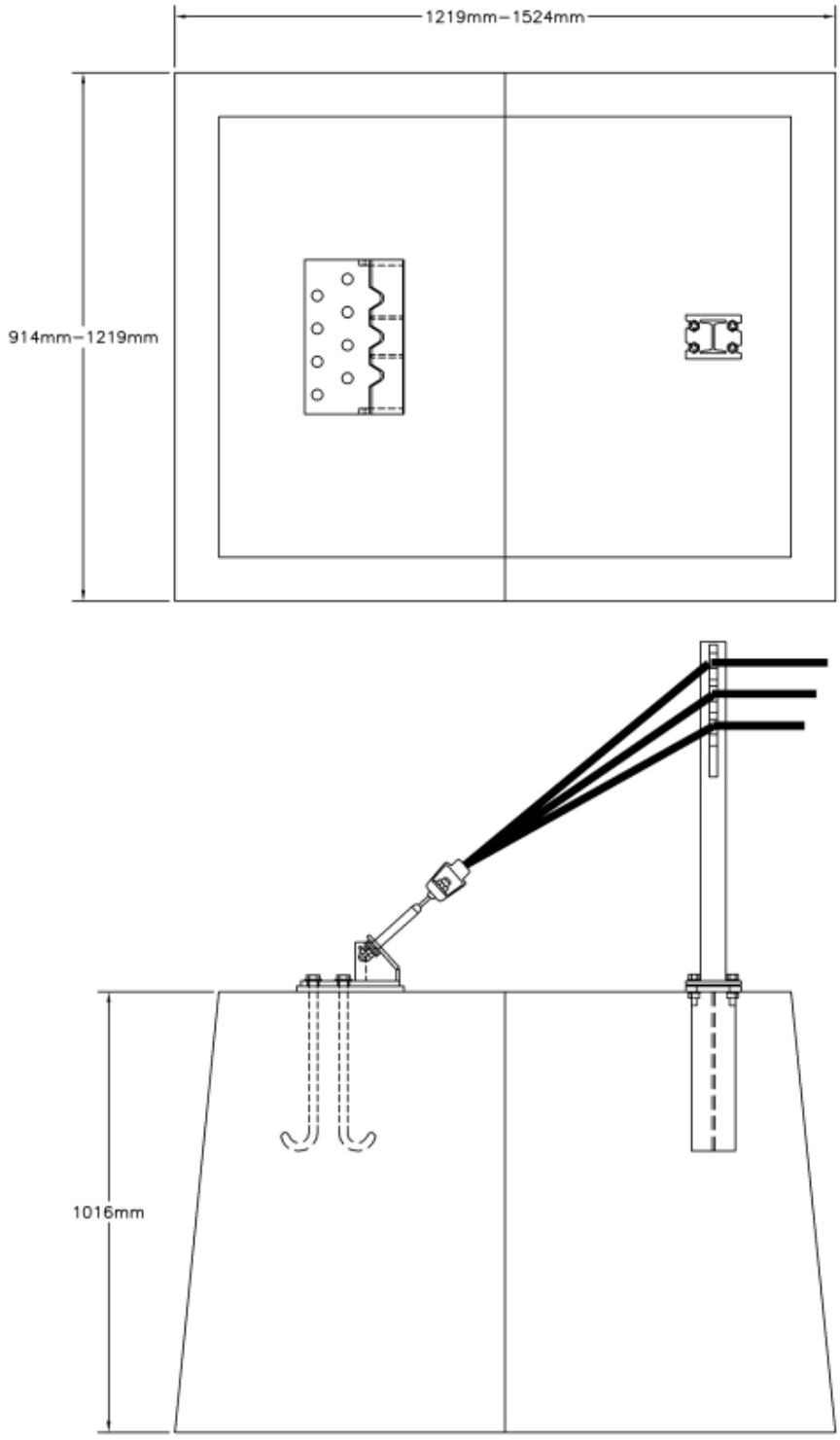

Figure 1. Existing Anchor Design

airborne. Following the loss of ground contact, the impact side of the vehicle may drop and allow the large lateral forces produced by the cable to generate a destabilizing moment that acts on an already unstable vehicle. This instability can cause the vehicle to rollover the embankment.

3.2.2 Anchor

Three-cable guardrail is typically installed along open highways and is not necessarily within close proximity to populated communities. Therefore, the size and weight of the current concrete anchor design presents economic limitations. When cast-in-place concrete is used for the construction of the anchor, it is often the only concrete on the project, thus producing additional job costs for the delivery of fresh concrete. The large mass of the precast option requires the use of special equipment to lift and set the anchor. Since this equipment would not otherwise be required to complete the project, additional expenses are again incurred. The need for extra equipment or ready-mix concrete can be eliminated if alternate anchor designs can be proven to be effective. Therefore, design alternatives that resolve these problems could significantly reduce the cost of three-cable guardrail installation.

4 ANCHOR DESIGN

4.1 Proposed Anchor Alternatives

Initially, three very different anchor design options were considered to simplify construction of the three-cable guardrail system. The derived alternatives include a reinforced concrete block, a reinforced concrete shaft, and a driven steel post. The concrete block option mimics that of the existing design, but utilizes a smaller concrete block that can be lifted with existing equipment. The reinforced concrete shaft provides a simplified concrete design alternative, but still relies on the use of cast-in-place concrete. The steel post design incorporates a large steel beam that is driven into the ground.

4.1.1 Concrete Block

The revised concrete block design is 1,524-mm long x 1,015-mm deep x 610-mm wide (60-in. x 40-in. x 24-in.) and weighs approximately 2,268 kg (5,000 lbs), as shown in Figure 2. The corresponding English-unit drawing is shown in Appendix A. The block fabricated with 27.58-MPa (4,000-psi) minimum compressive strength concrete contains Grade 60 No. 4 reinforcement bars. The size and quantity reductions produce lower material costs as well as lower project costs since heavy equipment to lift and set the existing large-mass concrete block is not needed. Nonetheless, the size and weight of the new block make this design option relatively costly.

4.1.2 Reinforced Concrete Shaft

The drilled shaft concrete anchor does not eliminate the use of concrete, but it does provide a more economical alternative by reducing the volume of concrete and simplifying excavation. The drilled anchor has a 457-mm (18-in.) diameter and is 1,829-mm (72-in.) deep.

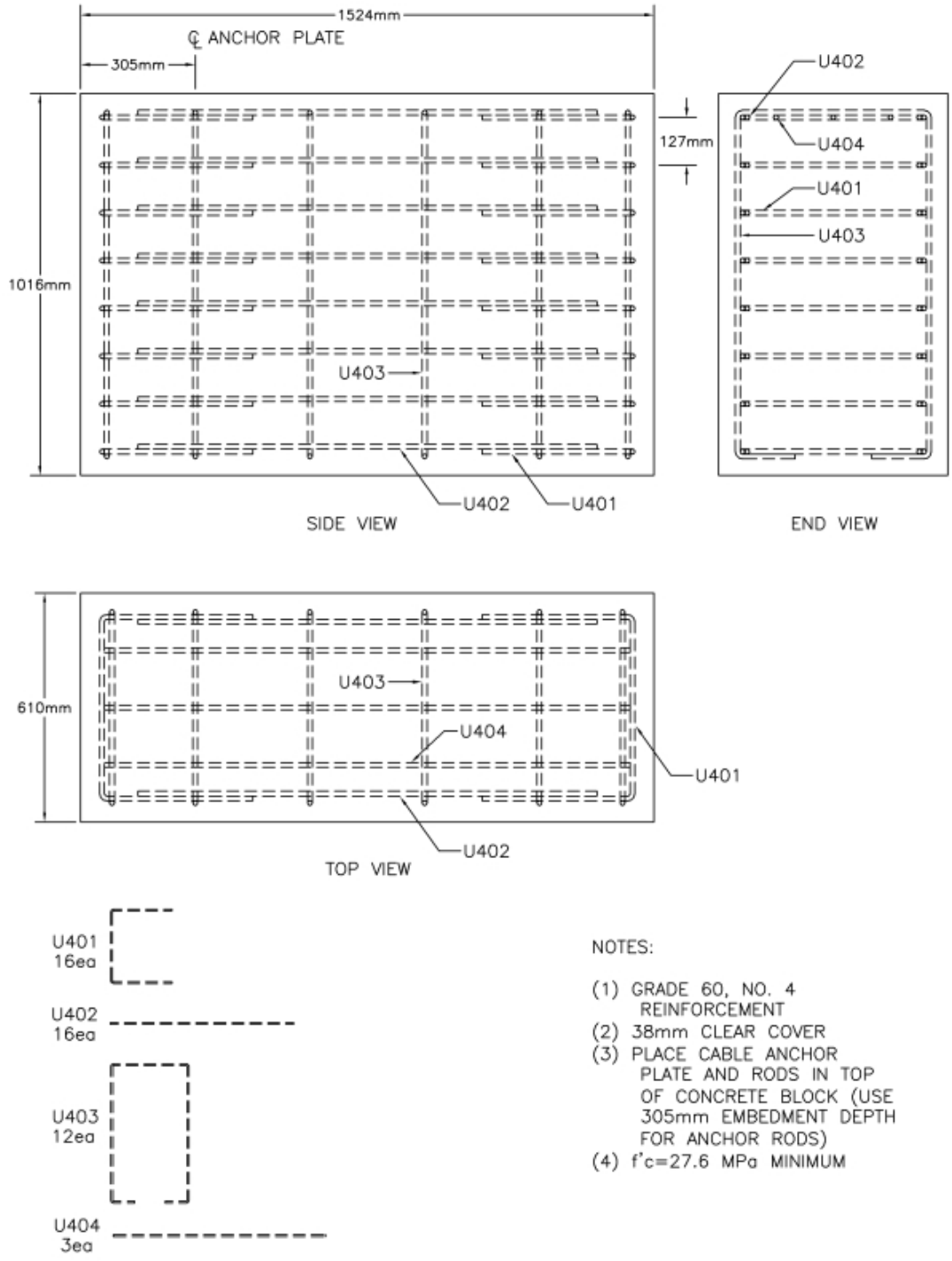

Figure 2. Design Option No. 1 – Reinforced Concrete Block

The anchor is reinforced with a spiral rebar cage fabricated with Grade 60 steel, as shown in Figure 3. The corresponding English-unit drawing is shown in Appendix A. The spiral reinforcement was designed with a 38-mm (1.5-in.) clear cover over No. 3 rebar and ten No. 4 vertical bars equally spaced around the interior circumference. A concrete mix with compressive strength of 27.58 MPa (4,000 psi) was also specified. Anchor rods embedded 305 mm (12 in.) into the structure were used to secure the cable anchor bracket. This design option provides another simple alternative and utilizes equipment that is usually available on a guardrail construction site.

4.1.3 Steel Post

The steel post alternative effectively eliminates the need for concrete, utilizes readily available equipment, and creates further simplicity in the construction process. A W152x37.2 (W6x25) steel section with a 248-MPa (36-ksi) yield strength and a 2,438 mm (96-in.) overall length was selected for the design, as shown in Figure 4. The addition of a 610-mm x 610-mm x 13-mm (24-in. x 24-in. x ½-in.) soil bearing plate provides further resistance against lateral forces. In this case, the anchor bracket is bolted to a steel plate welded to the top of the post. The corresponding English-unit drawing is shown in Appendix A.

4.2 Bogie Testing

The anchor capacity of each anchor alternative was to be determined by dynamic bogie testing. Full-scale crash testing has shown that a single cable is capable of successfully capturing high-energy impacts. As noted previously, 3x7 cables used in these barriers have shown maximum load capacities near 178 kN (40,000 lbs). Knowing this, an initial evaluation calculated that the peak resisting force of the anchor equals 534 kN (120,000 lbs). This value was

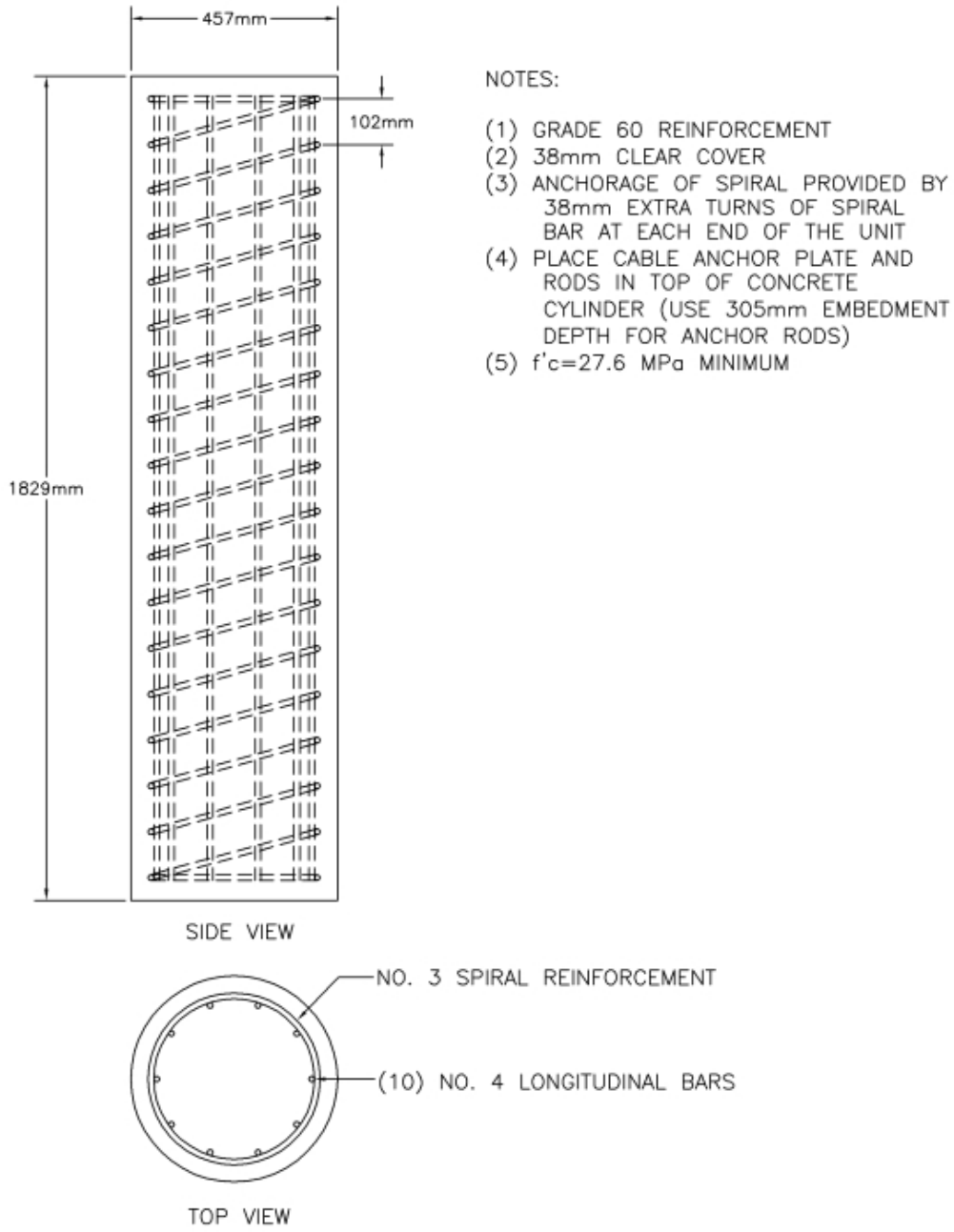

Figure 3. Design Option No. 2 – Drilled Concrete Shaft

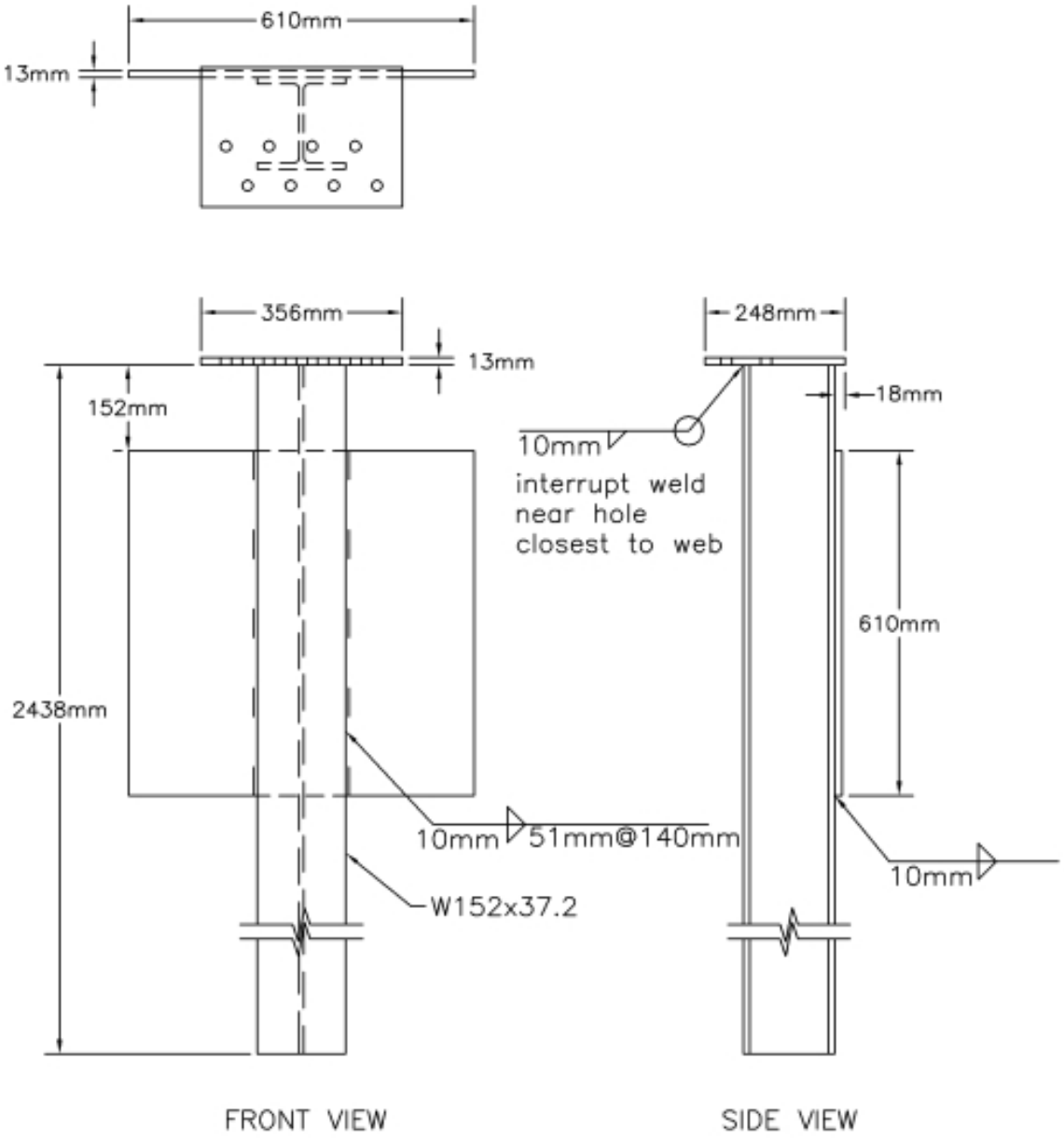

Figure 4. Design Option No. 3 – Driven Steel Post

considered to be unreasonably high and was found not to correlate to prior field studies. Combining the knowledge gained from previous cable barrier testing with the fact that a single cable is capable of successfully capturing high-energy impacts, it was believed that an anchor system could perform adequately if it could withstand a 178-kN (40,000-lb) tensile load. A series of bogie tests were conducted to verify that each revised anchor design could sustain a 178-kN (40,000-lbs) load with deflections of 152 mm (6 in.) or less.

The bogie testing involved a 2,223-kg (4,900-lb) bogie tethered to each design. The bogie vehicle was then towed up to the target speed and released. When the bogie reached the end of the cable tether, dynamic lateral loads were applied to the anchor. The target speed of the bogie was selected to provide a minimum dynamic load of 178 kN (40,000 lbs). The target speed was identified by assuming that both the cable tether and the soil acted as linear springs. The energy absorbed by the cable and soil spring was then estimated and set equal to the target kinetic energy of the bogie vehicle.

A string potentiometer (Linear Variable Displacement Transducer, LVDT) and high-speed video were used to monitor anchor motions during the testing. Bogie vehicle accelerometer data was used to estimate the maximum anchor load. The tests were designed to identify anchor yield forces, peak loading capacities, and associated displacements that could be expected during an impact.

4.2.1 Procedure

The bogie vehicle test configuration is shown in Figures 5 and 6. The rigid-frame bogie vehicle was to be towed to a target speed of 35.4 km/h (22 mph) for all three anchor tests.

Figure 5. Bogie Test Vehicle and Guidance System

Figure 6. Bogie Anchor Setup

A triaxial piezoresistive accelerometer system with a range of ±200 G's was mounted on the bogie vehicle to measure the accelerations in the longitudinal, lateral, and vertical directions at a sample rate of 3,200 Hz. The environmental shock and vibration sensor/recorder system, Model EDR-3, was developed by Instrumental Sensor Technology (IST) of Okemos, Michigan. The EDR-3 was configured with 256 Kb of RAM memory and a 1,120 Hz lowpass filter. "DynaMax 1 (DM-1)" and "DADiSP" were the two software packages selected to digitize, analyze, and plot the accelerometer data.

Three pressure-activated tape switches, spaced at 1,000 mm (39.37 in.) intervals, were used to determine the speed of the bogie vehicle just before the anchor began to be loaded. Each tape switch fired a strobe light which sent an electronic timing signal to the data acquisition system as the bogie vehicle's front tire passed over it. Test vehicle speeds were then determined from the relationship between the signal time periods and the 1,000-mm (39.37-in.) switch spacing. Accurate measurements of initial bogie velocity were compared with velocity changes obtained through integration of accelerometer data as a test validation check.

Anchor motions were monitored with a high-speed Red Lake E/cam video camera operating at a speed of 500 frames/sec. The high-speed photography in combination with a grid background presented a simplistic means of measuring anchor deflection versus time. A string potentiometer mounted near the anchor base was used as a secondary mode of deflection analysis. The test matrix for this set of dynamic bogie testing is shown in Table 1. It should be noted that during an additional test, test no. CA-2, the bogie cable connection to the bogie vehicle failed. This failure prompted the modification of the bogie vehicle resulting in an increased bogie weight for test nos. CA-3 and CA-4.

Table 1. Dynamic Bogie Test Matrix for Anchor Design Alternatives

Test Name	Description	Bogie Weight		Target Velocity	
		kg	lbs	km/h	mph
CA-1	Steel Post	2224	4902	35.4	22.0
CA-3	Concrete Shaft	2263	4990	35.4	22.0
CA-4	Concrete Block	2263	4990	35.4	22.0

4.2.2 Results

For the purpose of this research study, the cable guardrail anchor dynamic bogie test results were summarized by force-deflection curves. As previously stated, these results verified the capacity of each design option. The data obtained from each test assisted in the determination of various mechanical properties and behaviors used in the development of the finite element models (FEM).

Each anchor test force-displacement results are summarized in Table 2 and in Figures 7 through 9. In order to be directly applicable to the finite element modeling program, BARRIER VII, an elastic-plastic relationship was fitted to the force-deflection data (25).

The reinforced concrete block option represented the strongest design and is characterized by a 254-kN (57-kip) peak resisting force. The drilled shaft produced a maximum lateral force equal to 205 kN (46 kips). The driven steel post proved to be the weakest anchor and sustained a 187-kN (42-kip) peak load. The results indicate that the minimum criterion set for the anchor force and displacement were met by the concrete shaft and concrete block anchor designs. Although the steel post anchor design was slightly out of the targeted range of the initially set anchor force and displacement criterion and was the weakest anchor design, the researchers believed it would still be a viable anchor design option and would be capable of

developing the necessary anchor loads. Therefore, based on these results, BARRIER VII modeling was utilized to investigate the system behavior of each anchor design.

Table 2. Dynamic Bogie Test Results for Anchor Design Alternatives

Test Name	Description	Max. Anchor Force		Yield Displacement		Elastic Stiffness		Maximum Displacement	
		kN	kips	mm	in.	kN/mm	k/in.	mm	in.
CA-1	Steel Post	186.8	42.0	259	10.2	0.72	4.10	259	10.2
CA-3	Concrete Shaft	204.6	46.0	152	6.0	1.17	6.67	381	15.0
CA-4	Concrete Block	253.5	57.0	191	7.5	1.17	6.67	381	15.0

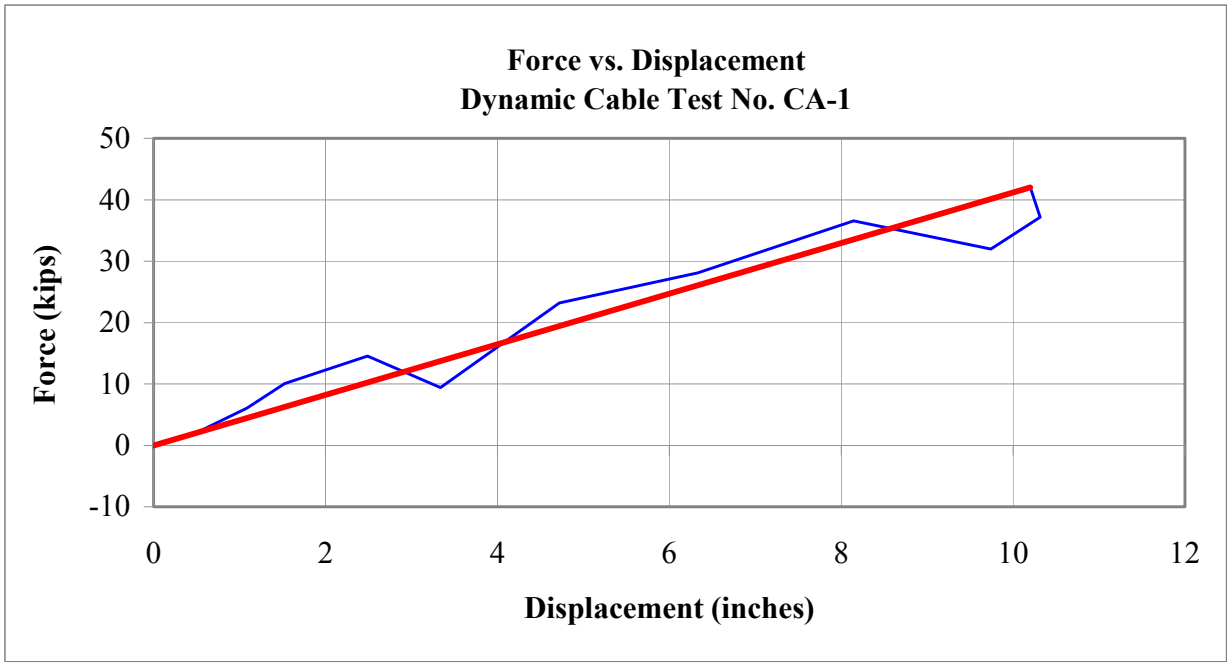

Figure 7. Force-Displacement Curve for Driven Steel Post, Test CA-1

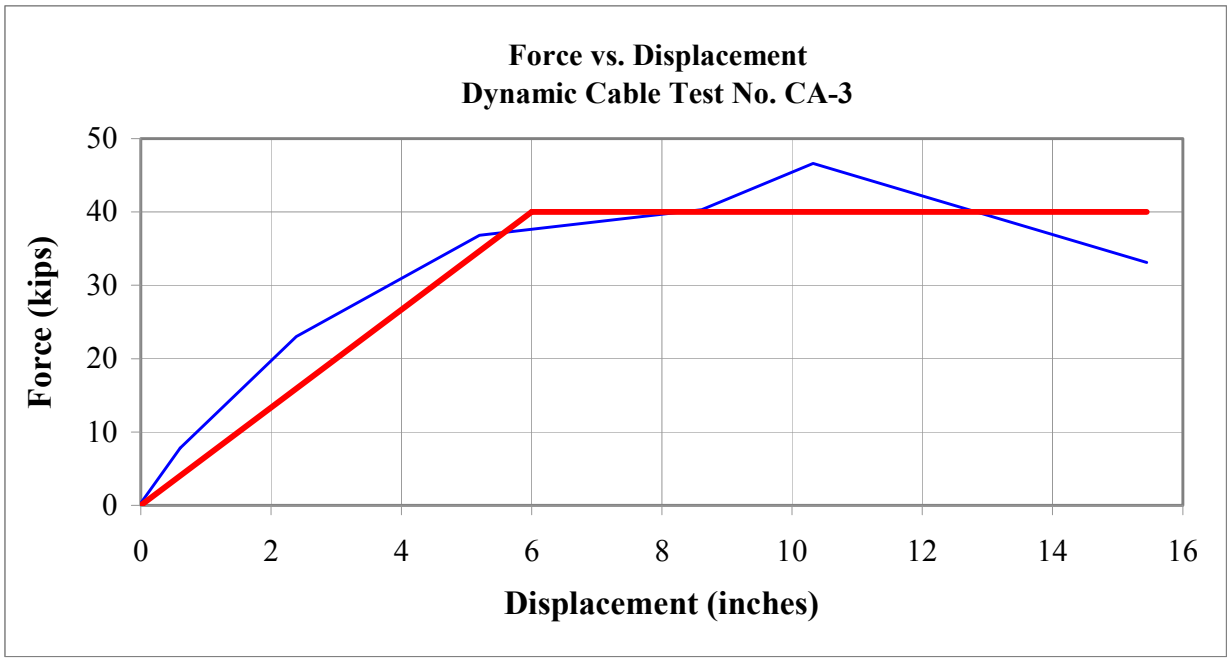

Figure 8. Force-Displacement Curve for Drilled Concrete Shaft, Test CA-3

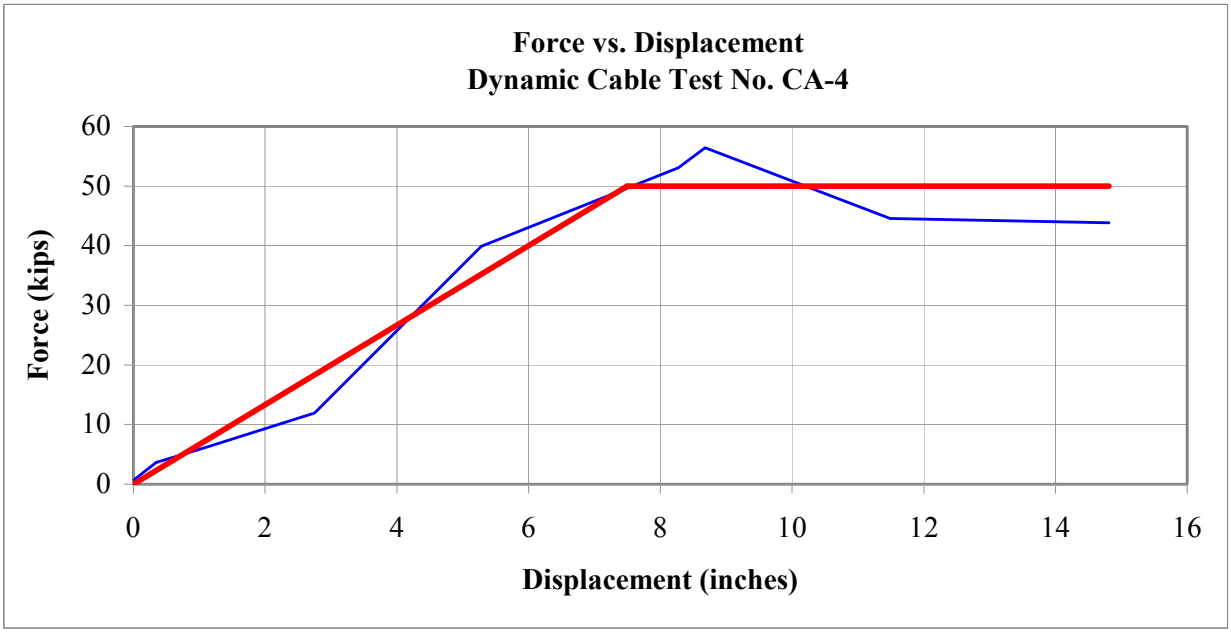

Figure 9. Force-Displacement Curve for Reinforced Concrete Block, Test CA-4

5 COMPUTER MODELING

5.1 Introduction

BARRIER VII has proven to be a powerful tool for predicting barrier performance and is often used in roadside barrier design (25). The program is designed to analyze the behavior of an automobile or other vehicle striking a deformable protective barrier while accounting for dynamic effects, large displacements, and inelastic behavior. Finite element modeling is often utilized to compare design concepts in the initial stages of design. BARRIER VII is normally calibrated against full-scale crash test results in order to gain maximum confidence in the analysis process.

5.1.1 BARRIER VII

BARRIER VII models are idealized as a two-dimensional framework comprised of diverse elements. Barriers are modeled as a series of beam, column, and spring elements. The beam elements incorporate elasto-plasto behavior at the ends of each element without failure. The posts are modeled in an elastic-plastic manner with a defined deflection limit. Once the deflection limit is met, the post elements are removed from the model. Additional elements include cable, spring, and damping members. Vehicles are idealized as rigid bodies of arbitrary shape surrounded by a cushion of discrete inelastic springs. The BARRIER VII solution procedure is defined by a dynamic step-by-step analysis and has been well validated through years of modeling flexible and semi-rigid barriers.

5.1.2 Limitations

Although proven to be a powerful tool, BARRIER VII does have some limitations. Simulation models are limited to a 2-D analysis in a horizontal plane, thus eliminating the

consideration of out-of-plane effects including vertical displacement of both the vehicle and barrier. The number of barrier nodes, members, and contact interfaces are also limited. In addition, contact interfaces for which interaction takes place must be clearly defined. Despite the limitations from which BARRIER VII operates, it is still a powerful tool in roadside barrier design.

5.2 Model Development

5.2.1 Model Description

The three-cable guardrail system used in this application represents that of recent tests. Previous testing has shown that the cable system must be long enough to provide sufficient length outside of the impact region to eliminate end effects. After reviewing previous NCHRP No. 350 testing of cable barriers, a 148-m (485-ft) overall system length was selected. Cable, post, and spring members were used in the simulation effort, as shown in Figure 10. Due to the limits on the number of nodes and members, only two cable lines were modeled as contact interfaces. The upper-most and lower-most cables, with mounting heights set at 762 and 610 mm (30 and 24 in.), respectively, were modeled. Post members were used for both line posts and end anchors. The line post height was selected to match the mounting height of the upper cable. Since the end terminal anchors were modeled as post members, cable-mounting heights were detailed. These assigned heights were set at 108 and 83 mm (4.25 and 3.25 in.) and were representative of actual heights associated with standard cable anchor brackets. Since BARRIER VII does not allow two different rail elements to be connected at a single node, minor height variations were utilized. Spring members were used to characterize the spring compensating cable assemblies located near each end of the cables.

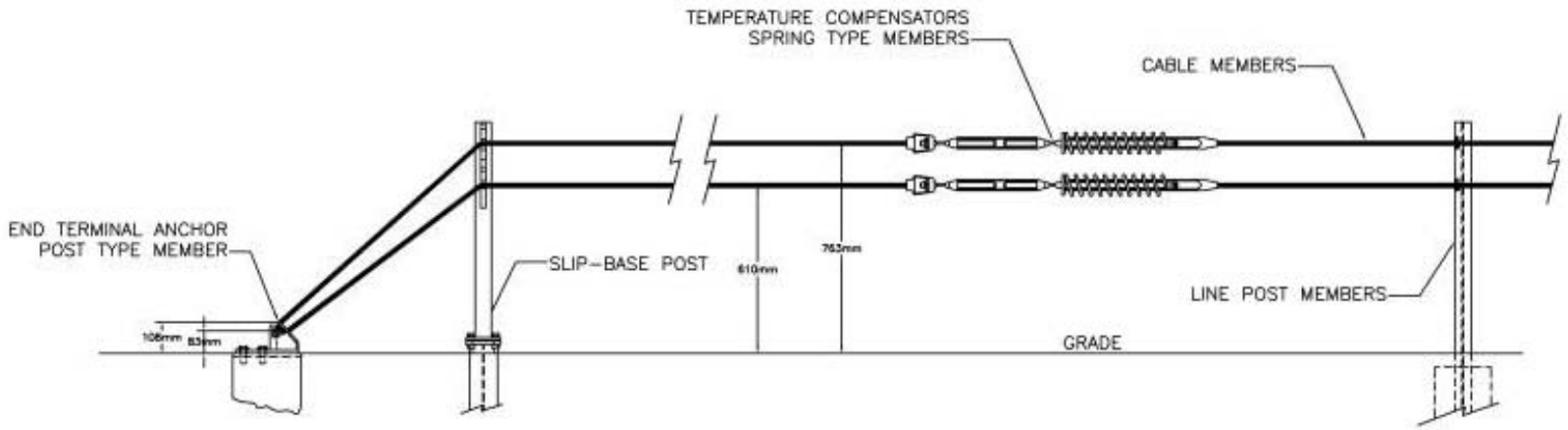

Figure 10. Description of Barrier VII Model

5.2.2 Input Parameters

Investigation of previous tests and barrier systems assisted in determining barrier input parameters. The material and geometric properties of the wire-rope cable were obtained from manufacturer specifications and are summarized in Table 3.

Table 3. BARRIER VII Cable Input Parameters

X-Sectional Area		Unit Weight		Young's Modululs		Yield Tensile Force	
mm^2	$in.^2$	kg/m	lb/ft	MPa	ksi	kN	kips
155.0	0.240	1.22	0.819	12.62	18,300	152.1	34.2

Dynamic behavior and material properties of line posts were derived from dynamic bogie testing similar to that performed on the anchor alternatives as well as video footage from previous cable tests. The dynamic bogie testing studied cable barrier posts in various foundation conditions, including soil conditions meeting the specifications of NCHRP Report No. 350. Additional details related to the dynamic bogie testing are provided in the referenced MwRSF research report (26). Similar to that of the anchor bogie tests, the results of the post tests were interpreted through linear approximations of the force-deflection plots. Results of the bogie testing are summarized in Table 4 and in Figures 11 and 12.

Table 4. Dynamic Bogie Test Results for S76x8.5 (S3x5.7) Posts

Test Name	Impact Axis	Yield Force		Yield Displacement		Elastic Stiffness		Base Moment	
		kN	kips	mm	in.	kN/mm	k/in.	kN-m	k-in.
CPB-2:CPB-4	Strong	16.0	3.6	127	5.0	0.13	0.72	11.0	97.2
CPB-5:CPB-7	Weak	7.6	1.7	127	5.0	0.06	0.34	5.2	45.9

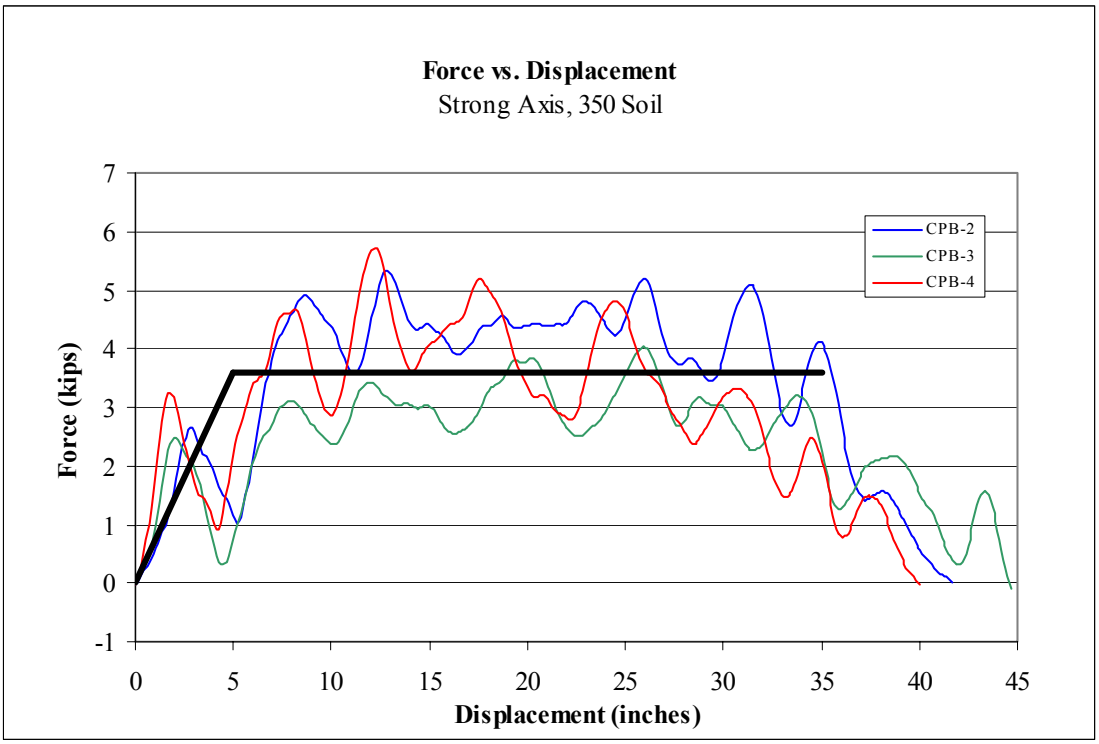

Figure 11. Force-Displacement Curve for Bogie Tests CPB-2 through CPB-4

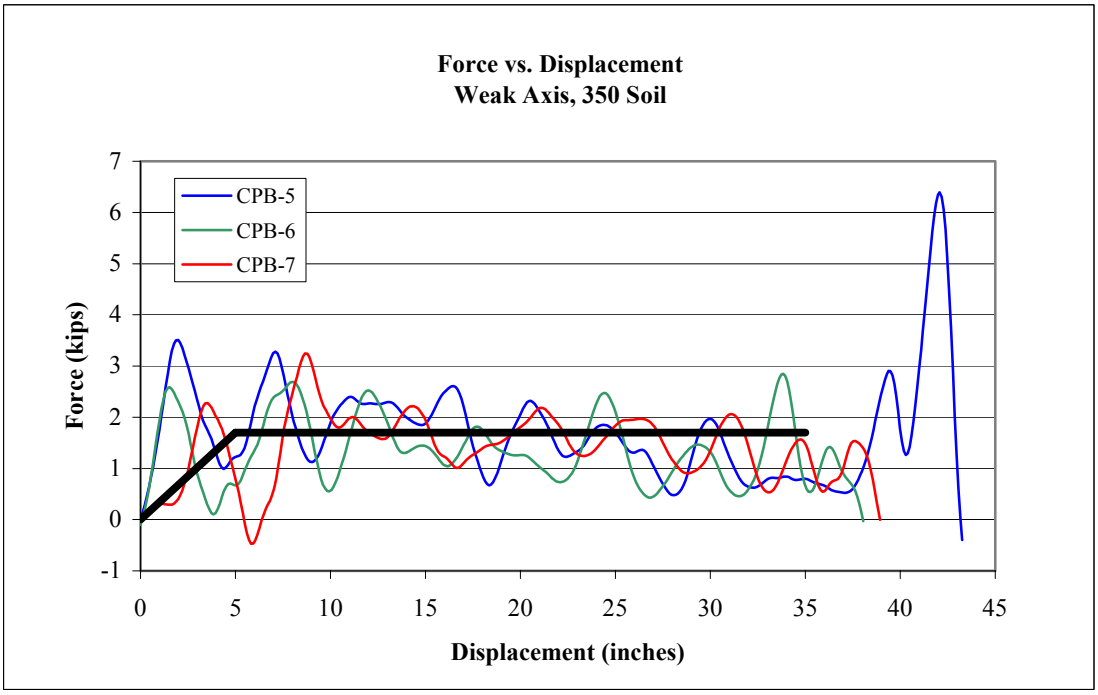

Figure 12. Force-Displacement Curve for Bogie Tests CPB-5 through CPB-7

Most of these results were used as input parameters for the BARRIER VII model, but some values were adjusted to develop a behavior that was more common to true impact scenarios. For example, a reduction in the weak-axis moment was employed to account for the relative free movement of the cable through hook bolts attached to each post. The combination of the bogie test results and video footage of prior full-scale crash tests assisted in determining both the longitudinal and lateral deflections (22). Slip-base post properties were estimated using classical structural analysis techniques. The input parameters for both the line and slip-base posts are shown in Table 5. It should be noted that the weak and strong axes are represented by A-axis and B-axis, respectively.

Table 5. BARRIER VII Input Parameters for Line Post Members

Post Type	Post Height				Stiffness				Effective Weight	
	Upper Cable		Lower Cable		Along A-Axis		Along B-Axis			
	mm	in.	mm	in.	kN/mm	k/in.	kN/mm	k/in.	kg	lb
Line	762	30.0	610	24.0	0.06	0.34	0.13	0.72	6.9	15.20
Slip-Base	762	30.0	610	24.0	0.11	0.63	0.61	3.46	6.9	15.20

Post Type	Base Moment				Shear Force			
	About B-Axis		About A-Axis		A-Axis		B-Axis	
	kN-mm	k-in.	kN-m	k-in.	kN	kips	kN	kips
Line	1.7	15.0	11.0	97.2	160.1	36.0	66.7	15.0
Slip-Base	1.7	15.0	11.0	97.2	160.1	36.0	66.7	15.0

Post Type	Deflection			
	A-Axis		B-Axis	
	mm	in.	mm	in.
Line	508	20.0	381	15.0
Slip-Base	508	20.0	381	15.0

As previously stated, the anchor alternatives were modeled as post-type members. The BARRIER VII input constraints were determined from the force-deflection plots produced from

the bogie test results discussed previously. For the purposes of modeling, properties and behavior of all anchors were assumed to be the same in both the weak-axis and strong-axis directions. It is noted that the effective weights of the three anchor designs were each reduced to an equal weight of 34.0 kg (75 lbs). In this case, the weight parameter served only as a source of stability in the computer model since the weight of each anchor was previously accounted for in the results set forth by the dynamic bogie testing. These input values are summarized in Table 6.

Table 6. BARRIER VII Input Parameters for Anchor Post Members

Anchor Post Type	Post Height				Stiffness Along A & B Axes		Effective Weight	
	Upper Cable		Lower Cable					
	mm	in.	mm	in.	kN/mm	k/in.	kg	lb
Steel Post	108	4.27	83	3.27	0.72	4.10	34	75
Concrete Shaft	108	4.27	83	3.27	1.17	6.67	34	75
Concrete Block	108	4.27	83	3.27	1.17	6.67	34	75

Anchor Post Type	Base Moment About A & B Axes		Shear Force Along A & B Axes		Deflection Along A & B Axes	
	kN-m	k-in.	kN	kips	mm	in.
Steel Post	20.3	180.0	186.8	42.0	259	10.2
Drilled Shaft	19.2	170.0	177.9	40.0	445	17.5
Concrete Block	24.3	215.0	222.4	50.0	445	17.5

The temperature compensators were the last of the barrier elements to be modeled. The properties for these spring-type members were obtained from existing state standards and physical measurements and computations. The BARRIER VII input data is summarized in Table 7.

Along with barrier input data, vehicle control data needed to be specified. The vehicle was modeled as a rigid body of arbitrary shape surrounded by a cushion of discrete inelastic springs. Input parameters include the vehicle weight, impact speed, impact angle, and impact

location, as detailed in Table 8. Additional vehicle data is defined in the referenced BARRIER VII manual (25) and Appendices B and C.

Table 7. BARRIER VII Input Parameters for Spring-Type Members

Spring Stiffness		Compression Bottoming		Post Compression Stiffness		Tension Bottoming		Post Tension Stiffness		Weight	
kN/mm	k/in.	mm	in.	kN/mm	k/in.	mm	in.	kN/mm	k/in.	kg	lbs
0.08	0.45	203	8.0	0.08	0.45	203	8.0	52.5	300.0	12.2	27.0

Table 8. BARRIER VII Input Parameters for Impacting Vehicle

Vehicle Weight		Impact Velocity		Impact Angle	Impact Location	
kg	lbs	km/h	mph	degrees	m	ft
1996	4400	100	62.14	25	623.6	2046

Recall that previous research has shown that a single cable can contain and redirect impacting vehicles. The expected results of such an occurrence were explored in the simulation effort. For all anchor options, models were developed where both cable lines served as contact interfaces. These models were then modified to simulate both the top and bottom cables as single contact interfaces. An additional simulation model was also developed in an attempt to effectively model a three-cable system. To account for the presence of the third cable the cross-sectional areas and yield strengths of the upper and lower cables were increased to 1.5 times the original values. The bogie test results on the three proposed anchors indicated that the driven steel post was the most efficient design capable of meeting minimum criterion because it presented the lowest force-resisting capacity and largest longitudinal displacement. Nevertheless, all three anchors were modeled and analyzed to reconfirm initial assessments as well as establish

a comparison base for system behavior of each anchor alternative. The BARRIER VII simulation matrix is detailed in Table 9. The models served as the foundation for validation efforts and templates for extending the modeling to sloping installations.

Table 9. BARRIER VII Simulation Matrix

Simulation	Description	Contact Interface
SP-1A	Driven Steel Post	Upper & Lower Cable
SP-1B	Driven Steel Post	Upper Cable
SP-1C	Driven Steel Post	Lower Cable
SP-1D	Driven Steel Post	Upper & Lower Cable (Three-Cable Model)
DS-1A	Drilled Shaft	Upper & Lower Cable
DS-1B	Drilled Shaft	Upper Cable
DS-1C	Drilled Shaft	Lower Cable
DS-1D	Drilled Shaft	Upper & Lower Cable (Three-Cable Model)
CB-1A	Concrete Block	Upper & Lower Cable
CB-1B	Concrete Block	Upper Cable
CB-1C	Concrete Block	Lower Cable
CB-1D	Concrete Block	Upper & Lower Cable (Three-Cable Model)

5.3 Validation Efforts

Initial simulations assessed the behavior of the three-cable guardrail system located on a flat surface. The simulation results are summarized in Table 10 and were used in the validation of the BARRIER VII models. Video and documented results of similar three-cable barrier tests served as the source of validation. Video footage confirmed that the cable released from the line post at approximately 381 mm (15 in.) of displacement measured from the top of the post. One crash test was performed on a 145-m (476-ft) long cable guardrail system using a 2,000-kg (4,409-lb) pickup truck impacting at a nominal speed and angle of 101.4 km/h (63.0 mph) and 24.8 degrees, respectively. During this test, a 3.4-m (11-ft) maximum lateral deflection was observed, which was comparable to the 3.7-m (12-ft) deflection predicted by BARRIER VII.

Other comparisons were made between the approximate parallel time and the length of contact prior to parallel. These results are summarized in Table 11.

Table 10. BARRIER VII Results for Flat-Surface Model

Simulation	T_{upper}		T_{lower}		δ_{upper}		δ_{lower}		$\delta_{lateral}$		Location		Time
	kN	kips	kN	kips	mm	in.	mm	in.	mm	in.	m	ft	sec
SP-1A	13.9	3.12	89.1	20.04	114	4.5	87	3.4	3741	147.3	62.33	204.5	0.660
SP-1B	70.6	15.88	4.0	0.90	106	4.2	81	3.2	4516	177.8	64.16	210.5	0.735
SP-1C	4.0	0.90	80.6	18.13	97	3.8	75	2.9	4021	158.3	62.94	206.5	0.695
SP-1D	7.4	1.66	114.2	25.67	124	4.9	97	3.8	3696	145.5	61.72	202.5	0.630
DS-1A	32.0	7.19	79.8	17.93	77	3.1	60	2.3	3703	145.8	61.72	202.5	0.630
DS-1B	74.8	16.82	4.0	0.90	68	2.7	52	2.0	4486	176.6	73.30	240.5	0.955
DS-1C	4.0	0.90	81.8	18.38	67	2.6	52	2.0	4003	157.6	62.94	206.5	0.675
DS-1D	25.9	5.83	106.8	24.01	89	3.5	69	2.7	3459	136.2	61.42	201.5	0.610
CB-1A	32.0	7.19	79.8	17.93	77	3.1	60	2.3	3703	145.8	61.72	202.5	0.630
CB-1B	74.8	16.82	4.0	0.90	68	2.7	52	2.0	4486	176.6	73.30	240.5	0.955
CB-1C	4.0	0.90	81.8	18.38	67	2.6	52	2.0	4003	157.6	62.94	206.5	0.675
CB-1D	25.9	5.83	106.8	24.01	89	3.5	69	2.7	3459	136.2	61.42	201.5	0.610

where: T_{upper} = Tensile Force in Upper Cable at Anchor
T_{lower} = Tensile Force in Lower Cable at Anchor
δ_{upper} = Displacement of Upper Anchor Connection
δ_{lower} = Displacement of Lower Anchor Connection
$\delta_{lateral}$ = Maximum Lateral Barrier Displacement
Location = Point of Maximum Lateral Displacement Measured from Upstream Anchor
Time = Time when Maximum Lateral Displacement Occurred

Table 11. Comparative Results of BARRIER VII to Field Testing

Means of Comparison	Field Testing	BARRIER VII
Maximum Lateral Barrier Deflection	3.41 m (11.2 ft)	3.66 m (12.0 ft)
Time to Parallel	0.450 sec	0.446 sec
Contact Length to Parallel	9.75 m (32.0 ft)	8.81 m (28.9 ft)

Slight variation in results can be attributed to the accuracy of the general input parameters of the BARRIER VII model. The results of the flat-surface simulations confirmed that all anchors would provide satisfactory performance if implemented into the cable barrier system. The driven steel post alternative was selected for the design because it presented the most

economical solution. In addition, the steel post design was the weakest design alternative and if it is proven adequate, the other two anchor design alternatives would also be adequate.

5.4 Slope Model

A primary objective of this research study was to investigate the behavior and adequacy of a three-cable barrier system adjacent to a 1.5H:1V slope. Thus, the finite element model was modified to accurately simulate the effects of the slope. Because the limitations of BARRIER VII do not allow for three-dimensional modeling, a different approach was taken. The only way the additional energy produced by the vehicle traveling down the slope could be addressed with BARRIER VII was to increase the energy in the vehicle at impact. Combining the definition of impact severity velocity and the energies provided the means of effectively modeling the slope, as shown in Equation 1.

$$\frac{1}{2}m\left(V_s \sin\theta\right)^2 = \frac{1}{2}m\left(V_{fs} \sin\theta\right)^2 + mgh \qquad \text{(Equation 1)}$$

where: m = mass of the impacting vehicle
g = gravitation acceleration
h = vertical component of slope (determined from flat-surface deflection)
V_s = effective vehicle velocity due to slope
V_{fs} = effective flat-surface vehicle velocity
θ = angle of impact
$V\sin\theta$ = effective barrier velocity

The vertical component of the slope represented of the potential drop in the vehicle's center of gravity as the vehicle encroached onto the steep slope. This potential drop was calculated from the average lateral barrier deflection obtained from the flat-surface simulations. With a 1.5H:1V slope geometry, a velocity of 110.3 km/h (68.55 mph) was computed to compensate for the energy increase as the vehicle traveled down the slope. The revised simulation matrix is shown in Table 12. Furthermore, a finite element model of the three-cable

guardrail is provided in Appendix B. A typical computer simulation input data file is detailed in Appendix C.

Note that based on the dynamic bogie testing of the anchor designs and the BARRIER VII model validation, the steel post option was proven to be the critical design case. If this anchor proved to be adequate, the other two designs would also be adequate. Therefore, this analysis was limited to the steel post design option only.

Table 12. BARRIER VII Simulation Matrix

Simulation	Description	Contact Interface
SP-2A	Driven Steel Post	Upper & Lower Cable
SP-2B	Driven Steel Post	Upper Cable
SP-2C	Driven Steel Post	Lower Cable
SP-2D	Driven Steel Post	Upper & Lower Cable (Three-Cable Model)

5.5 Results

The results of the simulated cable barrier set adjacent to a modeled slope focused primarily on the anchor displacement, the forces acting on the terminal anchor, and the maximum lateral displacement of the system. These results are summarized in Table 13. The BARRIER VII results predicted that an acceptable range of anchor displacements and base forces would be experienced when a cable system is installed adjacent to a 1.5H:1V slope. In addition, when a single contact interface was simulated, a 4.0-kN (0.9-kip) force remained in the cable which was effectively removed from the system. This force is attributed to the initial cable pre-tensioning.

The results of the BARRIER VII simulation also provided other pertinent information. In addition to the maximum lateral displacement of the barrier, the measured distance between

initial barrier contact and the point at which the vehicle exited the system was utilized in determining the needed dimensions of the field-constructed slope. The BARRIER VII analysis of the three-cable barrier installed adjacent to a 1.5H:1V slope, simulation run SP-2D, predicted a maximum lateral barrier deflection of approximately 4.19 m (13.75 ft) and a contact length of 41.45 m (136 ft).

The prediction of such a large lateral displacement in the barrier raised significant concern as to whether or not an impacting vehicle could remain stable. The 4.19-m (13.75-ft) lateral deflection determined from BARRIER VII corresponds to an approximate 1.98-m (6.5-ft) drop in the vehicle's center of gravity (c.g.) as it encroaches onto the slope. This significant drop greatly increases the potential of vehicle rollover. Based on these results and the frequent use of three-cable guardrail adjacent to slope, full-scale crash testing was warranted to determine the actual performance of the three-cable barrier installed in this manner.

Table 13. BARRIER VII Results for Slope Model

Simulation	T_{upper}		T_{lower}		δ_{upper}		δ_{lower}		$\delta_{lateral}$		Location		Time
	kN	kips	kN	kips	mm	in.	mm	in.	mm	in.	m	ft	sec
SP-2A	16.6	3.74	103.9	23.36	132	5.2	102	4.0	4356	171.5	73.30	240.5	0.865
SP-2B	78.3	17.61	4.0	0.90	119	4.7	91	3.6	5423	213.5	76.66	251.5	1.000
SP-2C	4.0	0.90	85.6	19.24	99	3.9	76	3.0	4651	183.13	74.52	244.5	0.920
SP-2D	7.7	1.74	131.7	29.58	135	5.3	104	4.1	4194	165.1	73.00	239.5	0.86

where: T_{upper} = Tensile Force in Upper Cable at Anchor
T_{lower} = Tensile Force in Lower Cable at Anchor
δ_{upper} = Displacement of Upper Anchor Connection
δ_{lower} = Displacement of Lower Anchor Connection
$\delta_{lateral}$ = Maximum Lateral Barrier Displacement
Location = Point of Maximum Lateral Displacement Measured from Upstream Anchor
Time = Time when Maximum Lateral Displacement Occurred

6 THREE-CABLE GUARDAIL (DRIVEN STEEL POST OPTION)

Based on the BARRIER VII simulation results, it was decided that a full-scale crash test was to be conducted to explore vehicle stability. The system design was selected based on the modeled barrier which was South Dakota's three cable barrier and included the weakest of the three anchor options.

The total length of the installation was 147.82 m (485 ft). The test installation consisted of four major structural components: (1) wire rope; (2) posts; (3) spring compensating cable end assemblies, and (4) anchor assemblies. Design details are shown in Figures 13 through 17. The corresponding English-unit drawings are shown in Appendix D. Photographs of the test installation are shown in Figures 18 and 19.

Three separate lines of 19-mm (¾-in.) diameter 3x7 wire rope defined the rail elements. The cable rails were supported by thirty-two guardrail posts with an uppermost mounting height of 762 mm (30 in.) and 76-mm (3-in.) incremental spacing for the lower cables, as shown in Figure 14. The 1,600-mm (63-in.) long S76x8.5 (S3x5.7) rolled steel section was used for the typical line post. The section incorporated a 762-mm (30-in.) embedment depth and a 203-mm x 610-mm x 6-mm (8-in. x 24-in. x 1/4-in.) soil bearing plate welded along the post flange edge, as shown in Figures 15 and 17. The guardrail posts were set 305-mm (12-in.) back from the slope breakpoint.

Due to the fact that the existing anchorage design also served as the mounting pad for the slip-base post system, a revised design included a redeveloped anchorage for the slip-base posts. The proposed design integrated the slip-base mechanism mounted to a 1,829-mm (72-in.) long W152x13.4 (W6x9) steel post, as shown in Figures 15 and 17.

The anchor bracket post, previously analyzed through dynamic bogie testing and computer simulation, was configured with a W152x37.2 (W6x25) steel post and embedded to a depth of 2,438 mm (96 in.), as shown in Figures 14 and 16. A 13-mm (½-in) thick by 610-mm (24-in.) square soil plate was welded to the post flange by a series of 10-mm (⅜-in.) fillet welds. Furthermore, the cable anchor bracket was bolted to a 13-mm x 356-mm x 248-mm (½-in. x 14-in. x 9 ¾-in.) plate welded to the top of the post.

A 64-m long x 10-m wide (210-ft x 33-ft) pit was excavated behind the cable system. In order to develop a 1.5H:1V slope, the pit's profile was identified by horizontal and vertical components of 6.1 m (20 ft) and 4.0 m (13 ft), respectively, as shown in Figures 13 and 18.

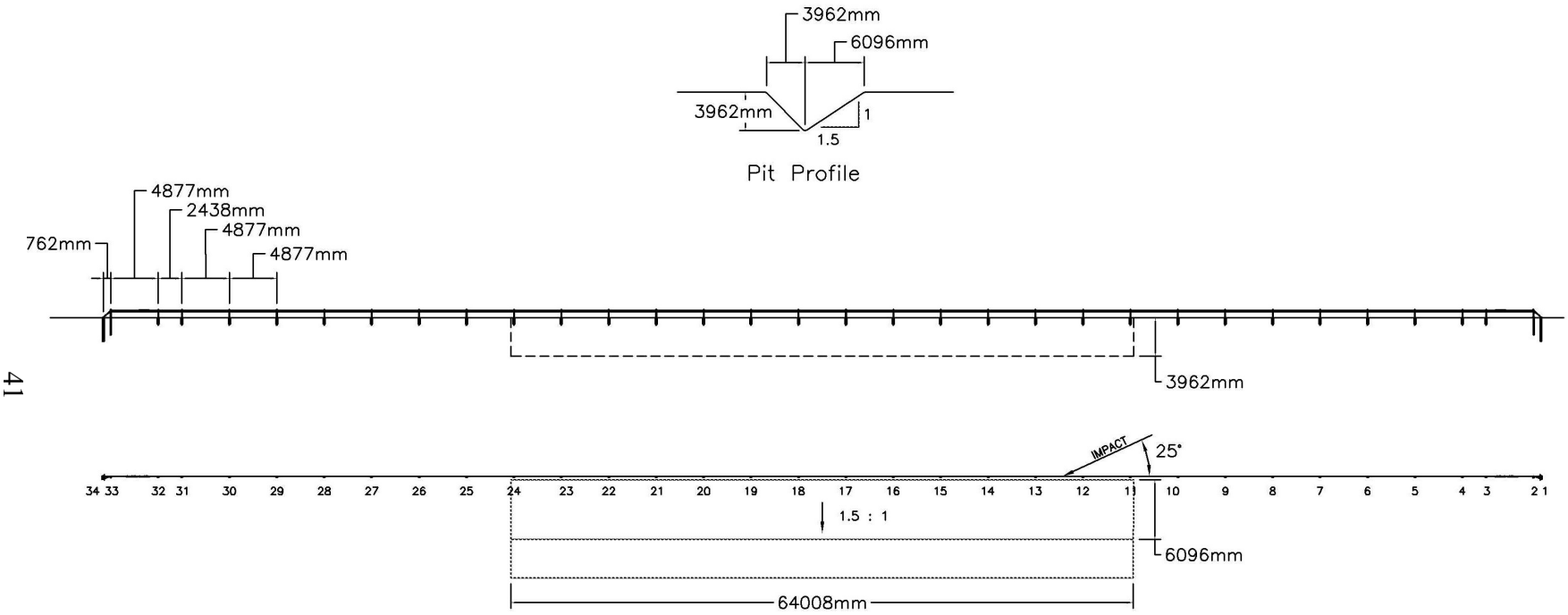

Figure 13. Three-Cable Guardrail Geometry

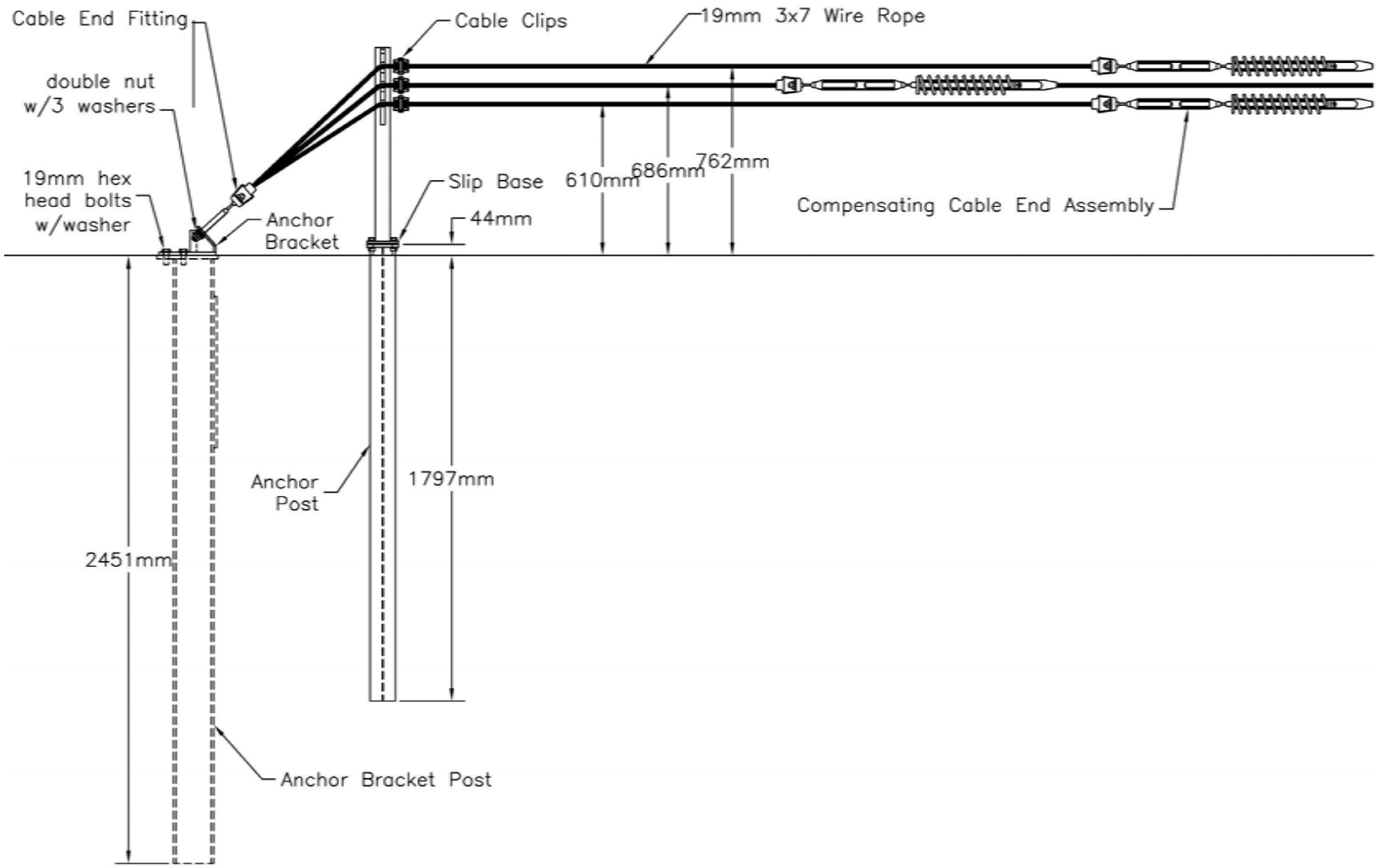

Figure 14. Three-Cable Guardrail End Terminal Overview

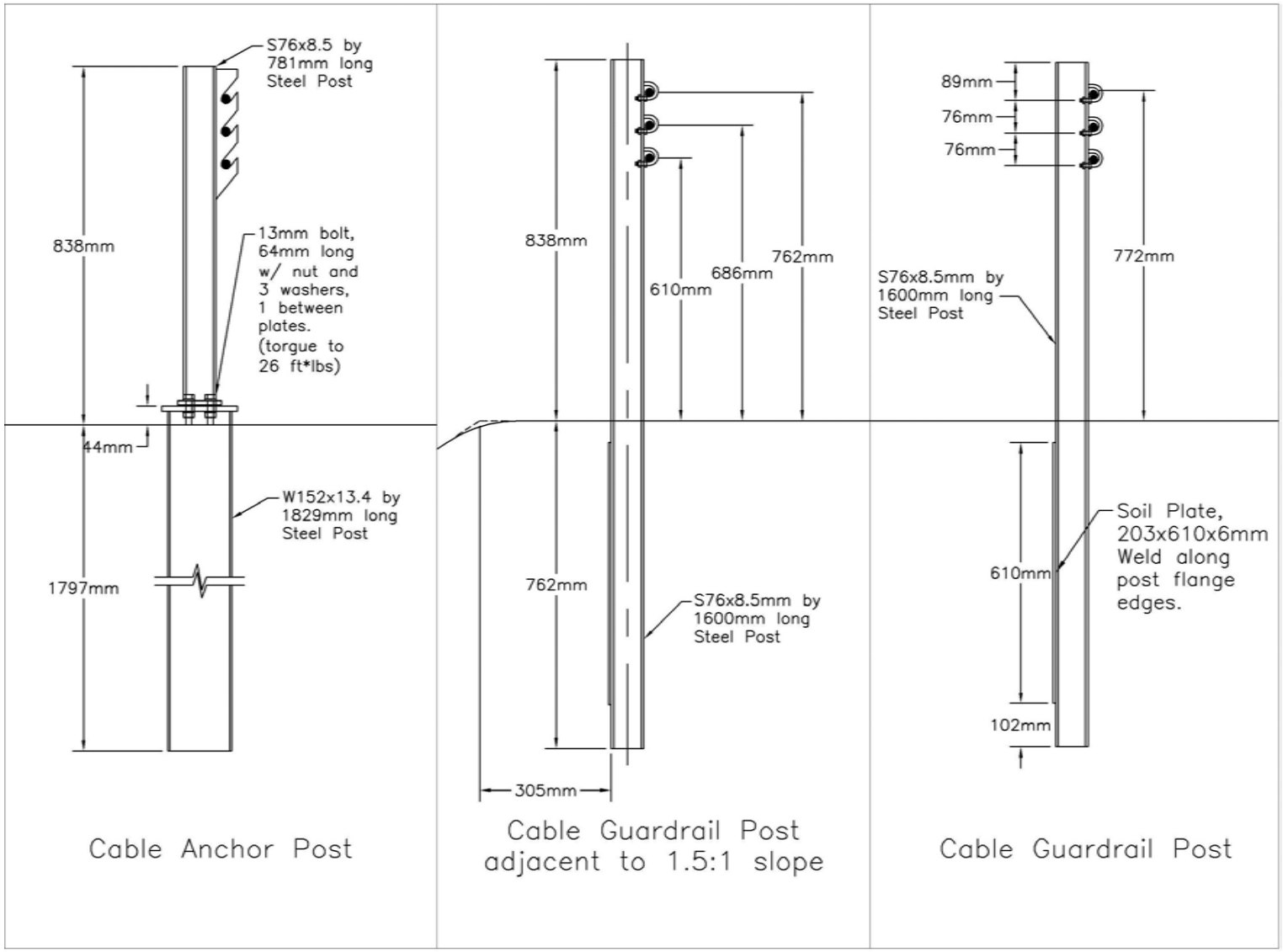

Figure 15. Typical Three-Cable Guardrail Post Overview

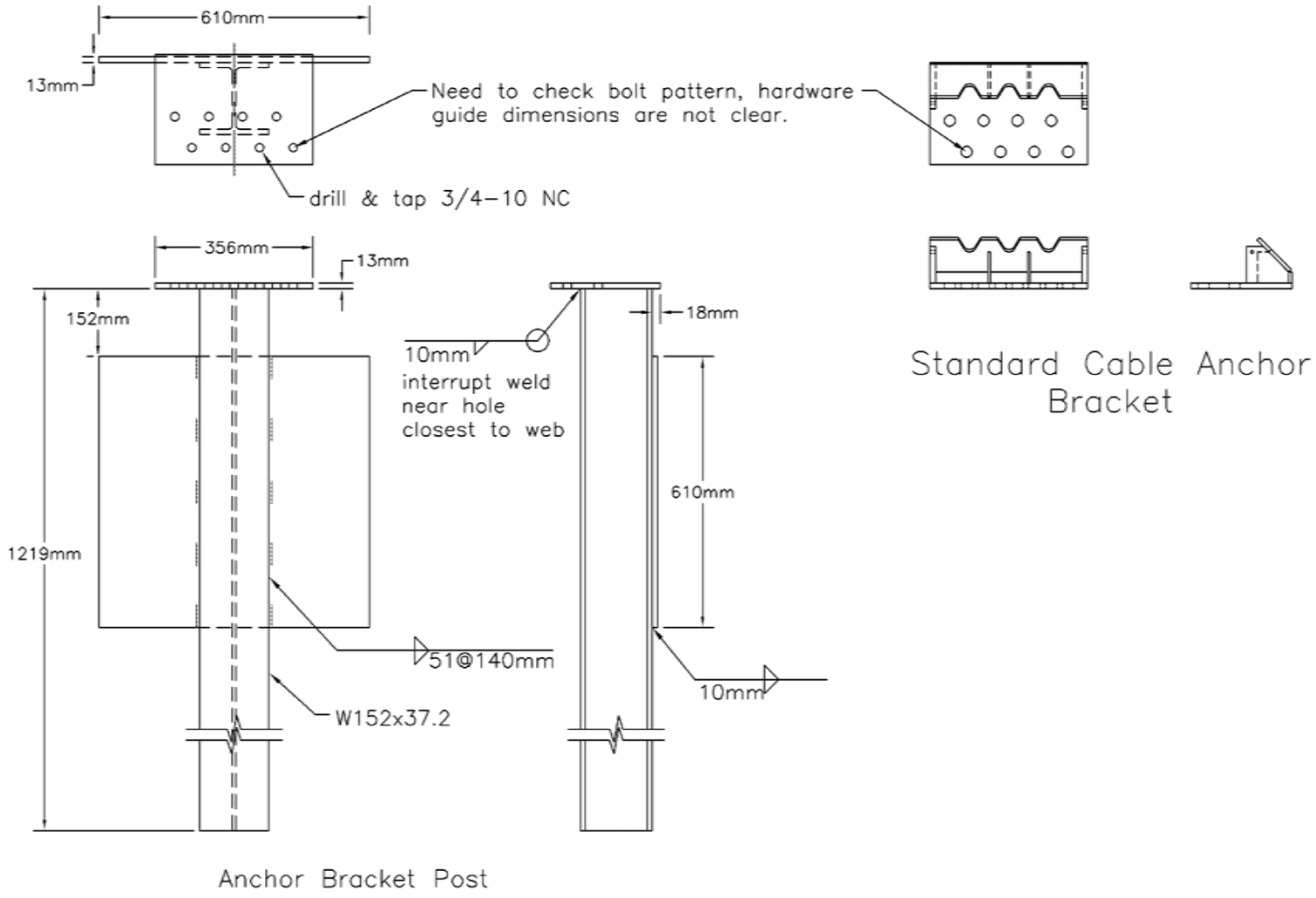

Figure 16. End Anchor and Cable Bracket Details

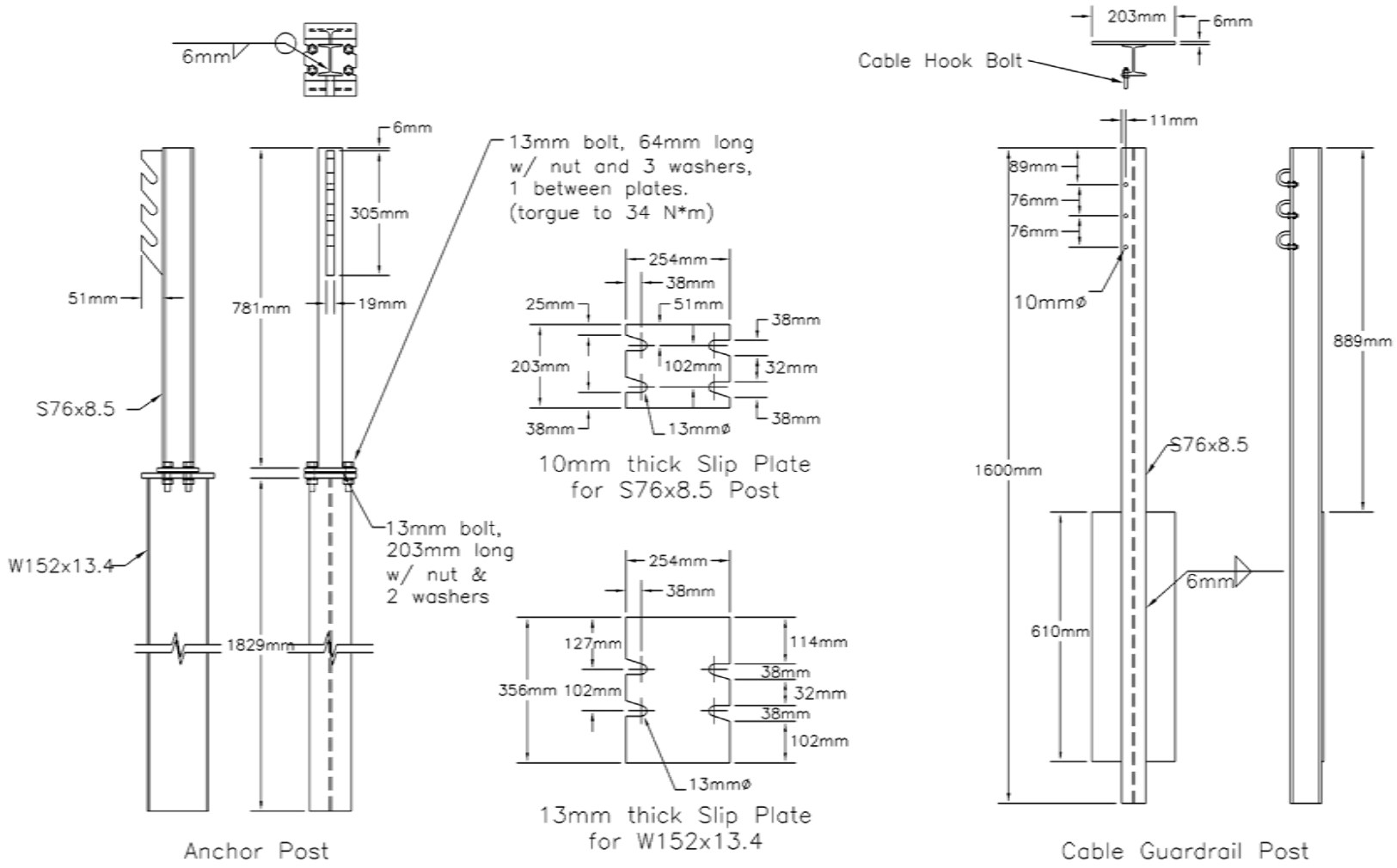

Figure 17. Line and Slip-Base Post Details

Figure 18. Three-Cable Guardrail System Adjacent to Slope

Figure 19. Three-Cable Guardrail System Adjacent to Slope

7 TEST REQUIREMENTS AND EVALUATION CRITERIA

7.1 Test Requirements

Longitudinal barriers, such as three-cable guardrail, must satisfy the requirements provided in NCHRP Report No. 350 to be accepted for use on National Highway System (NHS) new construction projects or as a replacement for existing designs not meeting current safety standards. According to TL-3 of NCHRP Report No. 350, longitudinal barriers must be subjected to two full-scale crash tests. The two crash tests are as follows:

1. Test Designation 3-10. An 820-kg (1,808-lb) small car impacting the barrier at a nominal speed and angle of 100.0 km/h (62.14 mph) and 20 degrees, respectively.

2. Test Designation 3-11. A 2,000-kg (4,409-lb) pickup truck impacting the barrier at a nominal speed and angle of 100.0 km/h (62.14 mph) and 25 degrees, respectively.

However, the higher impact energy associated with the pickup truck test produces larger barrier deflections and greatly increases the likelihood of vehicle rollover as compared to the small car test. Therefore, the 2,000-kg (4,409-lb) pickup truck test was selected as sufficient to evaluate the performance of the cable guardrail adjacent to steep slopes, and the 820-kg (1,808-lb) small car test was considered unnecessary for this project. The test conditions for TL-3 longitudinal barriers are summarized in Table 14.

7.2 Evaluation Criteria

Evaluation criteria for full-scale vehicle crash testing are based in three appraisal areas: (1) structural adequacy; (2) occupant risk; and (3) vehicle trajectory after collision. Criteria for structural adequacy are intended to evaluate the ability of the barrier to contain, redirect, or allow controlled vehicle penetration in a predictable manner. Occupant risk evaluates the degree of

hazard to occupants in the impacting vehicle. Vehicle trajectory after collision is a measure of the potential for the post-impact trajectory of the vehicle to cause subsequent multi-vehicle accidents. This criterion also indicates the potential safety hazard for the occupants of the other vehicle or the occupants of the impacting vehicle when subjected to secondary collisions with other fixed objects. These three evaluation criteria are defined in Table 15. The full-scale vehicle crash test was conducted and reported in accordance with the procedures provided in NCHRP Report No. 350.

Table 14. NCHRP Report No. 350 Test Level 3 Crash Test Conditions

Test Article	Test Designation	Test Vehicle	Impact Conditions			Evaluation Criteria
			Speed		Angle (degrees)	
			(km/h)	(mph)		
Longitudinal Barrier	3-10	820C	100	62.1	20	A,D,F,H,I,K,M
	3-11	2000P	100	62.1	25	A,D,F,K,L,M

Table 15. NCHRP Report No. 350 Evaluation Criteria for Crash Tests

Structural Adequacy	A. Test article should contain and redirect the vehicle; the vehicle should not penetrate, underride, or override the installation although controlled lateral deflection of the test article is acceptable.
Occupant Risk	D. Detached elements, fragments or other debris from the test article should not penetrate or show potential for penetrating the occupant compartment, or present an undue hazard to other traffic, pedestrians, or personnel in a work zone. Deformations of, or intrusions into, the occupant compartment that could cause serious injuries should not be permitted.
	F. The vehicle should remain upright during and after collision although moderate roll, pitching, and yawing are acceptable.
	H. Longitudinal and lateral occupant impact velocities should fall below the preferred value of 9 m/s (29.53 ft/s), or at least below the maximum allowable value of 12 m/s (39.37 ft/s).
	I. Longitudinal and lateral occupant ridedown accelerations should fall below the preferred value of 15 g's, or at least below the maximum allowable value of 20 g's.
Vehicle Trajectory	K. After collision it is preferable that the vehicle's trajectory not intrude into adjacent traffic lanes.
	L. The occupant impact velocity in the longitudinal direction should not exceed 12 m/sec (39.37 ft/sec), and the occupant ridedown acceleration in the longitudinal direction should not exceed 20 G's.
	M. The exit angle from the test article preferably should be less than 60 percent of test impact angle measured at time of vehicle loss of contact with test device.

8 TEST CONDITIONS

8.1 Test Facility

The testing facility is located at the Lincoln Air-Park on the northwest (NW) side of the Lincoln Municipal Airport and is approximately 8.0 km (5.0 miles) NW of the University of Nebraska-Lincoln.

8.2 Vehicle Tow and Guidance System

A reverse cable tow system with a 1:2 mechanical advantage was used to propel the test vehicle. The distance traveled and the speed of the tow vehicle was one-half that of the test vehicle. The test vehicle was released from the tow cable before impact with the cable guardrail.

A vehicle guidance system developed by Hinch (27) was used to steer the test vehicle. A guide-flag, attached to the front-left wheel and the guide cable, was sheared off before impact. The 9.5-mm (0.375-in.) diameter guide cable was tensioned to approximately 15.6 kN (3,500 lbs), and supported laterally and vertically every 30.48 m (100 ft) by hinged stanchions. The hinged stanchions stood upright while holding up the guide cable, but as the vehicle was towed down the line, the guide-flag struck and knocked each stanchion to the ground. The vehicle guidance system was approximately 457-m (1,500-ft) long.

8.3 Test Vehicle

For test CS-1, a 1995 GMC 2500 ¾-ton pickup truck was used as the test vehicle. The test inertial and gross static weights were 2,034 kg (4,484 lbs). The test vehicle is shown in Figure 20, and vehicle dimensions are shown in Figure 21.

The longitudinal component of the center of gravity was determined using the measured axle weights. The location of the final center of gravity is shown in Figures 20 and 21.

Figure 20. Test Vehicle, Test CS-1

Date: 11/1/01 Test Number: CS-1 Model: 2500

Make: GMC Vehicle I.D.#: 1GDGC24K8SE519215

Tire Size: 245/75 R16 Year: 1995 Odometer: 223207

*(All Measurements Refer to Impacting Side)

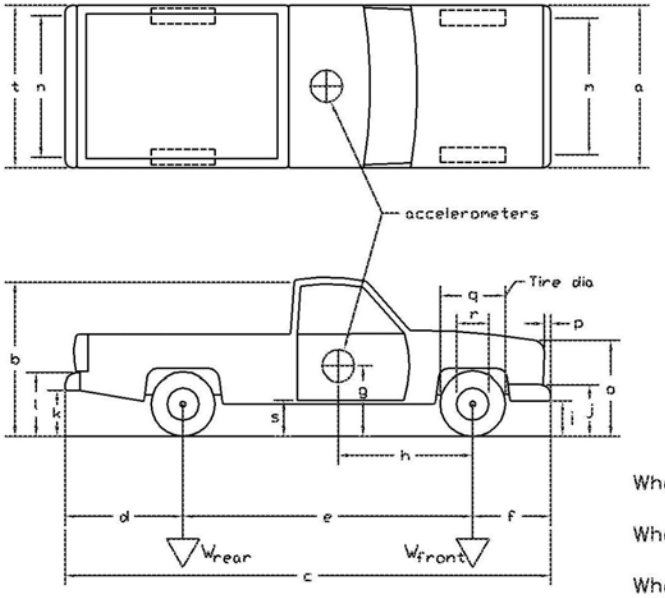

Vehicle Geometry – mm (in.)

a	1861 (73.25)	b	1887 (73.5)
c	5537 (218.0)	d	1302 (51.25)
e	3327 (131.0)	f	908 (35.75)
g	667 (26.25)	h	1372 (54.0)
i	464 (18.25)	j	673 (26.5)
k	603 (23.75)	l	794 (31.25)
m	1591 (62.625)	n	1626 (64.0)
o	1029 (40.5)	p	83 (3.25)
q	762 (30.0)	r	445 (17.5)
s	483 (19.0)	t	1854 (73.0)

Wheel Center Height Front 365 (14.375)

Wheel Center Height Rear 362 (14.25)

Wheel Well Clearance (FR) 905 (35.625)

Wheel Well Clearance (RR) 953 (37.5)

Engine Type 8 CYL. GAS

Engine Size 5.7 L 350 CID

Transmission Type:

(Automatic) or Manual

FWD or (RWD) or 4WD

Weights – kg (lb)

	Curb	Test Inertial	Gross Static
W_{front}	1124 (2475)	1194 (2631)	1194 (2631)
W_{rear}	824 (1814)	840 (1851)	840 (1851)
W_{total}	1948 (4294)	2034 (4482)	2034 (4482)

Note any damage prior to test: Rusty box fenders/Small dents in box/lower d. side

Figure 21. Vehicle Dimensions, Test CS-1

Square, black and white-checkered targets were placed on the vehicle to aid in the analysis of the high-speed film and E/cam video, as shown in Figure 22. Round, checkered targets were placed at the center of gravity on the driver's side door, on the passenger's side door, and on the roof of the vehicle. The remaining targets were located for reference so they could be viewed from the high-speed cameras for film analysis.

The front wheels of the test vehicle were aligned for camber, caster, and toe-in values of zero so the vehicle would track properly along the guide cable. One 5B flash bulb was mounted on the hood and another mounted on the roof of the vehicle to pinpoint the time of impact with the cable guardrail on the high-speed film and E/cam video. The flash bulbs were fired by a pressure tape switch mounted on the front face of the bumper. A remote controlled brake system was installed in the test vehicle so the vehicle could be safely slowed to a stop after the test.

8.4 Data Acquisition Systems

8.4.1 Accelerometers

One triaxial piezoresistive accelerometer system with a range of ±200 G's was used to measure the acceleration in the longitudinal, lateral, and vertical directions at a sample rate of 10,000 Hz. The environmental shock and vibration sensor/recorder system, Model EDR-4M6, was developed by Instrumented Sensor Technology (IST) of Okemos, Michigan and includes three differential channels as well as three single-ended channels. The EDR-4 was configured with 6 Mb of RAM memory and a 1,500 Hz lowpass filter. Computer software, "DynaMax 1 (DM-1)" and "DADiSP," was used to digitize, analyze, and plot the accelerometer data.

A backup triaxial piezoresistive accelerometer system with a range of ±200 G's was also used to measure the longitudinal, lateral, and vertical accelerations at a sample rate of 3,200 Hz. The environmental shock and vibration sensor/recorder system, Model EDR-3, was also

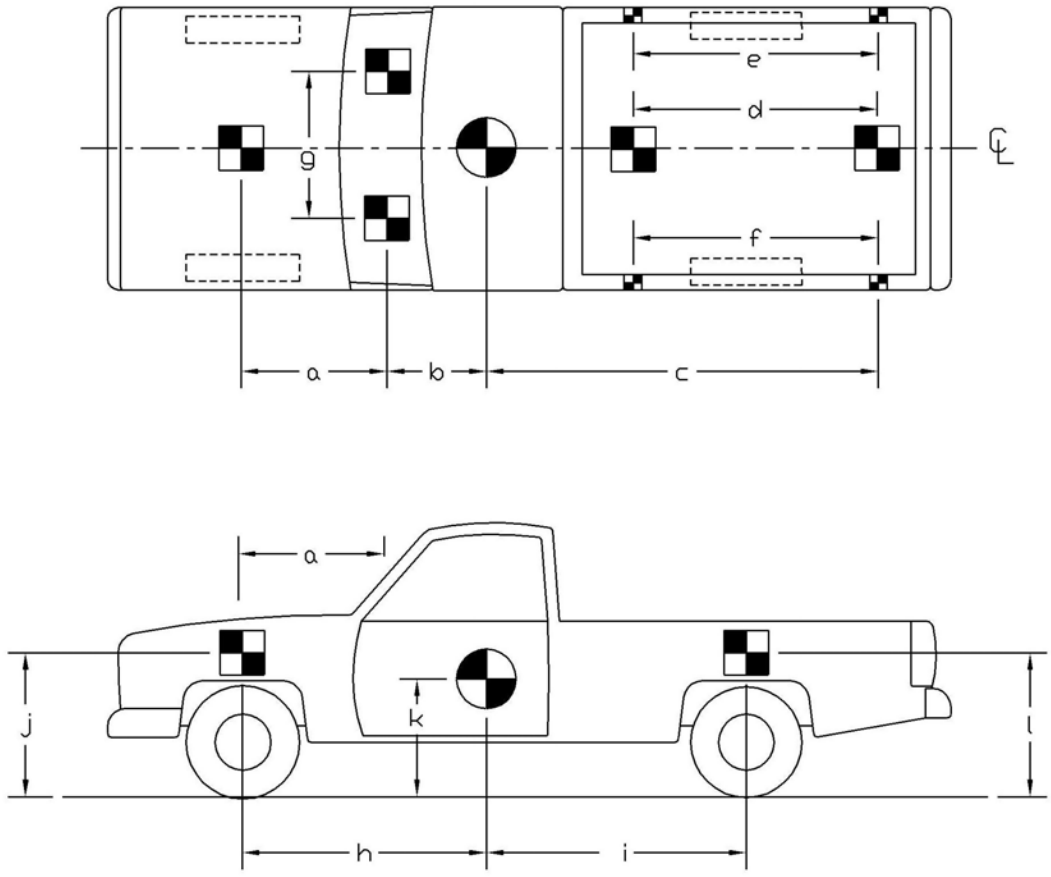

TEST #: CS-1

TARGET GEOMETRY -- mm (in.)

a	832 (32.75)	d	1899 (74.75)	g	1200 (47.25)	j	1006 (39.625)
b	699 (27.5)	e	2146 (84.5)	h	1372 (54.0)	k	667 (26.25)
c	2819 (111.0)	f	2146 (84.5)	i	1956 (77.0)	l	1054 (41.5)

Figure 22. Vehicle Target Locations, Test CS-1

developed by Instrumented Sensor Technology (IST) of Okemos, Michigan. EDR-3 was configured with 256 Kb of RAM memory and a 1,120 Hz lowpass filter. Computer software, "DynaMax 1 (DM-1)" and "DADiSP," was used to digitize, analyze, and plot the accelerometer data.

8.4.2 Rate Transducer

A Humphrey 3-axis transducer with a range of 360 degrees/second in each of the three directions (pitch, roll, and yaw) was used to measure the rates of motion of the test vehicle. The rate transducer was rigidly attached to the vehicle near the test vehicle's center of gravity. Rate transducer signals, excited by a 28-volt DC power source, were received through the three single-ended channels located externally on the EDR-4M6 and stored in the internal memory. The raw data measurements were then downloaded for analysis and plotted. Computer software, "DynaMax 1 (DM-1)" and "DADiSP", was used to digitize, analyze, and plot the transducer data.

8.4.3 High-Speed Photography

For test CS-1, one high-speed 16-mm Red Lake Locam camera, with an operating speed of approximately 500 frames/sec, was used to film the crash test. Five high-speed Red Lake E/cam video cameras, with operating speeds of 500 frames/sec, were also used to film the crash test. Five Canon digital video cameras, with a standard operating speed of 29.97 frames/sec, were also used to film the crash test. A Locam, with a wide-angle 12.5-mm lens, and two Canon digital video cameras were placed above the test installation to provide a field of view perpendicular to the ground. A high-speed E/cam video camera, a Canon digital video camera, and a Nikon 995 digital camera were placed downstream from the impact point and behind the barrier and had a field of view parallel to the impacting vehicle. A high-speed E/cam video

camera and a Canon digital video camera were placed upstream from the impact point and behind the barrier. Another high-speed E/cam video camera was placed downstream from the impact point and behind the barrier, but closer to the impact. Another high-speed E/cam video camera was placed upstream from the impact point and behind the barrier, but closer to the impact. An additional high-speed E/cam video camera was placed upstream from the impact point and on the traffic side of the barrier. A Canon digital video camera, with a panning view, was placed on the traffic side of the barrier and had a field of view perpendicular to the barrier. A schematic of all twelve camera locations for test CS-1 is shown in Figure 23. The Locam film and E/cam videos were analyzed using the Vanguard Motion Analyzer and the Redlake Motion Scope software, respectively. Actual camera speed and camera divergence factors were conducted in the analysis of the high-speed film.

8.4.4 Pressure Tape Switches

For test CS-1, five pressure-activated tape switches, spaced at 2-m (6-ft 6 ¾-in.) intervals, were used to determine the speed of the vehicle before impact. Each tape switch fired a strobe light, which sent an electronic timing signal to the data acquisition system as the left-front tire of the vehicle passed over it. Test vehicle speed was determined from electronic timing mark data recorded using the "Test Point" software. Strobe lights and high-speed film analysis are used only as a backup in the event that vehicle speed cannot be determined from the electronic data.

8.4.5 Three-Cable End Terminal Instrumentation

Electronic sensors were placed near the terminal anchor of the three-cable guardrail system. The types of sensors used for the crash test were load cells and string potentiometers and are described following.

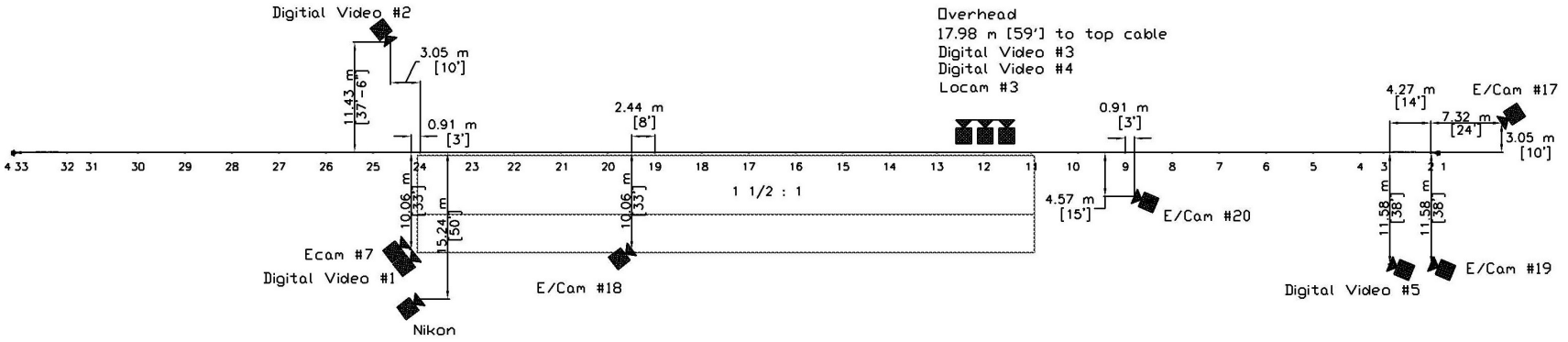

Figure 23. Location of High-Speed Cameras, Test CS-1

8.4.5.1 Load Cells

Six load cells were installed along the three-cable guardrail system. The load cells were positioned in line and at both ends of the three individual cables to measure the forces transferred to the end terminal anchors. The positioning of the load cells is shown in Figure 24.

The load cells were Transducer Techniques TLL-50K load cells with a load range up to 222.4 kN (50,000 lbs). During the test, output voltage signals from the string potentiometers were sent to a Keithly Metrabyte DAS-1802HC data acquisition board, acquired with "Test Point," and stored permanently on the computer. The sample rate of the load cells was 10,000 samples per second (10,000 Hz).

8.4.5.2 String Potentiometers

A string potentiometer (linear variable displacement transducer) was installed on the end terminal anchor to monitor longitudinal displacement of the anchor. The positioning of the string potentiometer is shown in Figure 24.

The string potentiometer used was a UniMeasure PA-50 string potentiometer with a range of 1.27 m (50 in.). A Measurements Group Vishay Model 2310 signal conditioning amplifier was used to condition and amplify the low-level signals to high-level outputs for multichannel, simultaneous dynamic recording on "Test Point" software. After each signal was amplified, it was sent to a Keithly Metrabyte DAS-1802HC data acquisition board, and then stored permanently on the computer. The sample rate of the string potentiometers was 10,000 samples per second (10,000 Hz).

Figure 24. Three-Cable End Terminal Instrumentation

9 CRASH TEST NO. 1

9.1 Test CS-1

The 2,034-kg (4,484-lb) pickup truck impacted the three-cable guardrail system at a speed of 98.1 km/h (61.0 mph) and at an angle of 26.2 degrees. A summary of the test results and the sequential photographs are shown in Figure 25. The summary of the test results and sequential photographs in English units are shown in Appendix E. Additional sequential photographs are shown in Figures 26 through 29. Documentary photographs of the crash test are shown in Figure 30.

9.2 Test Description

Initial impact was to occur 2,134 mm (84 in.) downstream from post no. 12, as shown in Figure 31. Actual vehicle impact occurred 2,743 mm (108 in.) downstream from post no. 12. At 0.046 sec, post nos. 12 and 13 showed lateral and downstream longitudinal deflection. At 0.076 sec, the truck contacted post no. 13. At this same time, the cables began to wrap around the truck's left-front corner while the left-front tire traveled off the slope breakpoint. At 0.176 sec, the left-front tire became airborne as the right-front tire reached the slope breakpoint. It is noted that post nos. 12 through 15 showed continued lateral deflection while the cables released from post no. 14 which had rotated to a 45-degree angle. At 0.234 sec, the truck began to yaw as both left tires and the right-front tire became airborne. At this same time, post no. 14 deflected to nearly parallel with the traveled surface. At 0.274 sec, post no. 14 pulled out of the ground, and post no. 16 began to deflect. At 0.330 sec, the top, middle, and bottom cables were positioned at the headlight, above the bumper, and on the bumper, respectively. It was at this time that the vehicle became completely airborne and pitched downward, rolled counter-clockwise (CCW)

toward the barrier, and continued to yaw. The front of the airborne vehicle engaged the cable barrier, and the front of the vehicle dropped. This drop caused the cables to engage the rear of the vehicle at a position lower than the center of gravity, producing a "tripping" effect. The combination of pitch and roll caused the vehicle to roll over the cables. At 0.396 sec, two cables released from post no. 16, post nos. 11 through 17 were deflected, and the vehicle continued to roll, pitch, and yaw. At 0.532 sec, the truck reached an approximate 45-degree roll angle. As the vehicle yawed approximately parallel to the original system, it began to release from the cables due to an excessive roll angle. At 0.558 sec, post no. 17 rotated to a 45-degree angle, and post nos. 18 and 19 deflected. At 0.682 sec, the truck rolled 90 degrees. At this same time, the cables and attached posts began to rebound toward the traffic side. The vehicle came to rest on its right side at the bottom of the pit and laterally back from post no. 21, or approximately 41.3-m (135 ft-4 in.) downstream from the impact point, as shown in Figures 25 and 32.

9.3 Barrier Damage

Damage to the barrier was moderate, as shown in Figures 33 through 35. Barrier damage consisted mostly of damaged line posts, stretched cable, and soil failure. The maximum permanent set deflection of the upstream anchor was 45 mm (1.75 in.). Diagonal soil cracks, 406-mm (16-in.) long, and soil disturbance was found around the upstream anchor, as shown in Figure 33. Post no. 2 demonstrated twisting and bending at the base, resulting in weld failure on the tension side. Permanent set was not visible below grade at post no. 2. Post no. 3 illustrated only slight twisting and bending at the grade line. No damage or soil movement was noted for post nos. 4 through 11. Post no. 12 deflected 140 mm (5.5 in.) at the ground and the cables remained attached. Post no. 13 deflected 330 mm (13 in.) at the ground. The two lower cables released from post no. 13, with the respective hook bolts deformed. Post no. 14 was pushed

backward 254 mm (10 in.) at the ground and bent above the soil plate in the downstream direction. All three cables disengaged from post no. 14. Post no. 15 pulled completely out of the ground and was found at the bottom of the pit. Post no. 16 deflected 330 mm (13 in.) at the ground without any post bending. All three cables disengaged from post no. 16. Post no. 17 pulled completely out of the ground and was found 914-mm (36-in.) downstream and 1,219-mm (48-in.) laterally down the slope. Post no. 18 remained undamaged, but was pushed back 279 mm (11 in.) at the ground with the top cable unattached. Posts no. 19 and 20 rotated slightly, with deflections of 102 mm (4 in.) and 25 mm (1 in.) at the ground level, respectively. The remainder of the downstream posts showed no evidence of movement.

9.4 Vehicle Damage

The entire vehicle exterior and occupant compartment was severely damaged, as expected from a rollover on a steep slope. Vehicle damage is illustrated in Figure 36. Occupant compartment deformations for given locations are provided in Appendix F. It should be noted that the impact side showed the least amount of damage.

9.5 Occupant Risk Values

The longitudinal and lateral occupant impact velocities were determined to be 1.30 m/sec (4.27 ft/sec) and 2.69 m/sec (8.84 ft/sec), respectively. The maximum 0.010-sec average occupant ridedown decelerations in the longitudinal direction were 4.98 g's and -7.97 g's. The maximum 0.010-sec average occupant ridedown deceleration in the lateral direction was 15.19 g's. It is noted that even though the barrier system failed, the occupant impact velocities (OIV's) and occupant ridedown decelerations (ORD's) were within suggested limits provided in NCHRP Report No. 350. The results of the occupant risk, determined from the accelerometer data, are

summarized in Figure 25. Results are shown graphically in Appendix G. The results from the rate transducer are also shown graphically in Appendix G.

9.6 Load Cell and String Potentiometer Results

The forces transferred to the upstream end anchor and the corresponding anchor displacements measured the effectiveness of the driven steel post anchor. As previously discussed, load cells were installed parallel to each cable and at both ends of the system to monitor the loads transferred to the anchor through the cables. A string potentiometer was also installed at the upstream end to record dynamic displacement of the steel post anchor. The results of the load cell data is summarized in Table 16.

Table 16. Load Cell Results, Test CS-1

Load Type	Location	Maximum Cable Load		Time
		kN	kips	sec
Maximum Combined Cable Load	Upstream	108.4	24.36	3.03
	Downstream	90.7	20.39	3.03
Maximum Load in Top Cable	Upstream	38.9	8.74	3.03
	Downstream	29.2	6.57	3.02
Maximum Load in Middle Cable	Upstream	30.8	6.93	3.02
	Downstream	38.2	8.58	2.84
Maximum Load in Bottom Cable	Upstream	49.3	11.09	2.88
	Downstream	34.2	7.68	3.03

The recorded data for both sensor types is shown in Figures 37 through 41. The total cable load was summed and plotted, as shown in Figure 37. As expected, the upstream anchor produced the higher load pattern. The maximum forces acting on the upstream and downstream anchors were 108.4 kN (24.36 kips) and 90.7 kN (20.39 kips), respectively. The dissection of the total cable loading to the contribution of each individual cable is shown Figures 38 through 40.

The load pattern for the top cable mimics that of the total load. The upstream anchor sustained a maximum load of 38.9 kN (8.74 kips) and the downstream anchor showed a maximum load of 29.2 kN (6.57 kip). The performance of the middle cable deviated from the expected pattern. In this case, the downstream anchor sustained the higher force. The downstream anchor sustained maximum load of 38.2 kN (8.58 kips) and the upstream anchor showed a maximum load of 30.8 kN (6.93 kips). Although the magnitude of the difference is relatively minor, these results cannot be explained with complete certainty at this time. One possible explanation is the possibility the cable hung up on the upstream posts, thereby decreasing anchor load. Another potential explanation is that the load cell wires connected to the data recorder were accidentally switched. The bottom cable illustrated expected behavior, resulting in a higher force at the upstream anchor. The resultant force applied to the upstream and downstream anchors by the bottom cable were determined to be 49.3 kN (11.09 kips) and 34.2 kN (7.68 kips), respectively.

Anchor displacement was also of primary concern in the evaluation of the anchor design. The displacement time history of the upstream anchor is shown in Figure 41. The driven steel post anchor on the upstream end of the barrier yielded a maximum displacement of approximately 66 mm (2.6 in.) at 0.566 sec. This simulated design alternative also predicted a permanent set displacement of 44 mm (1.72 in.), which correlated with the testing results.

It is noted that the anchor force and displacement values were significantly lower than the 178-kN (40-kip) load and 152-mm (6-in.) displacement values of the anchor's design. The lower test values can be attributed to the barrier's inability to contain the vehicle. Premature vehicle rollover did not allow for the full tensile forces to develop in the cable system. The functionality of the cable guardrail as a flexible barrier system and the presence of intermediate posts also

contribute to the reduced anchor load and displacement values. Since the cable barrier was a longer system, a portion of the transferred energy was dissipated in the intermediate line posts.

9.7 Discussion

The analysis of the test results for test CS-1 showed that the three-cable guardrail installed adjacent to a 1.5H:1V slope did not contain nor redirect the vehicle with controlled lateral displacements of the guardrail since the vehicle penetrated the system and did not remain upright after collision with the guardrail. Once the impacting vehicle became completely airborne, vehicle stability became a concern. Furthermore, the large lateral forces produced by the cable generated a large destabilizing moment that acted on the vehicle. The added instability caused the vehicle to roll over the cables and come to rest on the passenger side at the bottom of the pit. There were no detached elements nor fragments which showed potential for penetrating the occupant compartment nor presented undue hazards to other traffic. Therefore, test CS-1 conducted on the three-cable guardrail was determined to be unacceptable according to the TL-3 safety performance criteria found in NCHRP Report No. 350 due to vehicle rollover and penetration behind the system.

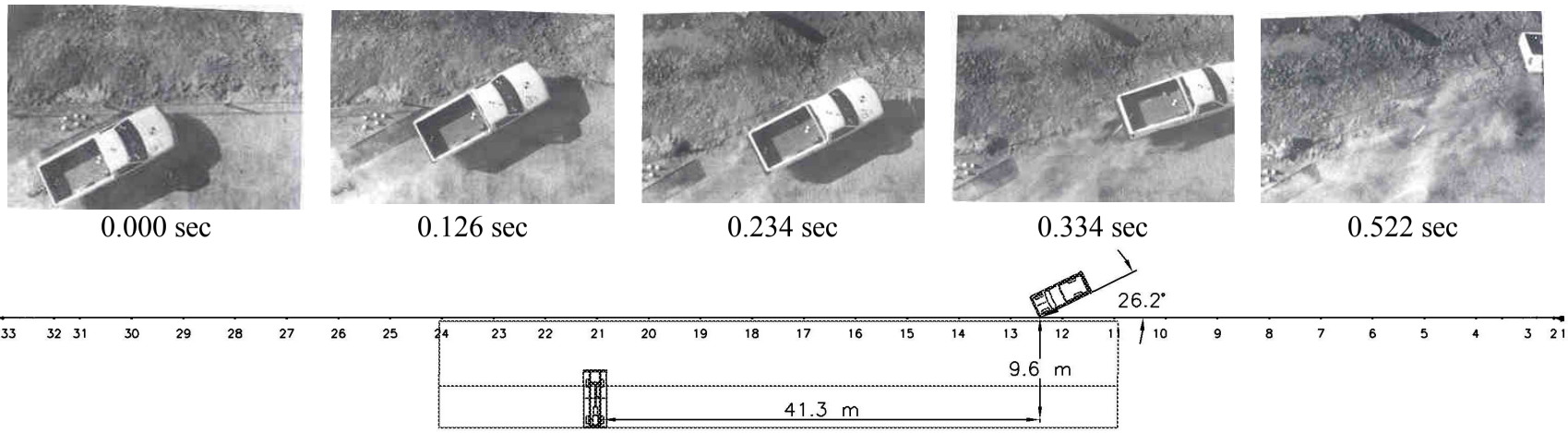

- Test Number CS-1
- Date 11/1/01
- Appurtenance ..... Three-cable guardrail installed adjacent to 1.5:1 slope
- Total Length ..... 147.83 m
- Wire Rope
  - Diameter ..... 19 mm
  - Top Mounting Height ..... 762 mm
  - Incremental Spacing ..... 76 mm
- Steel Posts
  - Post Nos. 1 and 34 ..... W152x37.2 by 2,438-mm long
  - Post Nos. 2 and 33 ..... S76x8.5 by 794-mm long with W152x13.4 by 1,829-mm long
  - Post Nos. 3 – 32 ..... S76x8.5 by 1,600-mm long
- Soil Type ..... Grading B – AASHTO M 147-65
- Vehicle Model ..... 1995 GMC 2500 ¾-ton pickup
  - Curb ..... 1,948 kg
  - Test Inertial ..... 2,034 kg
  - Gross Static ..... 2,034 kg
- Vehicle Speed
  - Impact ..... 98.1 km/h
  - Exit ..... NA
- Vehicle Angle
  - Impact ..... 26.2 deg
  - Exit ..... NA
- Vehicle Snagging ..... None
- Vehicle Pocketing ..... None
- Vehicle Stability ..... Unsatisfactory
- Occupant Ridedown Deceleration (10 msec avg.)
  - Longitudinal ..... 4.98 G's < 20 G's
  - Lateral (Not Required) ..... 15.19 G's
- Occupant Impact Velocity
  - Longitudinal ..... 1.30 m/s < 12 m/s
  - Lateral (Not Required) ..... 2.69 m/s
- Vehicle Damage ..... Extensive
  - TAD[28] ..... NA
  - SAE[29] ..... NA
- Vehicle Stopping Distance ..... 41.3 m downstream Located at bottom of slope
- Barrier Damage ..... Moderate
- Maximum Rail Deflections
  - Permanent Set ..... NA
  - Dynamic ..... NA

Figure 25. Summary of Test Results and Sequential Photographs, Test CS-1

0.000 sec

0.116 sec

0.198 sec

0.330 sec

0.384 sec

0.524 sec

0.590 sec

0.768 sec

Figure 26. Additional Sequential Photographs, Test CS-1

0.000 sec

0.122 sec

0.218 sec

0.334 sec

0.418 sec

0.458 sec

0.532 sec

0.650 sec

Figure 27. Additional Sequential Photographs, Test CS-1

0.000 sec

0.176 sec

0.222 sec

0.290 sec

0.326 sec

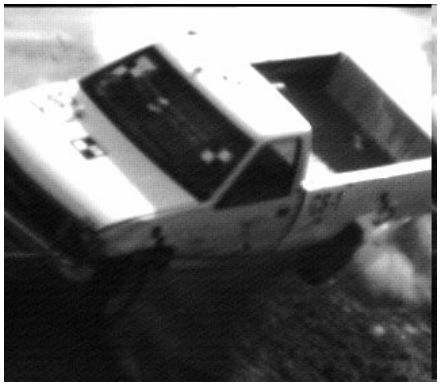

0.524 sec

Figure 28. Additional Sequential Photographs, Test CS-1

0.000 sec

0.200 sec

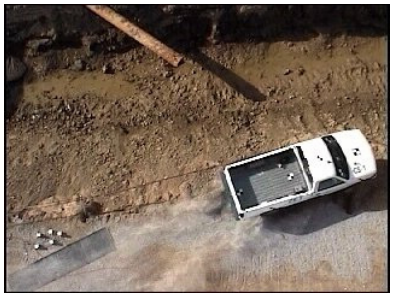

0.330 sec

0.400 sec

0.534 sec

0.701 sec

0.867 sec

Figure 29. Additional Sequential Photographs, Test CS-1

0.000 sec

0.300 sec

0.467 sec

0.734 sec

0.934 sec

1.335 sec

Figure 30. Documentary Photographs, Test CS-1

Figure 31. Impact Location, Test CS-1

Figure 32. Vehicle Final Position, Test CS-1

Figure 33. System Damage, Test CS-1

Figure 34. System Damage, Test CS-1

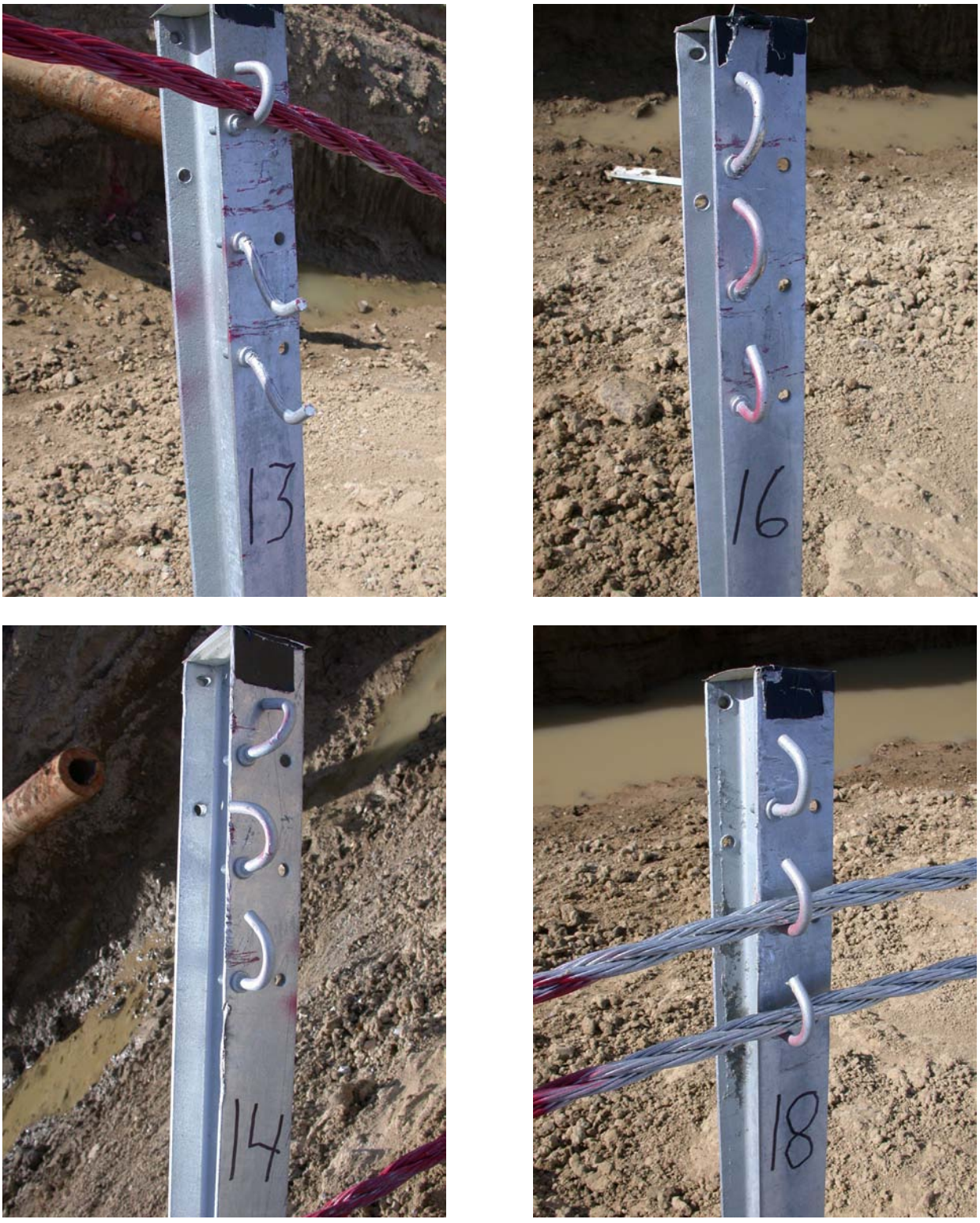

Figure 35. System Damage, Test CS-1

Figure 36. Vehicle Damage, Test CS-1

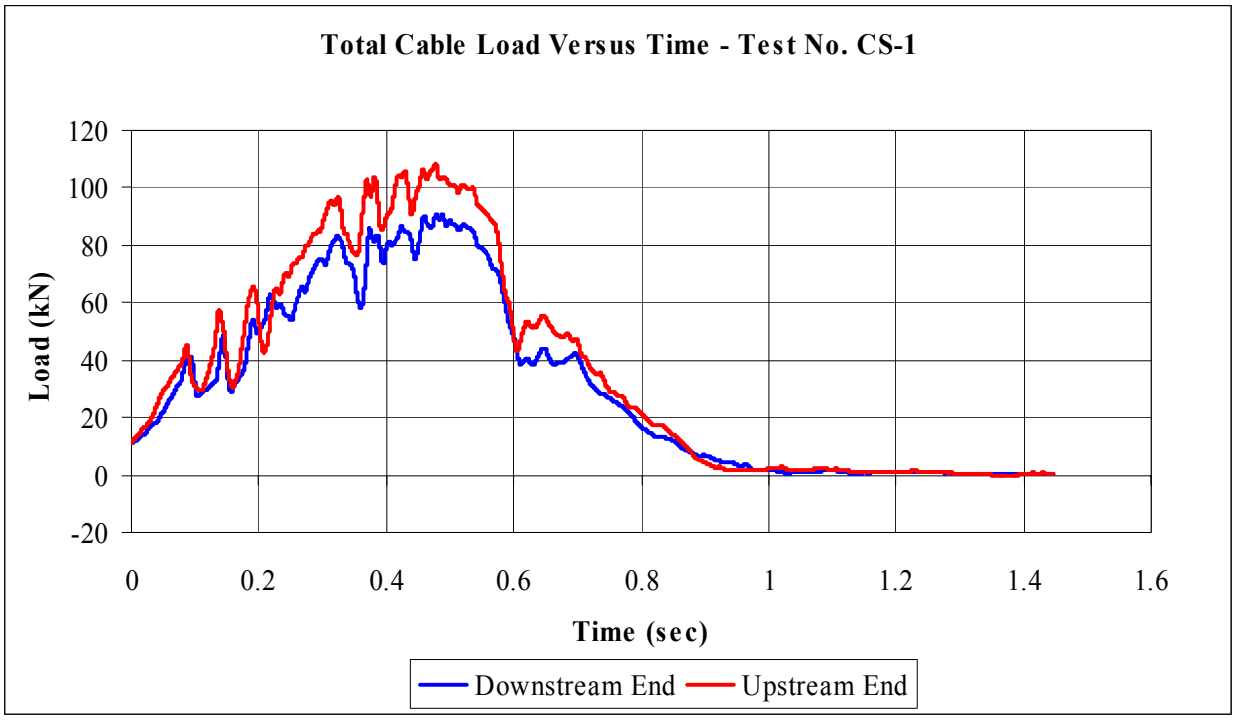

Figure 37. Force-Time History for Combined Cable Loading, Test CS-1

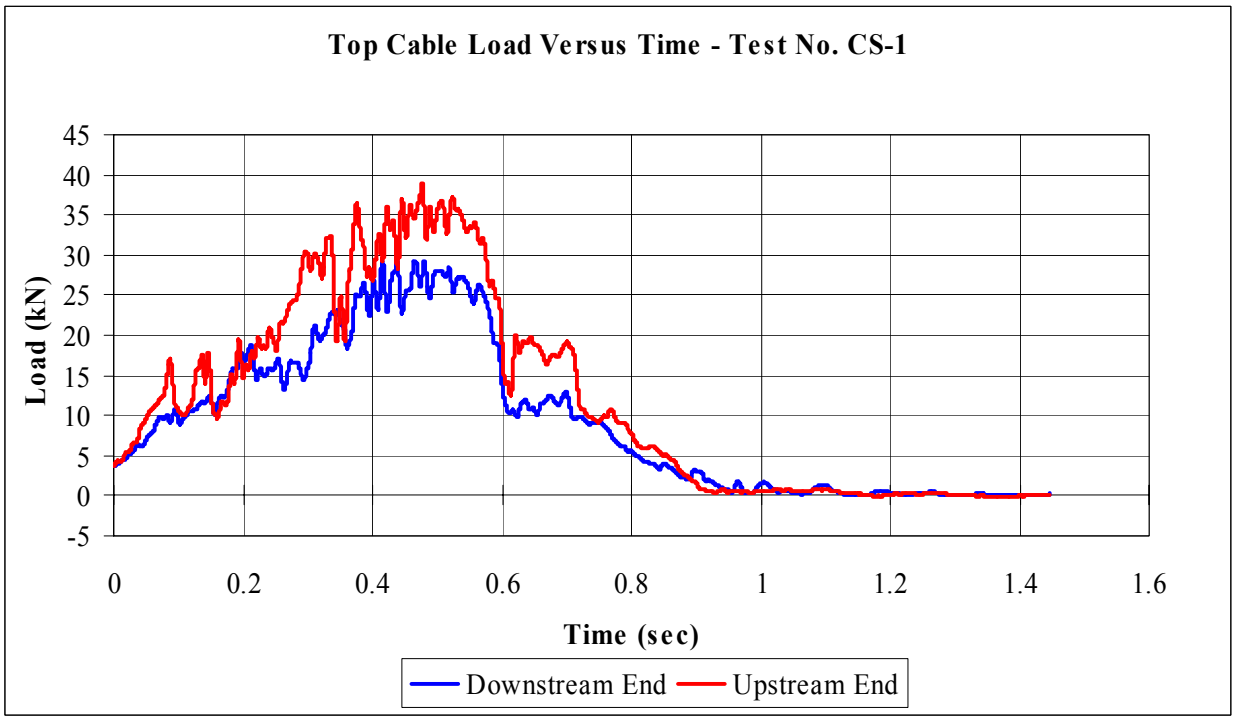

Figure 38. Force-Time History for Top Cable, Test CS-1

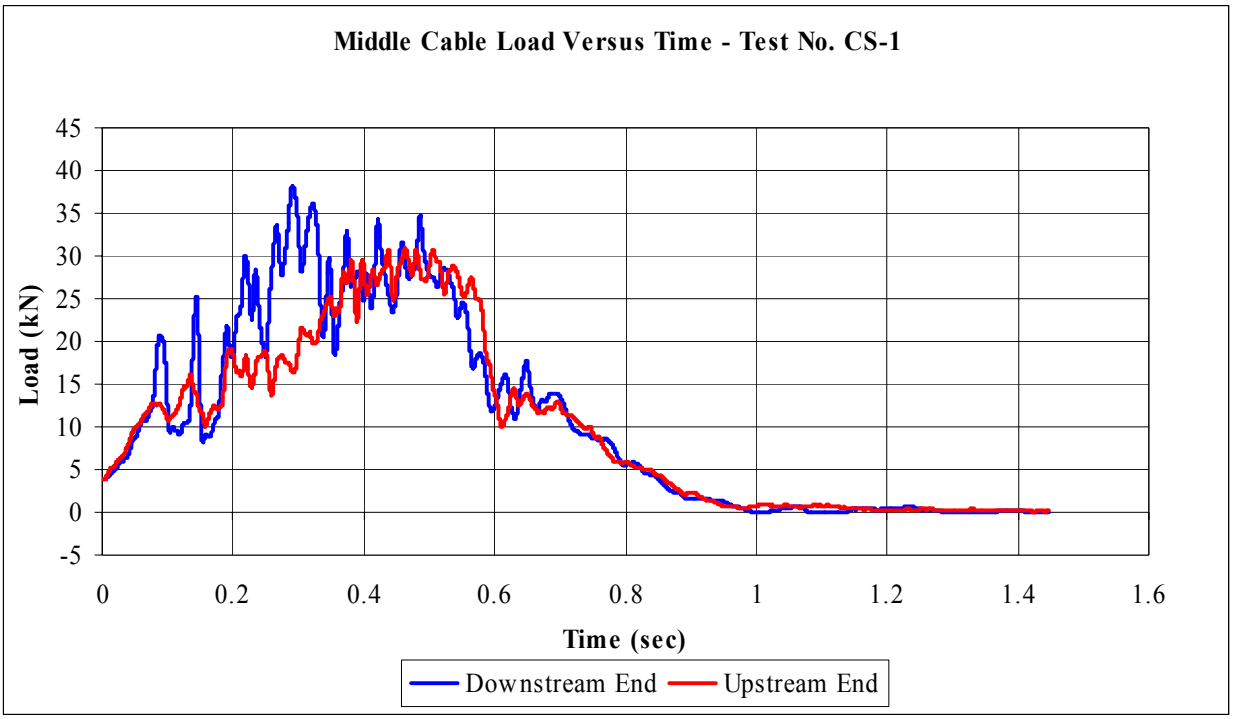

Figure 39. Force-Time History for Middle Cable, Test CS-1

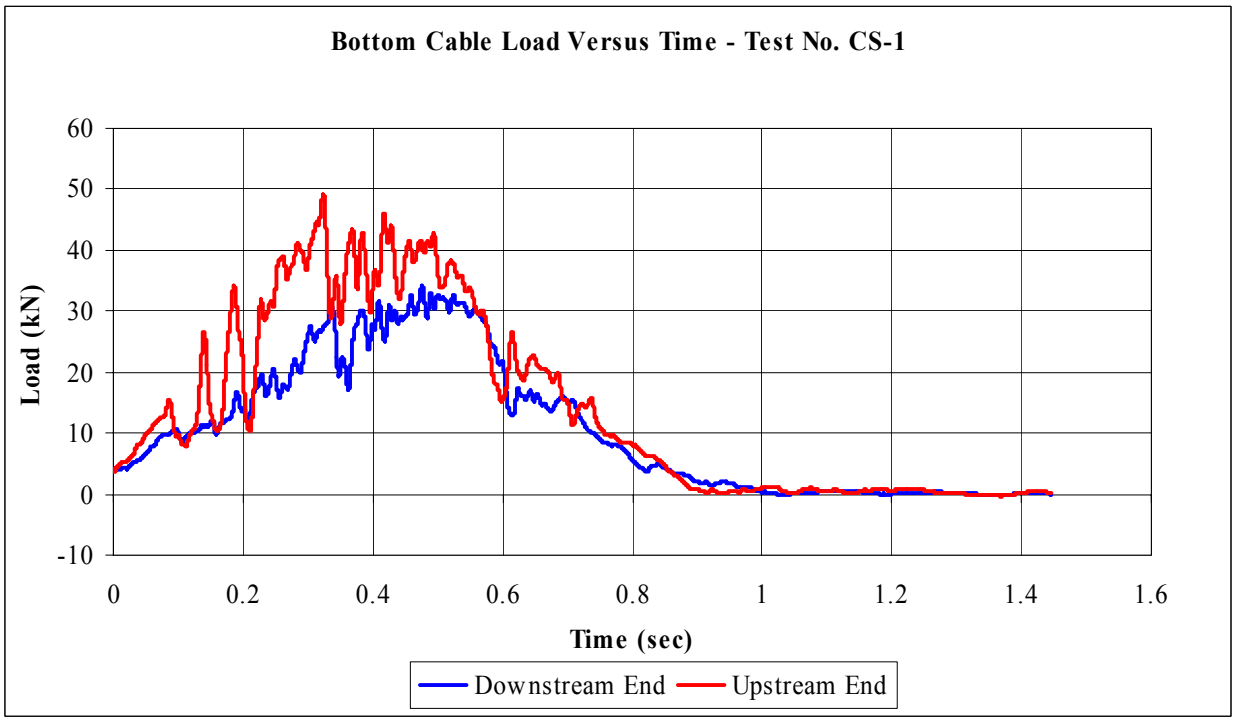

Figure 40. Force-Time History for Bottom Cable, Test CS-1

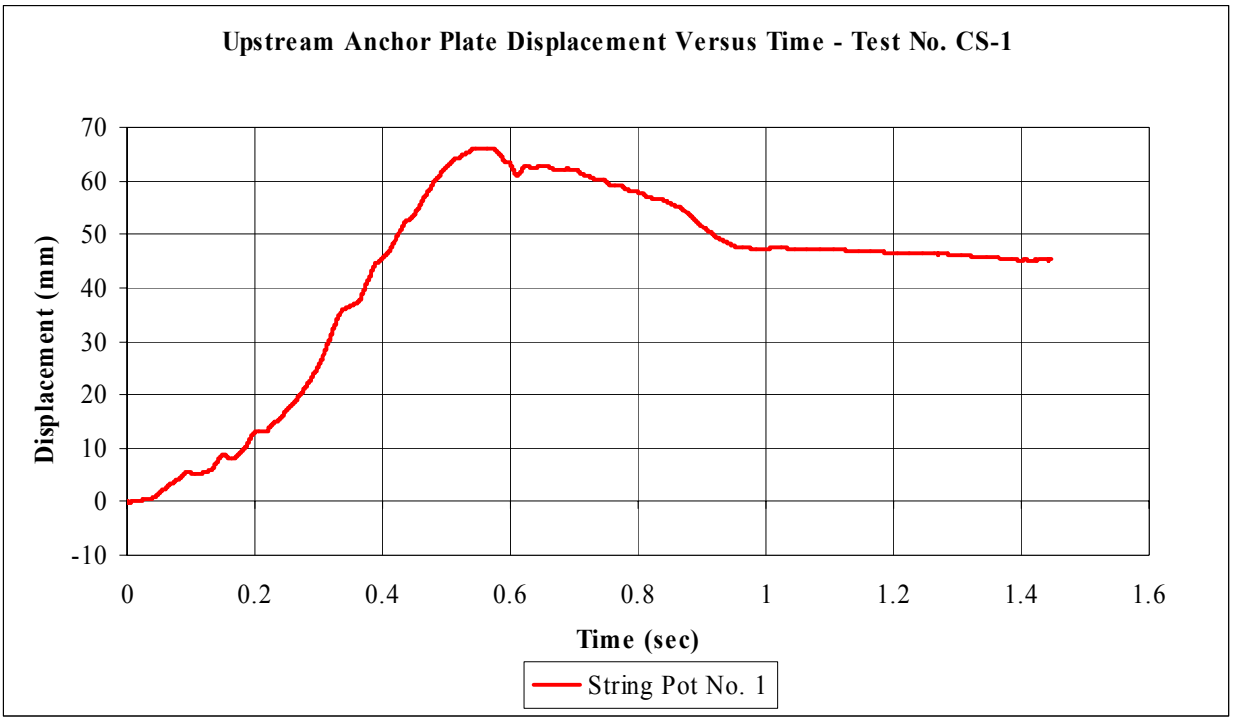

Figure 41. Displacement-Time History Plot for Upstream Anchor, Test CS-1

10 DISCUSSION AND DESIGN MODIFICATIONS

10.1 Discussion

The safety performance of a standard three-cable guardrail installed adjacent to a 1.5H:1V slope was examined through a full-scale crash test with a ¾-ton pickup truck. During this test, the vehicle became completely airborne as the cable barrier deformed and allowed it to encroach onto the steep slope. As a result, the front-impact side of the test vehicle dropped below the vehicle's center of gravity. The drop caused the re-directive forces applied by the cable system to be well below the c.g. of the vehicle. This induced a "tripping" effect and applied a roll moment on the vehicle. The destabilizing moment caused the vehicle to roll over the cables and come to rest at the bottom of the embankment.

Field performance of the three-cable barrier system was not accurately predicted by initial BARRIER VII modeling. Analysis of test CS-1 showed that the impacting vehicle did not travel down the sloped surface but remained relatively parallel to the flat surface traveled way. This lack of correlation between simulation and field testing required a review of the original parameters used to model the sloped surface. The basis for comparison between the BARRIER VII modeling and test no. CS-1 would be reverted back to the original flat-surface models.

Since the impacting vehicle was not successfully contained during test no. CS-1, a direct comparison between field testing and simulation could not be developed. However, from an analysis of barrier response in test no. CS-1, it was concluded that the resultant lateral forces in the cables had nearly achieved their peak values. Therefore, a correlation between the maximum lateral displacement of the barrier and the maximum longitudinal anchor displacement could be compared to the results of the flat-surface BARRIER VII model. Using the results of simulation run SP-2D, a comparative summary is detailed in Table 17.

Table 17. Comparison of Results from Test CS-1 to BARRIER VII

Means of Comparison	Test CS-1	BARRIER VII (Run SP-2D)
Maximum Lateral Barrier Displacment	2.59 m (8.5 ft)	4.19 m (13.75 ft)
Maximum Anchor Displacement	66 mm (2.6 in.)	104 mm (4.1 in.)
Maximum Anchor Force	108 kN (24.4 kips)	138 kN (31.0 kips)

This comparison suggested that the tested cable-guardrail system performed stiffer than the computer simulated models. The source of increased barrier stiffness was attributed to the increased stiffness of the steel post anchor system. Accordingly, the initial flat-surface BARRIER VII models were modified to account for an increased anchor stiffness of 1.5 times that of the original model. The revised simulation matrix and corresponding results are summarized in Tables 18 and 19, respectively.

Comparing the results of the revised simulation model SP-3D with those obtained in test no. CS-1, it was found that the maximum upstream anchor displacements and total upstream anchor forces were comparable to the model predicted values. These results are summarized in Table 20.

Table 18. Revised Barrier VII Simulation Matrix

Simulation	Description	Contact Interface
SP-3A	Driven Steel Post	Upper & Lower Cable
SP-3B	Driven Steel Post	Upper Cable
SP-3C	Driven Steel Post	Lower Cable
SP-3D	Driven Steel Post	Upper & Lower Cable (Three-Cable Model)

Table 19. BARRIER VII Results for Revised CS-1 Model

Simulation	T_{upper}		T_{lower}		δ_{upper}		δ_{lower}		$\delta_{lateral}$		Location		Time
	kN	kips	kN	kips	mm	in.	mm	in.	mm	in.	m	ft	sec
SP-3A	26.9	6.05	80.6	18.12	81	3.2	64	2.5	3693	145.4	61.72	202.5	0.630
SP-3B	71.6	16.11	4.0	0.90	71	2.8	53	2.1	4481	176.4	73.30	240.5	0.955
SP-3C	4.0	0.90	81.0	18.22	74	2.9	56	2.2	3998	157.4	62.94	206.5	0.675
SP-3D	19.9	4.48	101.2	22.74	89	3.5	69	2.7	3581	140.8	61.72	202.5	0.625

where: T_{upper} = Tensile Force in Upper Cable at Anchor
T_{lower} = Tensile Force in Lower Cable at Anchor
δ_{upper} = Displacement of Upper Anchor Connection
δ_{lower} = Displacement of Lower Anchor Connection
$\delta_{lateral}$ = Maximum Lateral Barrier Displacement
Location = Point of Maximum Lateral Displacement Measured from Upstream Anchor
Time = Time when Maximum Lateral Displacement Occurred

Table 20. Comparison of Results from Test CS-1 to Modified BARRIER VII Model

Means of Comparison	Test CS-1	BARRIER VII (Run SP-3D)
Maximum Anchor Displacement	66 mm (2.6 in.)	69 mm (2.7 in.)
Maximum Anchor Force	108 kN (24.4 k)	117 kN (26.2 k)

The relationship between the time tracked anchor displacements and resultant anchor forces are shown in Figures 42 and 43. Data from test no. CS-1 was filtered with a CFC Class 60 filter while the 200 Hz data from BARRIER VII was unfiltered. The sudden drop in the resultant anchor force shown in the plot from test no. CS-1 denotes the approximate time of vehicle rollover and the loss of barrier contact.

These results indicate that although BARRIER VII performs a two-dimensional analysis, it is still applicable to the evaluation of a three-dimensional barrier installed adjacent to a steep slope. BARRIER VII can predict with a high level of accuracy the extent of motion over the slope. Thus, BARRIER VII served as the basis of comparison between the standard design and any modified design presented.

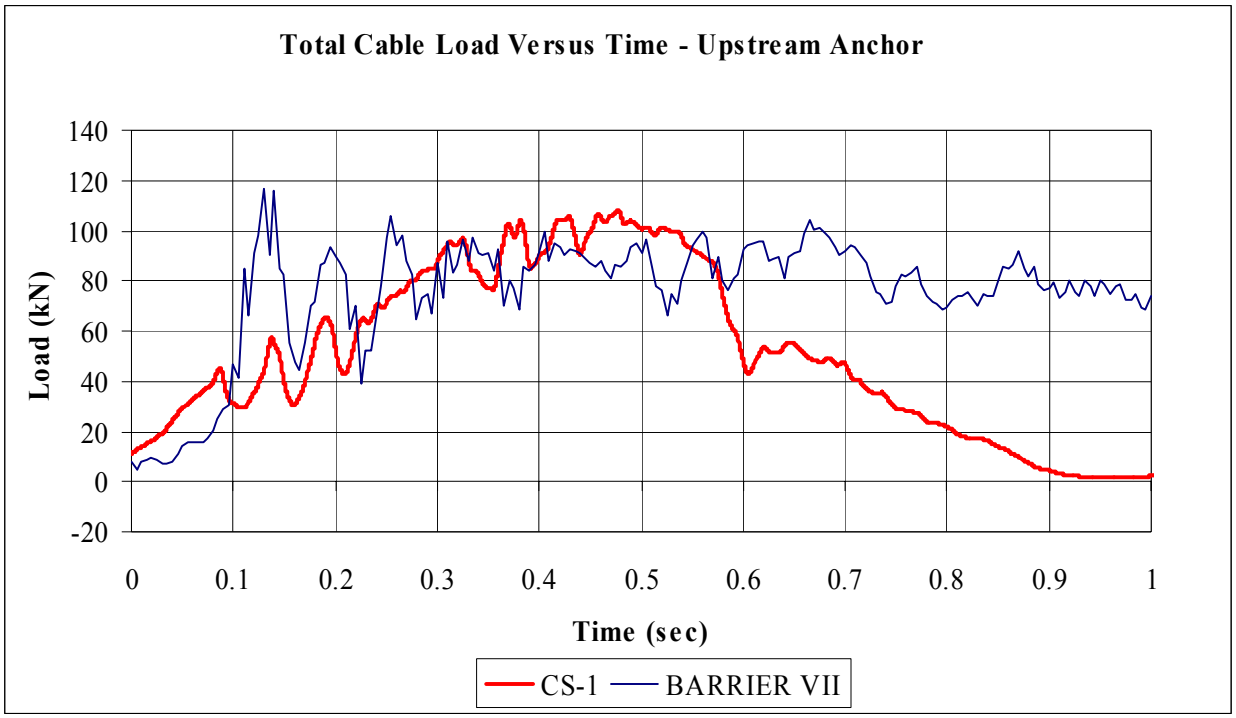

Figure 42. Force-Time History for Test CS-1 and BARRIER VII Model

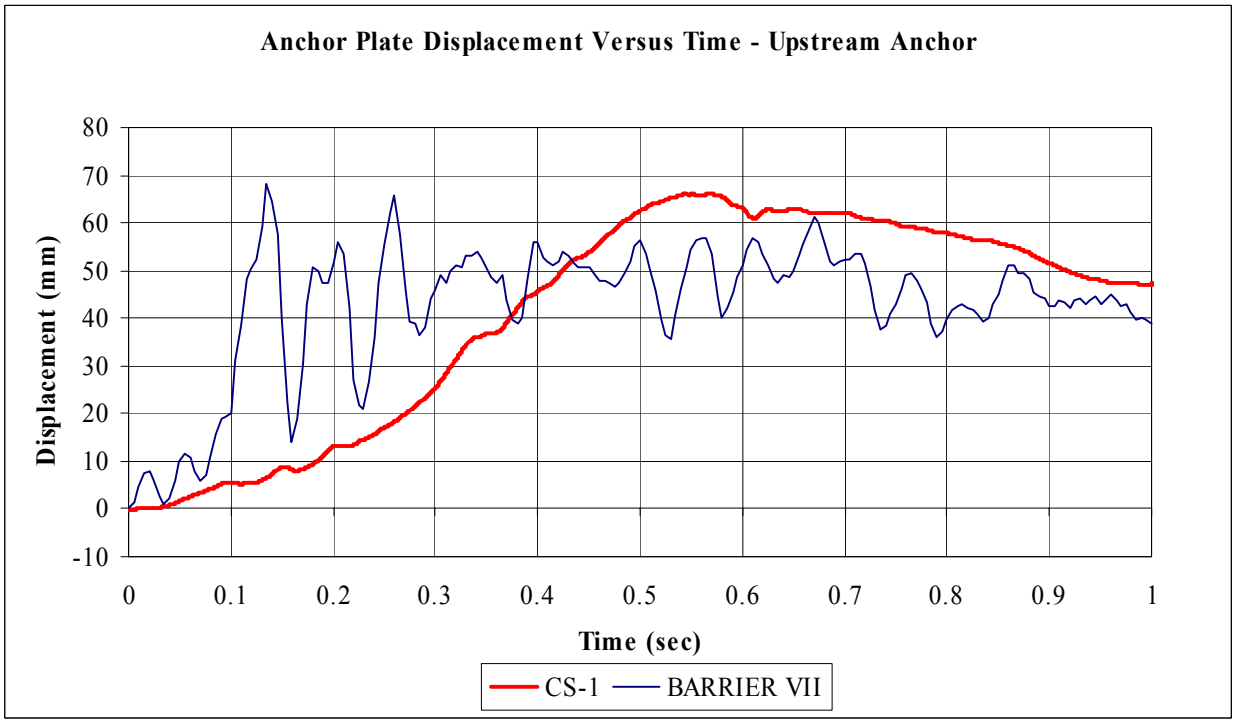

Figure 43. Displacement-Time History for Test CS-1 and BARRIER VII Model

10.2 Design Modifications

The poor performance observed in test no.CS-1 clearly warranted the need for design modifications to the three-cable guardrail system when placed adjacent to steep slopes. It was determined that the performance of the three-cable guardrail system (Design No. 1) could be significantly improved by reducing the lateral barrier deflection. In order to decrease the lateral deflections, the barrier stiffness was increased. This was accomplished by decreasing the post spacing to quarter-post spacing, thus reducing the post spacing from 4.88-m (16-ft) to 1.22-m (4-ft) centers. This increased barrier stiffness would reduce the potential for vehicle travel onto the embankment by decreasing lateral deflections. All other features of the three-cable guardrail system remained unchanged from its original configuration.

This modification, as well as the increased anchor stiffness derived from post-test analysis, was incorporated into a revised BARRIER VII finite element model. As previously discussed, it was determined that the flat-surface model more accurately portrayed the performance of the three-cable guardrail installed adjacent to a 1.5H:1V slope. The BARRIER VII simulation matrix and corresponding results are summarized in Tables 21 and 22, respectively.

Table 21. Revised BARRIER VII Simulation Matrix for Modified Post Spacing

Simulation	Description	Contact Interface
SP-4A	Driven Steel Post	Upper & Lower Cable
SP-4B	Driven Steel Post	Upper Cable
SP-4C	Driven Steel Post	Lower Cable
SP-4D	Driven Steel Post	Upper & Lower Cable (Three-Cable Model)

Table 22. BARRIER VII Results for Modified Post Spacing

Simulation	T_{upper}		T_{lower}		δ_{upper}		δ_{lower}		$\delta_{lateral}$		Location		Time
	kN	kips	kN	kips	mm	in.	mm	in.	mm	in.	m	ft	sec
SP-4A	25.8	5.79	42.0	9.45	51	2.0	38	1.5	2179	85.8	58.37	191.5	0.500
SP-4B	43.1	9.68	4.0	0.90	43	1.7	33	1.3	2139	84.2	58.06	190.5	0.480
SP-4C	4.0	0.90	53.7	12.08	33	1.3	25	1.0	1900	74.8	57.45	188.5	0.450
SP-4D	24.2	5.45	86.3	19.41	79	3.1	58	2.3	1588	62.5	56.24	184.5	0.380

where: T_{upper} = Tensile Force in Upper Cable at Anchor
T_{lower} = Tensile Force in Lower Cable at Anchor
δ_{upper} = Displacement of Upper Anchor Connection
δ_{lower} = Displacement of Lower Anchor Connection
$\delta_{lateral}$ = Maximum Lateral Barrier Displacement
Location = Point of Maximum Lateral Displacement Measured From Upstream Anchor
Time = Time when Maximum Lateral Displacement Occurred

Maintaining a comparative base, BARRIER VII model of simulation run SP-4D predicted a maximum lateral barrier deflection of 1,588 mm (62.5 in.). This reduced deflection corresponded to a reduction in potential vehicle c.g. drop to approximately 254 mm (10 in.). When evaluating the upper limit for the lateral deflection of the barrier, a 2,179-mm (85.8-in.) lateral displacement yields a potential vehicle c.g. drop of nearly 635 mm (25 in.). In order to further reduce this potential vehicle c.g, drop, an increased barrier offset from the slope breakpoint was evaluated. With the barrier system set 1,219-mm (4-ft) back from the slope breakpoint, the penetration of the vehicle onto the slope was approximately 914 mm (36 in.). Limiting the encroachment onto the slope limits the maximum vehicle c.g. drop. Considering only a 914-mm (36-in.) lateral penetration onto the slope, the potential vehicle c.g. drop is essentially limited to approximately 305 mm (12 in.). It is believed that this reduction in slope penetration will greatly reduce the propensity for the impacting vehicle c.g. to drop significantly and potentially cause vehicle rollover.

11 CONCLUSIONS AND RECOMMENDATIONS

A 147.82-m (485-ft) long, standard three-cable guardrail system installed adjacent to a 1.5H:1V slope was constructed and full-scale vehicle crash tested. A full-scale vehicle crash test was performed with a ¾-ton pickup on the standard three-cable guardrail system and was determined to be unacceptable according to the TL-3 criteria presented in NCHRP Report No. 350. Lateral vehicle penetration onto the slope allowed for the vehicle to become completely airborne, which resulted in the front-impact side of the vehicle dropping below the vehicle c.g. causing the redirective forces applied by the cable system to be significantly below the c.g. of the vehicle. This in turn, induced a "tripping" effect and applied a roll moment on the vehicle. The destabilizing moment caused the vehicle to roll over the cables and come to rest at the bottom of the embankment.

The poor performance observed in test no. CS-1 warranted design modifications. Consequently, additional computer simulation with BARRIER VII predicted that a reduced post spacing of 1.22 m (4 ft) showed an increase in the lateral barrier stiffness and consequently reduced lateral barrier deflections. The post-spacing reduction was coupled with an increased barrier offset from the slope breakpoint. Increasing the offset to 1.22 m (4 ft) would limit the penetration of the vehicle onto the slope and reduce the potential vehicle c.g. drop. It is believed that these design changes will significantly improve the safety performance of the standard three-cable guardrail system when installed adjacent to a 1.5H:1V slope. Therefore, it is recommended that a full-scale crash test be conducted on the modified cable barrier to verify its safety performance.

Furthermore, the redesign of the end terminal anchor was also a primary objective of the study. Three different alternatives were investigated and included: (1) a reinforced concrete

block that mimicked the existing design; (2) a reinforced drilled concrete shaft; and (3) a driven steel post. Although initial dynamic bogie testing and finite element modeling indicated that the driven steel post alternative was slightly out of the targeted range of the anchor force and displacement criterion and was the weakest design, the researchers believed that it would still a viable anchor design option and would be capable of developing the necessary anchor loads. During full-scale crash testing, the steel post anchor design perform as intended and provided adequate cable tension for the barrier system for resisting the large lateral forces developed in the cable barrier.

The success of the steel post anchor alternative indirectly proved that both the reduced concrete block and drilled concrete shaft anchor options will produce similar satisfactory results and that all three anchor alternatives present a cost-effective alternative to the current anchor system. However, since the impacting vehicle was not contained nor smoothly redirected, it is recommended that the new anchor alternatives continue to be evaluated in the future. Similarly, the performance of the anchor alternatives when impacted near the terminal end can only be evaluated and verified through the use of full-scale crash testing and should be undertaken prior to the implementation of any anchor alternative.

12 REFERENCES

1. Griffen, J., "Highway Safety Barrier System Will Cut Accident Rates", *Better Roads*, February 2002.

2. Sposito, B. and Johnson, S., *Three-Cable Median Barrier Final Report*, Oregon Department of Transportation, Research Report No. OR-RD-99-03, July 1998.

3. Graham, M.D., Burnett, W.C., Gibson, J.L., and Freer, R.H., *New Highway Barriers: The Practical Application of Theoretical Design*, Highway Research Record No. 174, 1967.

4. Whitmore, J.L., Picciocca, R.G., and Snyder, W.A., *Testing of Highway Barriers and Other Safety Accessories*, Research Report No. 38, Engineering Research and Development Bureau, New York State Department of Transportation, December 1976.

5. Ross, H.E., Sicking, D.L., Zimmer, R.A., and Michie, J.D., *Recommended Procedures for the Safety Performance Evaluation of Highway Features*, National Cooperative Research Program (NCHRP) Report No. 350, Transporation Research Board, Washington, D.C., 1993.

6. Coon, B.A., Faller, R.K., and Reid, J.D., *Cable Barrier Literature Review*, Final Report to the Midwest State's Regional Pooled Fund Program, Transportation Research Report No. TRP-03-118-02, Midwest Roadside Safety Facility, University of Nebraska-Lincoln, Lincoln, Nebraska, July 10, 2002.

7. Smith, P., *Development of a Three-Cable Guide Rail System and Other Guide Rail Tests, 1967 –1968*, Ontario Department of Highways, Report No. RR157, March 1970.

8. Phillips, R.G., Tyrell, A.B., Bryden, J.E., and Fortuniewicz, J.S., *Cable Guiderail Breakaway Terminal Ends*, Federal Highway Administration, Report No. FHWA/NY/RR-90/148, 1990.

9. Kenyon, W.D., *Cable Guardrail Tension*, Federal Highway Administration, Report No. FHWA/NY/RR-85/124, July 1985.

10. Yang, W., Bruno, N.J. and Kenyon, W.D., *Tension Loss in Cable Guiderail*, Special Report No. 104, Engineering Research and Development Bureau, New York State Department of Transportation, Albany, New York, July 1992.

11. Bateman, M.B., Howard, I.C., Johnson, A.R., and Walton, J.M., *A Model of the Performance of a Roadway Safety Fence and Its Use for Design*, Transportation Research Record 1647, 1998.

12. Bateman, M.B., Howard, I.C., Johnson, A.R., and Walton, J.M., "Computer Simulation of the Impact Performance of a Wire Rope Safety Fence", *International Journal of Impact Engineering*, Volume 25, 2001.

13. SwRI, *Test No. MSD-2*, SwRI Project No. 06-8299-01, Prepared for the Federal Highway Administration, January 1989.

14. SwRI, *Test No. MSD-2A*, SwRI Project No. 06-8299-01, Prepared for the Federal Highway Administration, January 1989.

15. SwRI, *Test No. MSD-4*, SwRI Project No. 06-8299-01, Prepared for the Federal Highway Administration, January 1989.

16. SwRI, *Crash Test Evaluation of A Franklin Post and Cable Guide System*, Test No. SD-1, SwRI Project 06-2696-001, Prepared for the South Dakota Department of Transportation, August 1989.

17. SwRI, *Crash Test Evaluation of A Franklin Post and Cable Guide System*, Test No. SD-2, SwRI Project 06-2696-001, Prepared for the South Dakota Department of Transportation, August 1989.

18. SwRI, *Crash Test Evaluation of A Franklin Post and Cable Guide System*, Test No. SD-3, SwRI Project 06-2696-001, Prepared for the South Dakota Department of Transportation, August 1989.

19. Mak, K.K. and Menges, W.C.*, Crash Testing and Evaluation of G1 Wire Rope Guardrail System*, Research Study No. RF 471470, Prepared for the Federal Highway Administration, Texas Transportation Institute, The Texas A&M University System, College Station, TX, December 1994.

20. Bullard, D.L. Jr. and Menges, W.L., *Crash Testing and Evaluation of the WSDOT Three Strand Cable Rail System*, Research Report No. 270687-WDT2, Prepared for the Washington State Department of Transportation, Texas Transportation Institute, The Texas A&M University System, College Station, TX, June 1996.

21. Buth, C.E., Menges, W.L., and Williams, W.F., *NCHRP Report 350 Test 3-34 of the New York Cable Rail Terminal*, Test Report No. 404211-6, Prepared for the Federal Highway Administration, Texas Transportation Institute, The Texas A&M University System, College Station, TX, October 1998.

22. Bullard, D.L., Menges, W.L., Buth, C.E., and Schoeneman, S.K., *NCHRP Report 350 Test 3-11 of the Washington Three-Strand Cable Barrier with New York Cable Terminal*, Test Report No. 404211-8, Prepared for the Federal Highway Administration, Texas Transportation Institute, The Texas A&M University System, College Station, TX, March 2000.

23. *Roadside Design Guide*, American Association of State Highway and Transportation Officials (AASHTO), Washington, D.C., January 1996.

24. Butler, R.R., Documentation of Internal Testing, Florida Wire and Cable, To D.L. Sicking, Midwest Roadside Safety Facility, June 2, 2000.

25. Powell, G.H., *BARRIER VII: A Computer Program for Evaluation of Automobile Barrier Systems*, Prepared for Federal Highway Administration, Report No. FHWA RD-73-51, April 1973.

26. Fating, R.M. and Reid, J.D., *Dynamic Impact Testing of S75x8.5 Steel Posts (Cable Barrier Posts),* Transportation Report No. TRP-03-117-07, Midwest Roadside Safety Facility, University of Nebraska-Lincoln, Lincoln, Nebraska, June 2002.

27. Hinch, J., Yang, T-L, and Owings, R., *Guidance Systems for Vehicle Testing*, ENSCO, Inc., Springfield, Virginia, 1986.

28. *Vehicle Damage Scale for Traffic Investigators*, Second Edition, Technical Bulletin No. 1, Traffic Accident Data (TAD) Project, National Safety Council, Chicago, Illinois, 1971.

29. *Collision Deformation Classification – Recommended Practice J224 March 1980*, Handbook Volume 4, Society of Automotive Engineers (SAE), Warrendale, Pennsylvania, 1985.

13 APPENDICES

APPENDIX A

Existing Anchor Design and Proposed Design Options

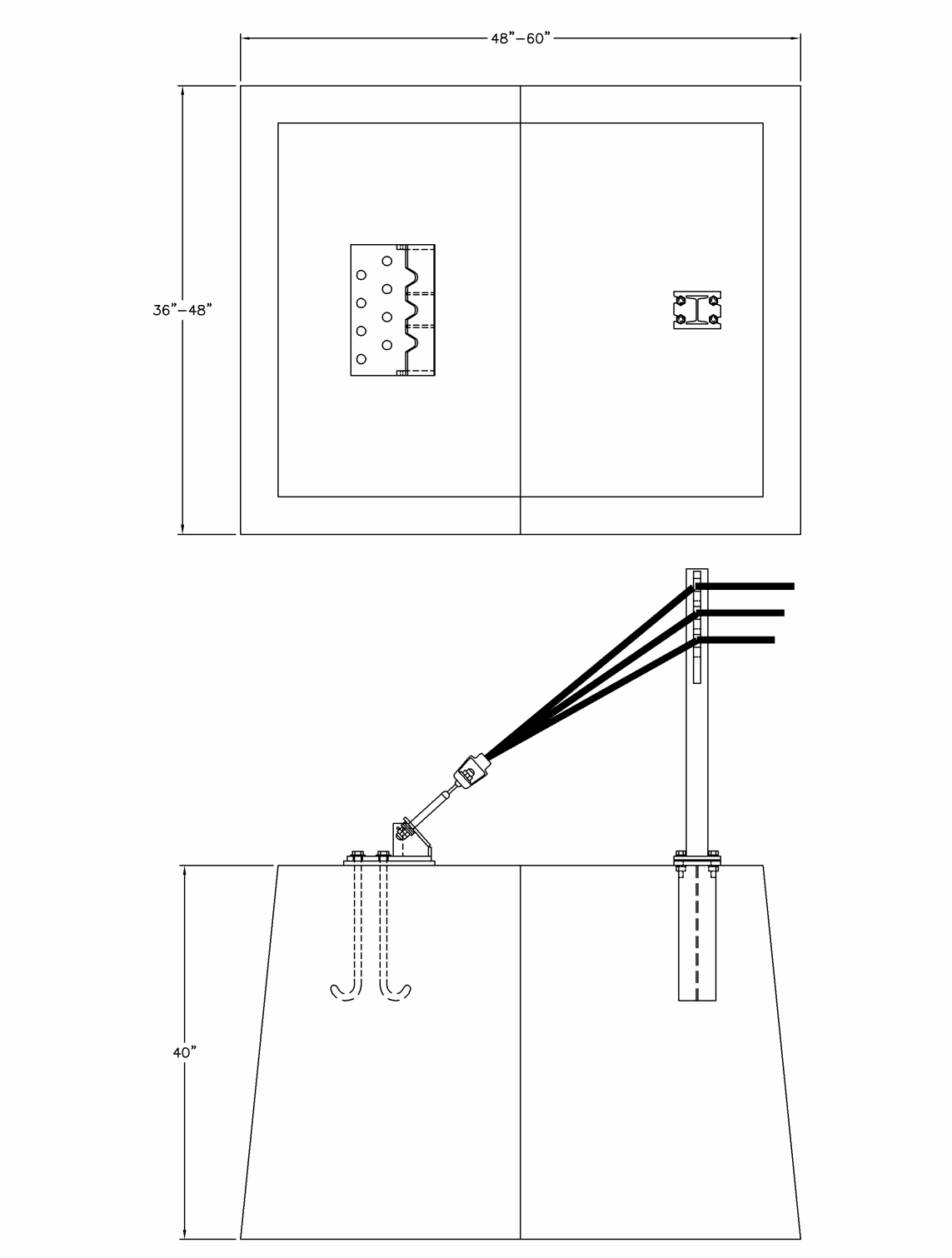

Figure A-1. Existing Anchor Design (English)

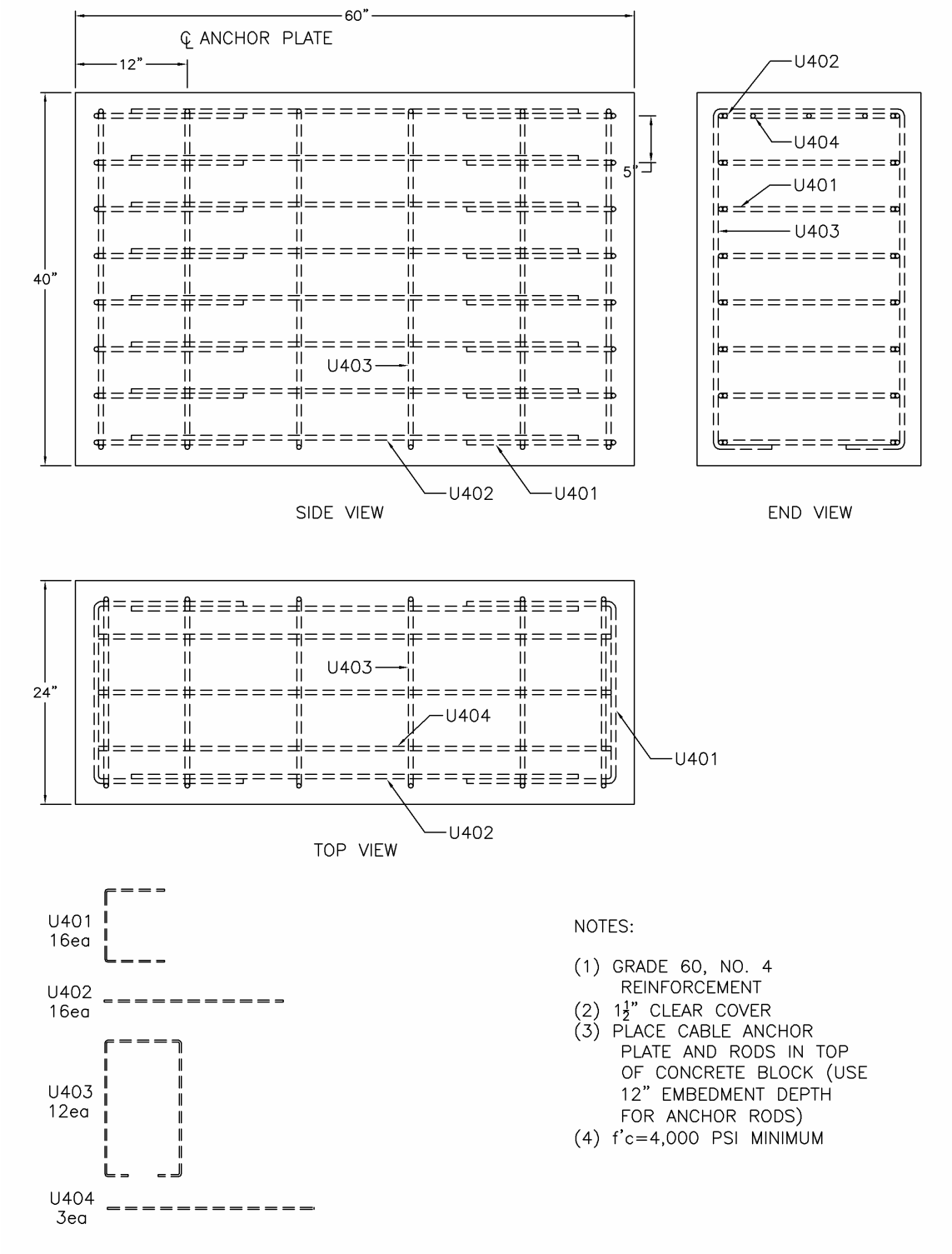

Figure A-2. Design Option No. 1 – Reinforced Concrete Block (English)

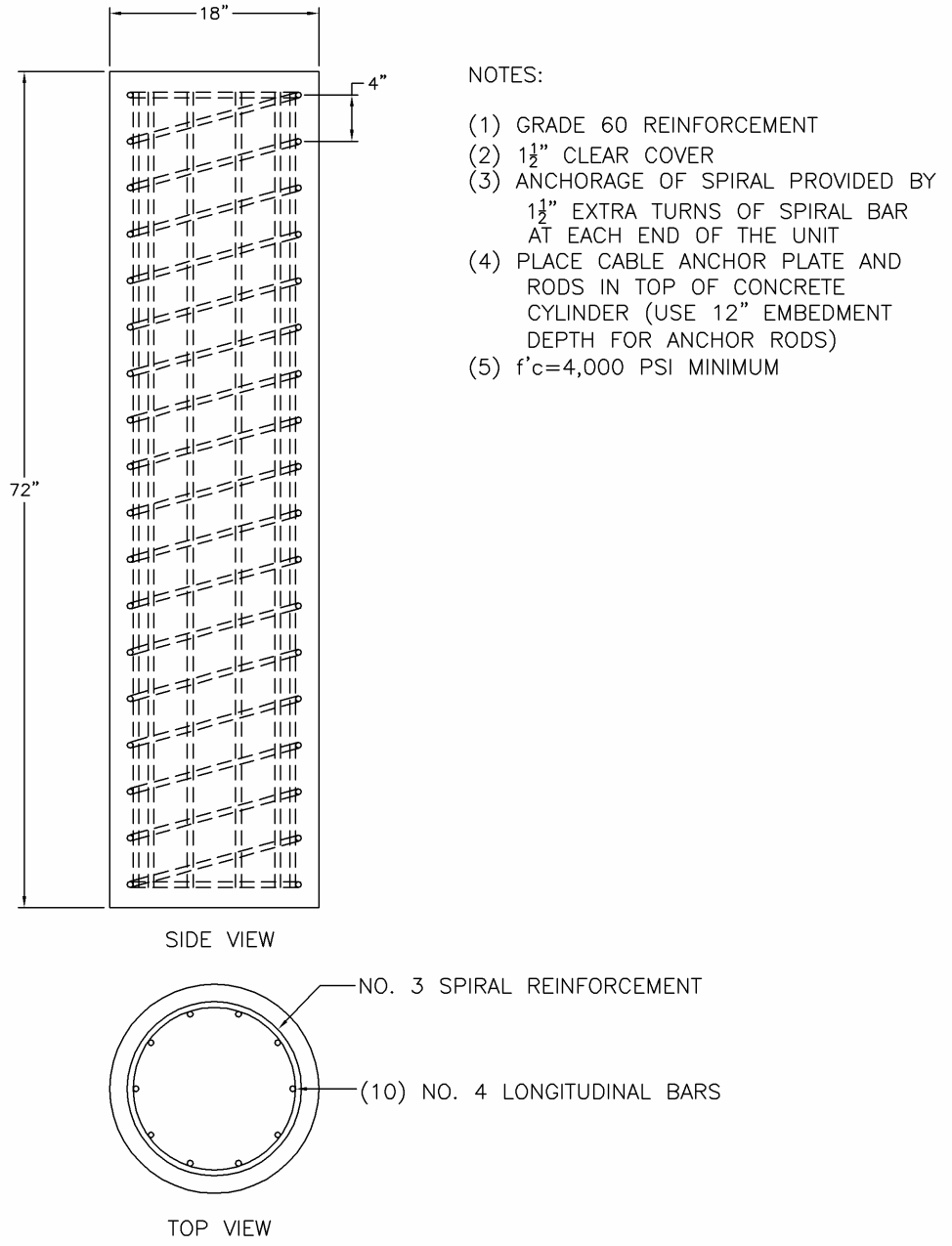

Figure A-3. Design Option No. 2 – Drilled Concrete Shaft (English)

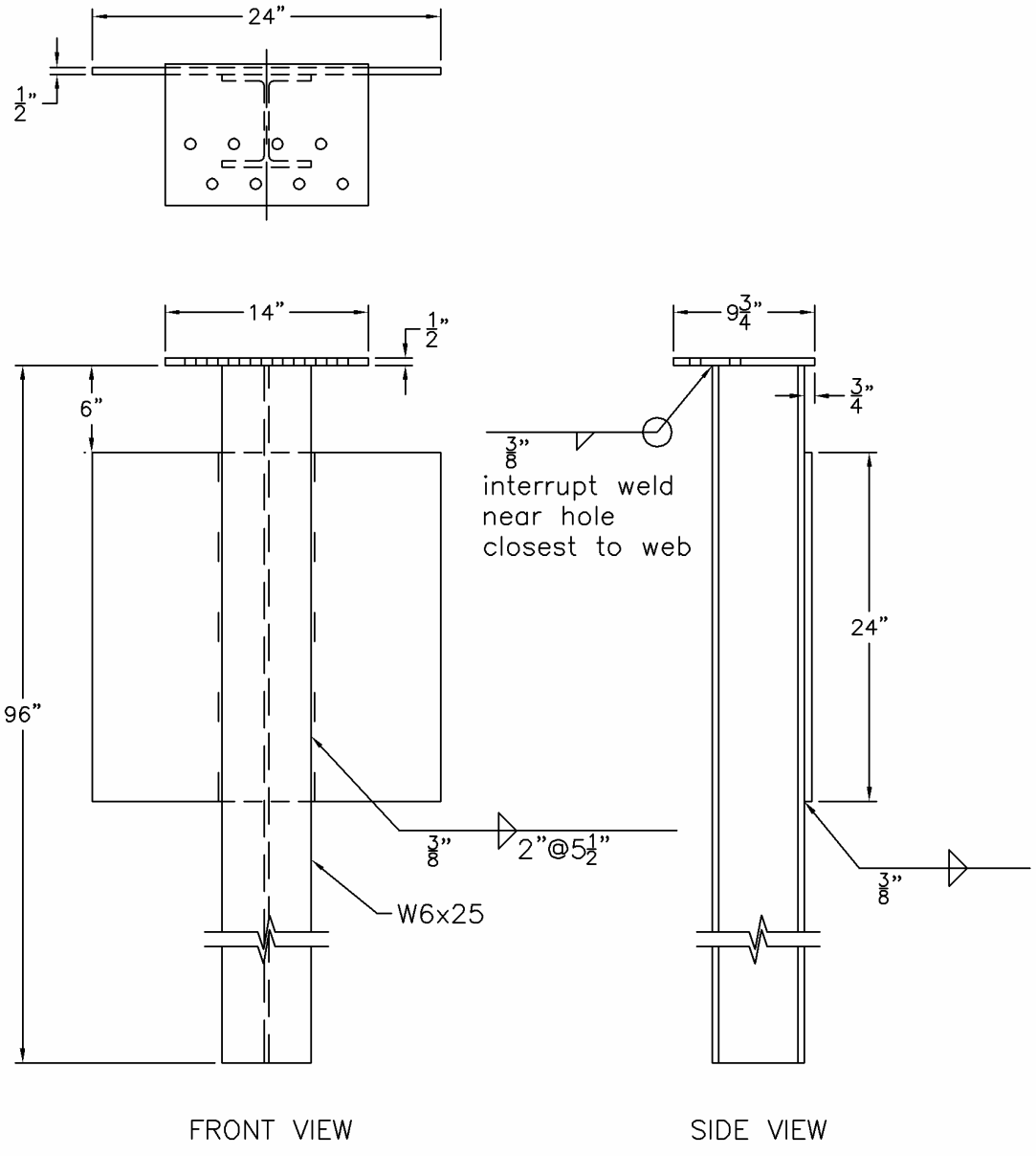

Figure A-4. Design Option No. 3 – Driven Steel Post (English)

APPENDIX B

BARRIER VII Computer Model

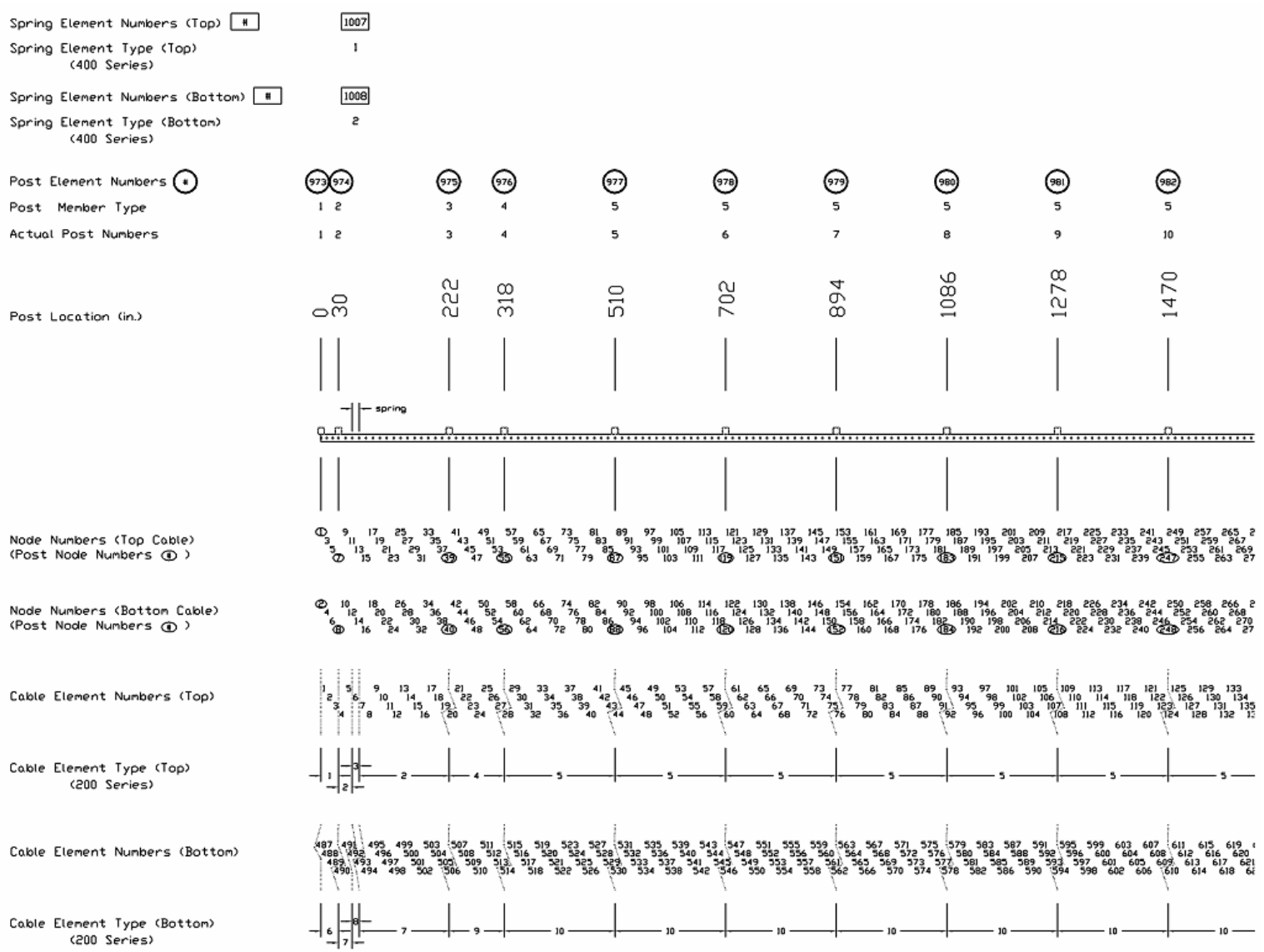

Figure B-1. Model of Three-Cable Guardrail System

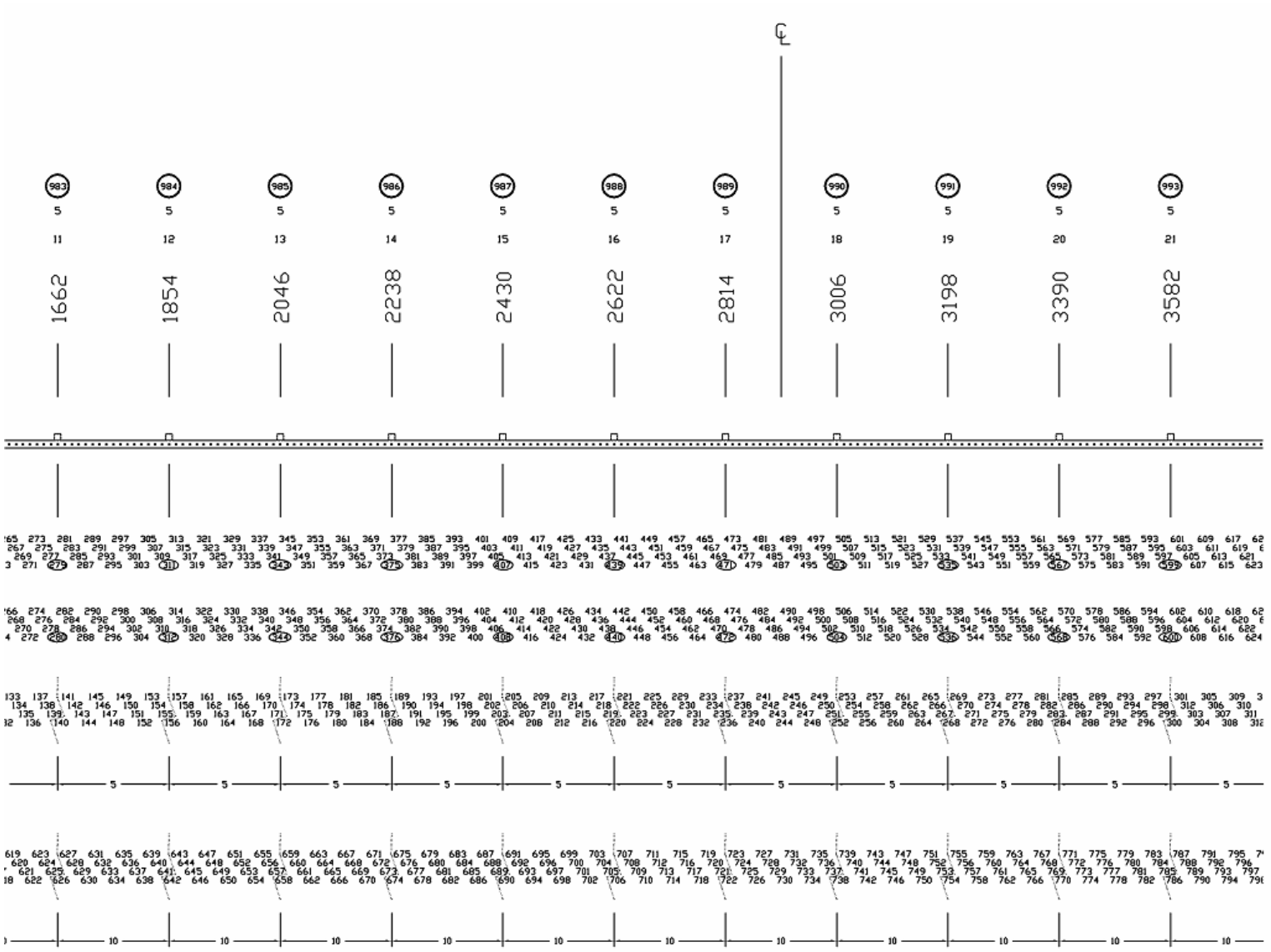

Figure B-2. Model of Three-Cable Guardrail System (Continued)

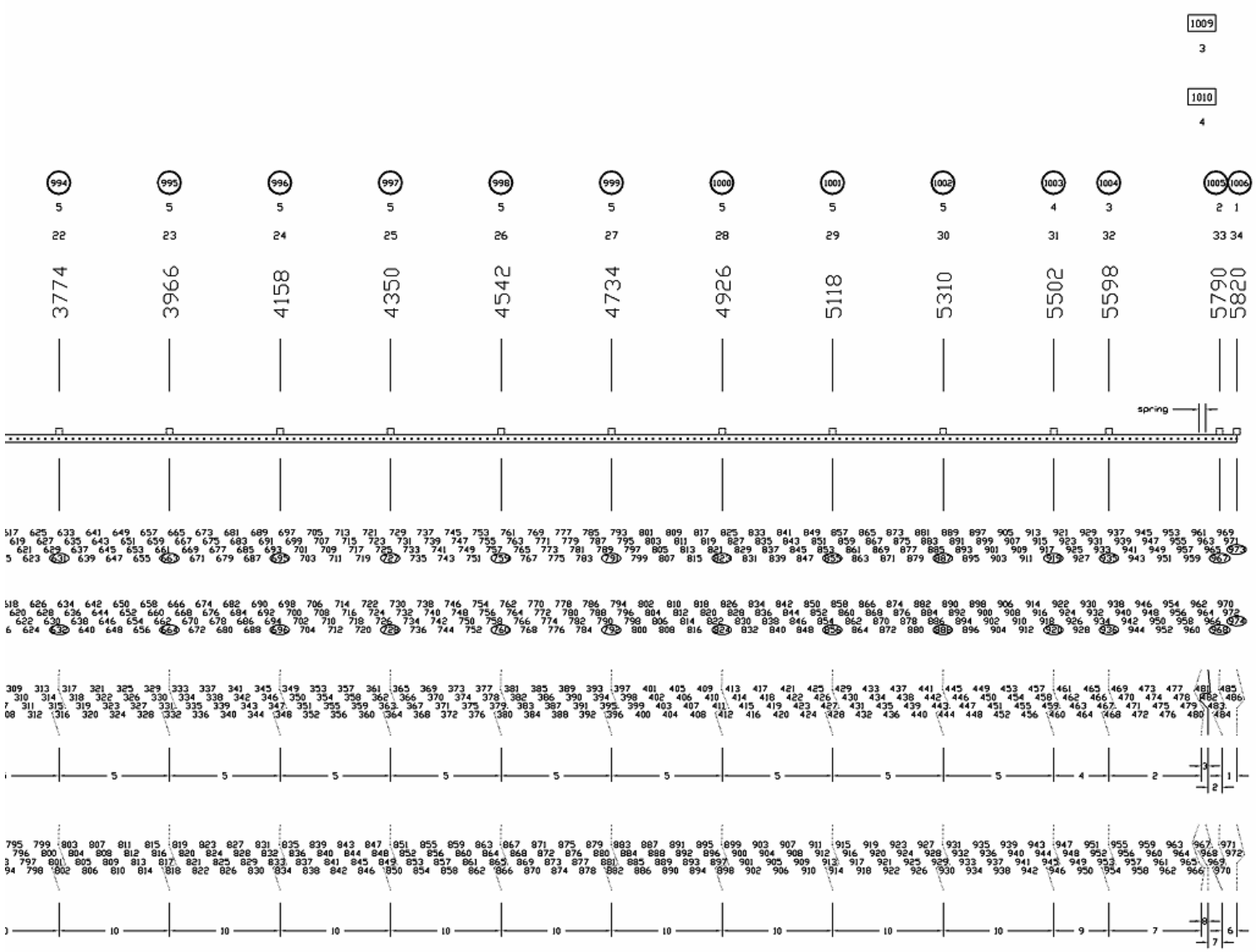

Figure B-3. Model of Three-Cable Guardrail System (Continued)

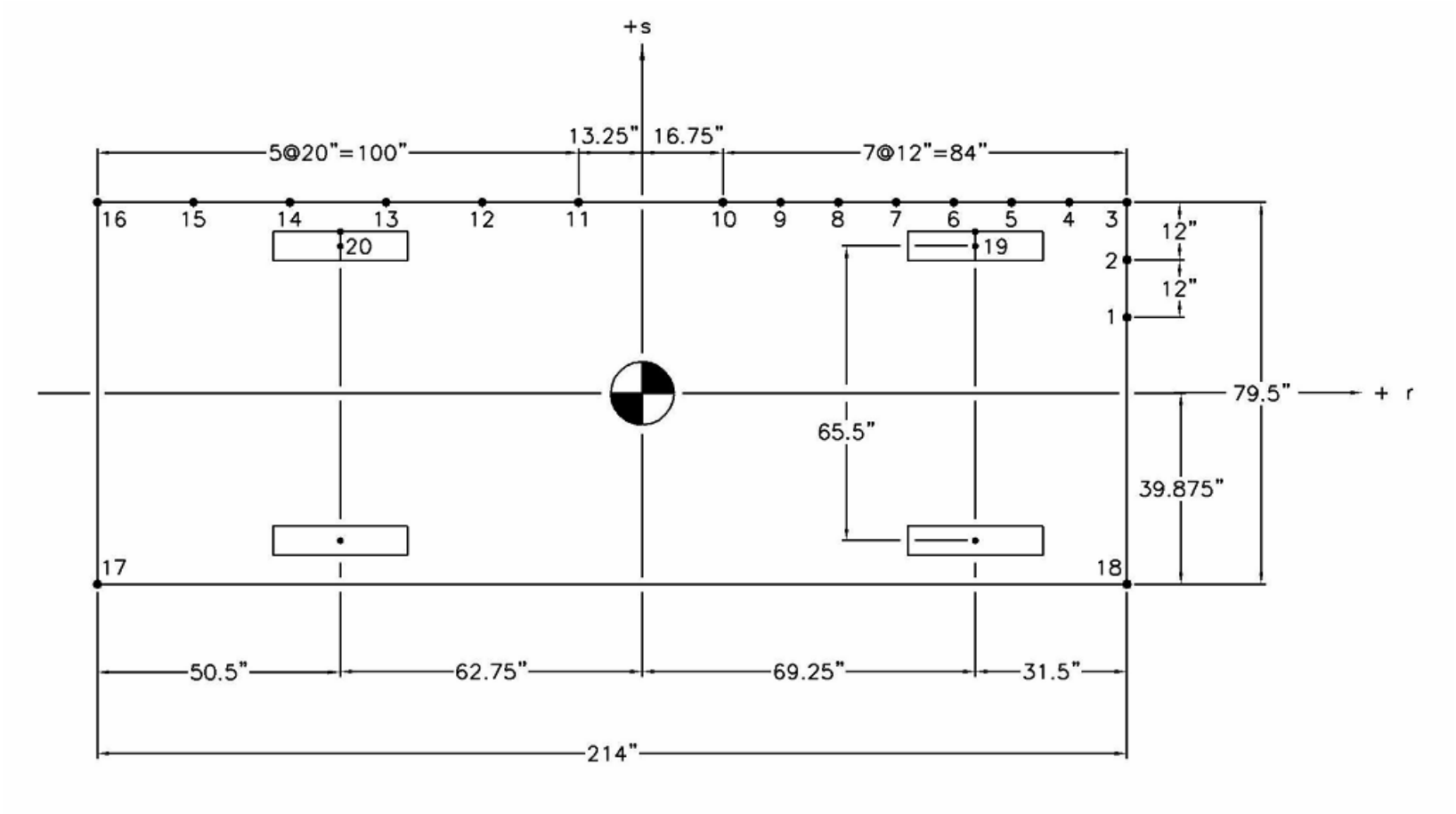

Figure B-4. Idealized Finite Element, 2 Dimensional Vehicle Model (2000P Pickup)

APPENDIX C

Typical BARRIER VII Input File

The sample input file for BARRIER VII included in Appendix C corresponds to the simulation SP-1A.

```
Three-Strand Cable Barrier on Slopes - SP-1A.dat - Pickup Truck 2000kg/100kph/25 degrees
  974   24   18    2 1006   56    3    0
    0.0001    0.0001     1.000  500    0       1.0
   10   50   50   50   50   50   10
    1      0.00      0.00
    2      0.00      0.00
    7     30.00      0.00
    8     30.00      0.00
   11     54.00      0.00
   12     54.00      0.00
   13     66.00      0.00
   14     66.00      0.00
   39    222.00      0.00
   40    222.00      0.00
   55    318.00      0.00
   56    318.00      0.00
  919   5502.00      0.00
  920   5502.00      0.00
  935   5598.00      0.00
  936   5598.00      0.00
  961   5754.00      0.00
  962   5754.00      0.00
  963   5766.00      0.00
  964   5766.00      0.00
  967   5790.00      0.00
  968   5790.00      0.00
  973   5820.00      0.00
  974   5820.00      0.00
    1    7    2    2
    2    8    2    2
    7   11    1    2
    8   12    1    2
   13   39   12    2
   14   40   12    2
   39   55    7    2
   40   56    7    2
   55  919  431    2
   56  920  431    2
  919  935    7    2
  920  936    7    2
  935  961   12    2
  936  962   12    2
  963  967    1    2
  964  968    1    2
  967  973    2    2
  968  974    2    2
    1  487      0.40
  973  971  969  967  965  963  961  959  957  955
  953  951  949  947  945  943  941  939  937  935
  933  931  929  927  925  923  921  919  917  915
  913  911  909  907  905  903  901  899  897  895
  893  891  889  887  885  883  881  879  877  875
  873  871  869  867  865  863  861  859  857  855
  853  851  849  847  845  843  841  839  837  835
  833  831  829  827  825  823  821  819  817  815
  813  811  809  807  805  803  801  799  797  795
  793  791  789  787  785  783  781  779  777  775
  773  771  769  767  765  763  761  759  757  755
  753  751  749  747  745  743  741  739  737  735
  733  731  729  727  725  723  721  719  717  715
  713  711  709  707  705  703  701  699  697  695
  693  691  689  687  685  683  681  679  677  675
  673  671  669  667  665  663  661  659  657  655
  653  651  649  647  645  643  641  639  637  635
  633  631  629  627  625  623  621  619  617  615
  613  611  609  607  605  603  601  599  597  595
  593  591  589  587  585  583  581  579  577  575
  573  571  569  567  565  563  561  559  557  555
  553  551  549  547  545  543  541  539  537  535
```

```
533  531  529  527  525  523  521  519  517  515
513  511  509  507  505  503  501  499  497  495
493  491  489  487  485  483  481  479  477  475
473  471  469  467  465  463  461  459  457  455
453  451  449  447  445  443  441  439  437  435
433  431  429  427  425  423  421  419  417  415
413  411  409  407  405  403  401  399  397  395
393  391  389  387  385  383  381  379  377  375
373  371  369  367  365  363  361  359  357  355
353  351  349  347  345  343  341  339  337  335
333  331  329  327  325  323  321  319  317  315
313  311  309  307  305  303  301  299  297  295
293  291  289  287  285  283  281  279  277  275
273  271  269  267  265  263  261  259  257  255
253  251  249  247  245  243  241  239  237  235
233  231  229  227  225  223  221  219  217  215
213  211  209  207  205  203  201  199  197  195
193  191  189  187  185  183  181  179  177  175
173  171  169  167  165  163  161  159  157  155
153  151  149  147  145  143  141  139  137  135
133  131  129  127  125  123  121  119  117  115
113  111  109  107  105  103  101   99   97   95
 93   91   89   87   85   83   81   79   77   75
 73   71   69   67   65   63   61   59   57   55
 53   51   49   47   45   43   41   39   37   35
 33   31   29   27   25   23   21   19   17   15
 13   11    9    7    5    3    1
  2  487       0.40
974  972  970  968  966  964  962  960  958  956
954  952  950  948  946  944  942  940  938  936
934  932  930  928  926  924  922  920  918  916
914  912  910  908  906  904  902  900  898  896
894  892  890  888  886  884  882  880  878  876
874  872  870  868  866  864  862  860  858  856
854  852  850  848  846  844  842  840  838  836
834  832  830  828  826  824  822  820  818  816
814  812  810  808  806  804  802  800  798  796
794  792  790  788  786  784  782  780  778  776
774  772  770  768  766  764  762  760  758  756
754  752  750  748  746  744  742  740  738  736
734  732  730  728  726  724  722  720  718  716
714  712  710  708  706  704  702  700  698  696
694  692  690  688  686  684  682  680  678  676
674  672  670  668  666  664  662  660  658  656
654  652  650  648  646  644  642  640  638  636
634  632  630  628  626  624  622  620  618  616
614  612  610  608  606  604  602  600  598  596
594  592  590  588  586  584  582  580  578  576
574  572  570  568  566  564  562  560  558  556
554  552  550  548  546  544  542  540  538  536
534  532  530  528  526  524  522  520  518  516
514  512  510  508  506  504  502  500  498  496
494  492  490  488  486  484  482  480  478  476
474  472  470  468  466  464  462  460  458  456
454  452  450  448  446  444  442  440  438  436
434  432  430  428  426  424  422  420  418  416
414  412  410  408  406  404  402  400  398  396
394  392  390  388  386  384  382  380  378  376
374  372  370  368  366  364  362  360  358  356
354  352  350  348  346  344  342  340  338  336
334  332  330  328  326  324  322  320  318  316
314  312  310  308  306  304  302  300  298  296
294  292  290  288  286  284  282  280  278  276
274  272  270  268  266  264  262  260  258  256
254  252  250  248  246  244  242  240  238  236
234  232  230  228  226  224  222  220  218  216
214  212  210  208  206  204  202  200  198  196
194  192  190  188  186  184  182  180  178  176
174  172  170  168  166  164  162  160  158  156
```

```
154  152  150  148  146  144  142  140  138  136
134  132  130  128  126  124  122  120  118  116
114  112  110  108  106  104  102  100   98   96
 94   92   90   88   86   84   82   80   78   76
 74   72   70   68   66   64   62   60   58   56
 54   52   50   48   46   44   42   40   38   36
 34   32   30   28   26   24   22   20   18   16
 14   12   10    8    6    4    2
200    8
  1     0.240     10.00   18300.0     0.819     34.20 0.10
  2     0.240     12.00   18300.0     0.819     34.20 0.10
  3     0.240     12.00   18300.0     0.819     34.20 0.10
  4     0.240     12.00   18300.0     0.819     34.20 0.10
  5     0.240     10.00   18300.0     0.819     34.20 0.10
  6     0.240     12.00   18300.0     0.819     34.20 0.10
  7     0.240     12.00   18300.0     0.819     34.20 0.10
  8     0.240     12.00   18300.0     0.819     34.20 0.10
300    5
  1      4.27      3.27      4.10      4.10     75.00    180.00    180.00 0.10
    42.0      42.0      10.2      10.2
  2     30.00     24.00      0.63      3.46     15.20     15.00     97.20 0.10
    36.0      15.0      20.0      15.0
  3     30.00     24.00      0.34      0.72     15.20     15.00     97.20 0.10
    36.0      15.0      20.0      15.0
  4     30.00     24.00      0.34      0.72     15.20     15.00     97.20 0.10
    36.0      15.0      20.0      15.0
  5     30.00     24.00      0.34      0.72     15.20     15.00     97.20 0.10
    36.0      15.0      20.0      15.0
400    4
  1      0.45       8.0      0.45       8.0    300.00 0.01      27.0
  2      0.45       8.0      0.45       8.0    300.00 0.01      27.0
  3      0.45       8.0      0.45       8.0    300.00 0.01      27.0
  4      0.45       8.0      0.45       8.0    300.00 0.01      27.0
  1    1    3    3    2  201       0.9       0.0
  4    7    9    5    2  202       0.9       0.0
  6   11   13              401       0.9
  7   13   15   19    2  202       0.9       0.0
 20   39   41   27    2  203       0.9       0.0
 28   55   57  459    2  204       0.9       0.0
460  919  921  467    2  203       0.9       0.0
468  935  937  480    2  202       0.9       0.0
481  961  963              403       0.9
482  963  965  483    2  202       0.9       0.0
484  967  969  486    2  201       0.9       0.0
487    2    4  489    2  205       0.9       0.0
490    8   10  491    2  206       0.9       0.0
492   12   14              402       0.9
493   14   16  505    2  206       0.9       0.0
506   40   42  513    2  207       0.9       0.0
514   56   58  945    2  208       0.9       0.0
946  920  922  953    2  207       0.9       0.0
954  936  938  966    2  206       0.9       0.0
967  962  964              404       0.9
968  964  966  969    2  206       0.9       0.0
970  968  970  972    2  205       0.9       0.0
973    1    2              301       0.0       0.0       0.0       0.0       0.0
974    7    8              302       0.0       0.0       0.0       0.0       0.0
975   39   40              303       0.0       0.0       0.0       0.0       0.0
976   55   56              304       0.0       0.0       0.0       0.0       0.0
977   87   88              305       0.0       0.0       0.0       0.0       0.0
978  119  120              305       0.0       0.0       0.0       0.0       0.0
979  151  152              305       0.0       0.0       0.0       0.0       0.0
980  183  184              305       0.0       0.0       0.0       0.0       0.0
981  215  216              305       0.0       0.0       0.0       0.0       0.0
982  247  248              305       0.0       0.0       0.0       0.0       0.0
983  279  280              305       0.0       0.0       0.0       0.0       0.0
984  311  312              305       0.0       0.0       0.0       0.0       0.0
985  343  344              305       0.0       0.0       0.0       0.0       0.0
986  375  376              305       0.0       0.0       0.0       0.0       0.0
```

```
 987  407  408            305       0.0       0.0       0.0       0.0       0.0
 988  439  440            305       0.0       0.0       0.0       0.0       0.0
 989  471  472            305       0.0       0.0       0.0       0.0       0.0
 990  503  504            305       0.0       0.0       0.0       0.0       0.0
 991  535  536            305       0.0       0.0       0.0       0.0       0.0
 992  567  568            305       0.0       0.0       0.0       0.0       0.0
 993  599  600            305       0.0       0.0       0.0       0.0       0.0
 994  631  632            305       0.0       0.0       0.0       0.0       0.0
 995  663  664            305       0.0       0.0       0.0       0.0       0.0
 996  695  696            305       0.0       0.0       0.0       0.0       0.0
 997  727  728            305       0.0       0.0       0.0       0.0       0.0
 998  759  760            305       0.0       0.0       0.0       0.0       0.0
 999  791  792            305       0.0       0.0       0.0       0.0       0.0
1000  823  824            305       0.0       0.0       0.0       0.0       0.0
1001  855  856            305       0.0       0.0       0.0       0.0       0.0
1002  887  888            305       0.0       0.0       0.0       0.0       0.0
1003  919  920            304       0.0       0.0       0.0       0.0       0.0
1004  935  936            303       0.0       0.0       0.0       0.0       0.0
1005  967  968            302       0.0       0.0       0.0       0.0       0.0
1006  973  974            301       0.0       0.0       0.0       0.0       0.0
   4400.0   40000.0   20    6    4    0    1
   1     0.055      0.12      6.00      17.0
   2     0.057      0.15      7.00      18.0
   3     0.062      0.18     10.00      12.0
   4     0.110      0.35     12.00       6.0
   5      0.35      0.45      6.00       5.0
   6      1.45      1.50     15.00       1.0
   1    100.75    15.875    1     12.00    1    1    0    0
   2    100.75    27.875    1     12.00    1    1    0    0
   3    100.75    39.875    2     12.00    1    1    0    0
   4     88.75    39.875    2     12.00    1    1    0    0
   5     76.75    39.875    2     12.00    1    1    0    0
   6     64.75    39.875    2     12.00    1    1    0    0
   7     52.75    39.875    2     12.00    1    1    0    0
   8     40.75    39.875    2     12.00    1    1    0    0
   9     28.75    39.875    2     12.00    1    1    0    0
  10     16.75    39.875    2     12.00    1    1    0    0
  11    -13.25    39.875    3     12.00    1    1    0    0
  12    -33.25    39.875    3     12.00    1    1    0    0
  13    -53.25    39.875    3     12.00    1    1    0    0
  14    -73.25    39.875    3     12.00    1    1    0    0
  15    -93.25    39.875    3     12.00    1    1    0    0
  16   -113.25    39.875    4     12.00    1    1    0    0
  17   -113.25   -39.875    4     12.00    0    0    0    0
  18    100.75   -39.875    1     12.00    0    0    0    0
  19     69.25     37.75    5      1.00    1    1    0    0
  20    -69.75     37.75    6      1.00    1    1    0    0
   1     69.25     32.75       0.0     608.0
   2     69.25    -32.75       0.0     608.0
   3    -62.75     32.75       0.0     492.0
   4    -62.75    -32.75       0.0     492.0
   1       0.0       0.0
   3   2046.00       0.0      25.0     62.14       0.0       0.0       1.0
```

APPENDIX D

Three-Cable Guardrail System Drawings in English Units

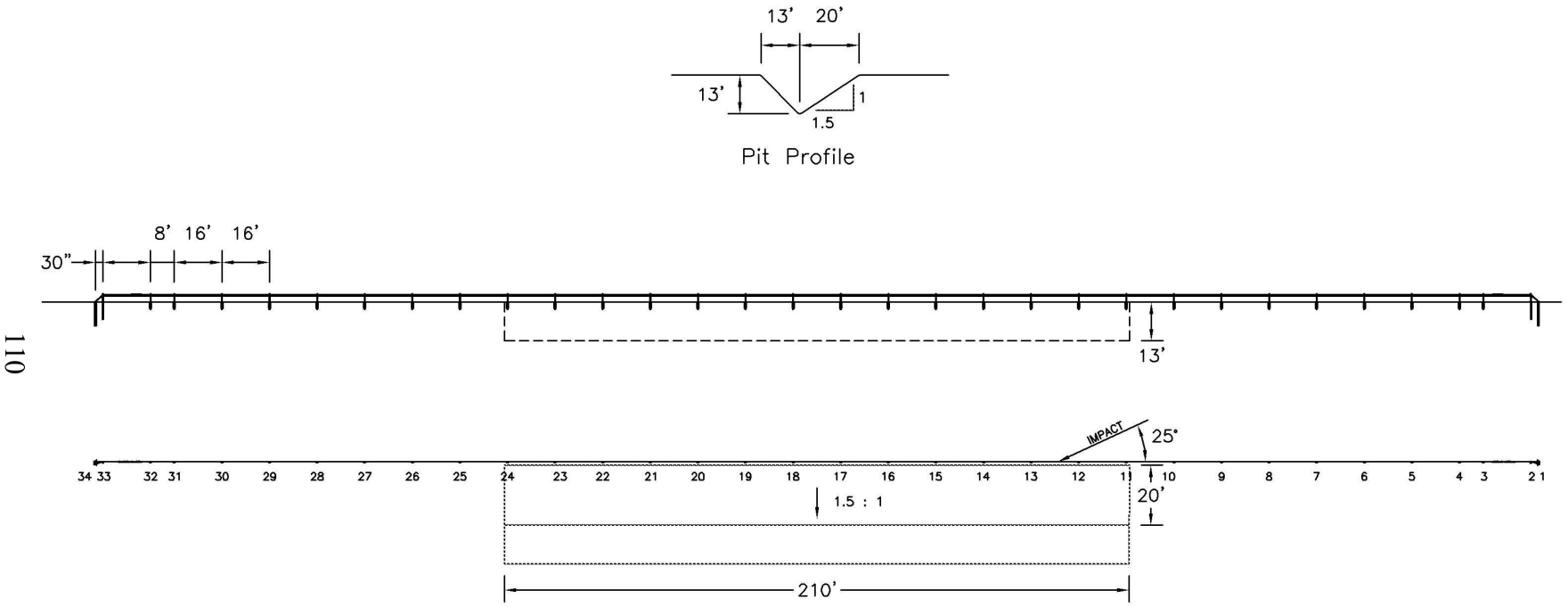

Figure D-1. Three-Cable Guardrail Geometry (English)

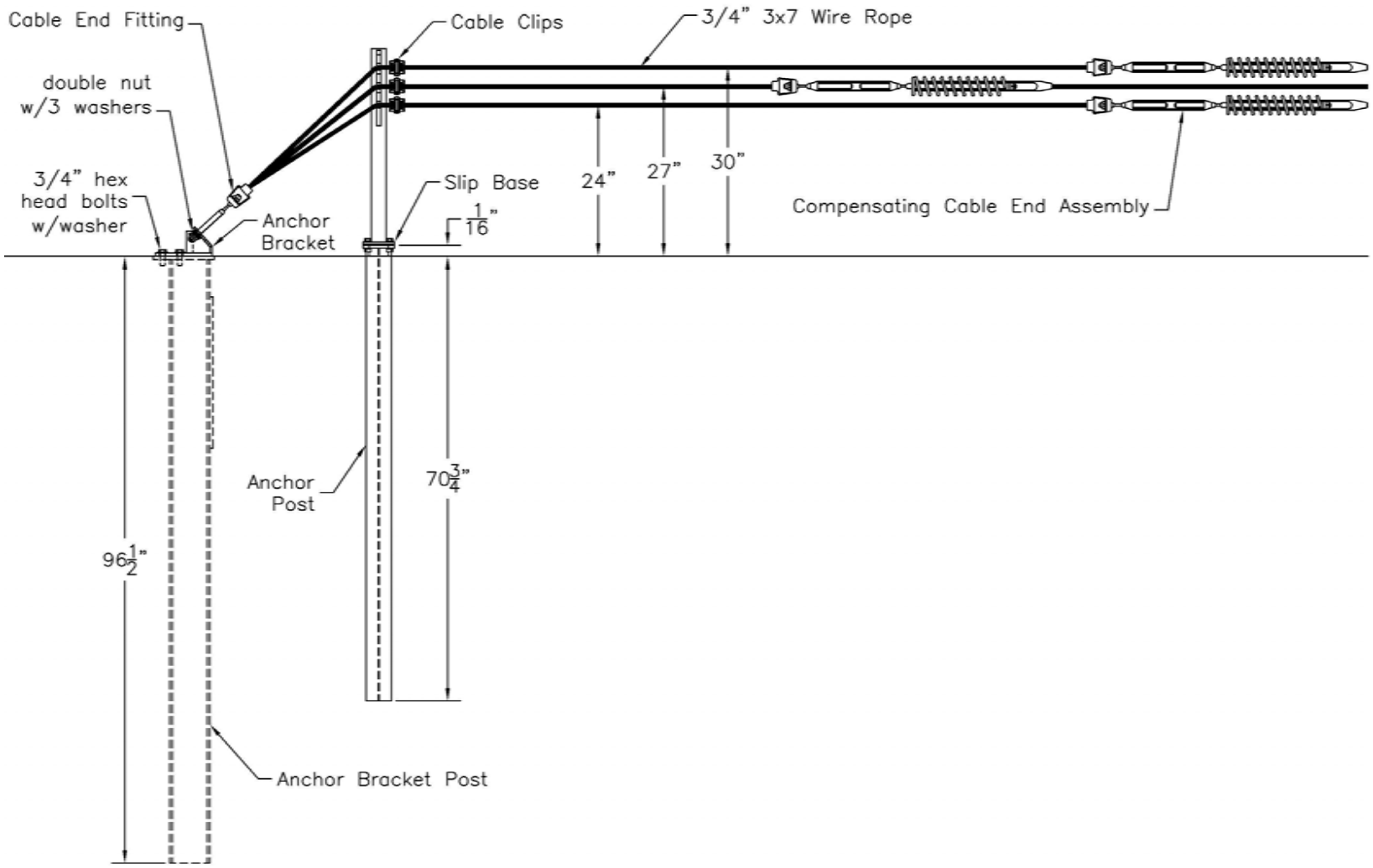

Figure D-2. Three-Cable Guardrail End Terminal Overview (English)

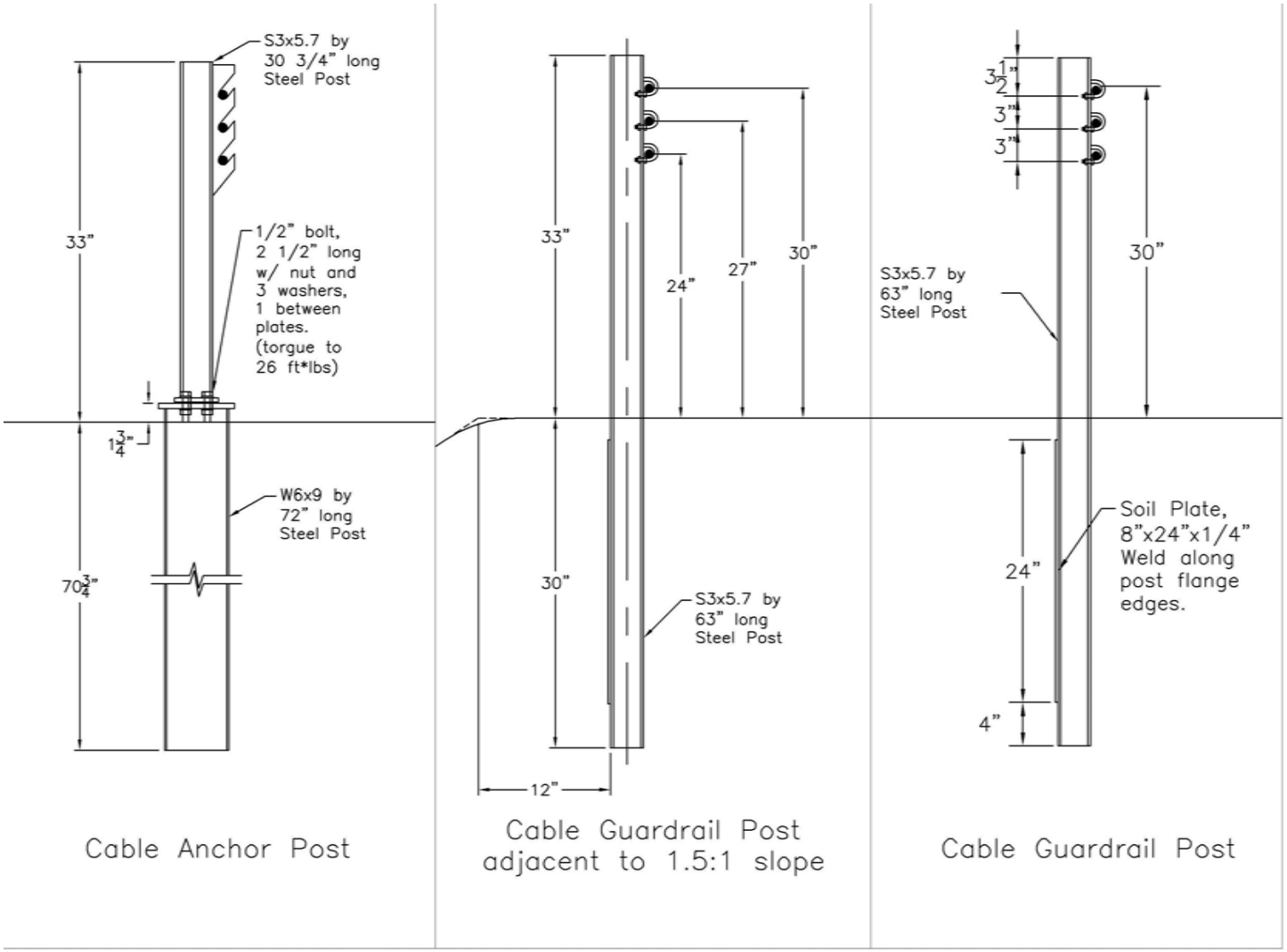

Figure D-3. Typical Three-Cable Guardrail Post Overview (English)

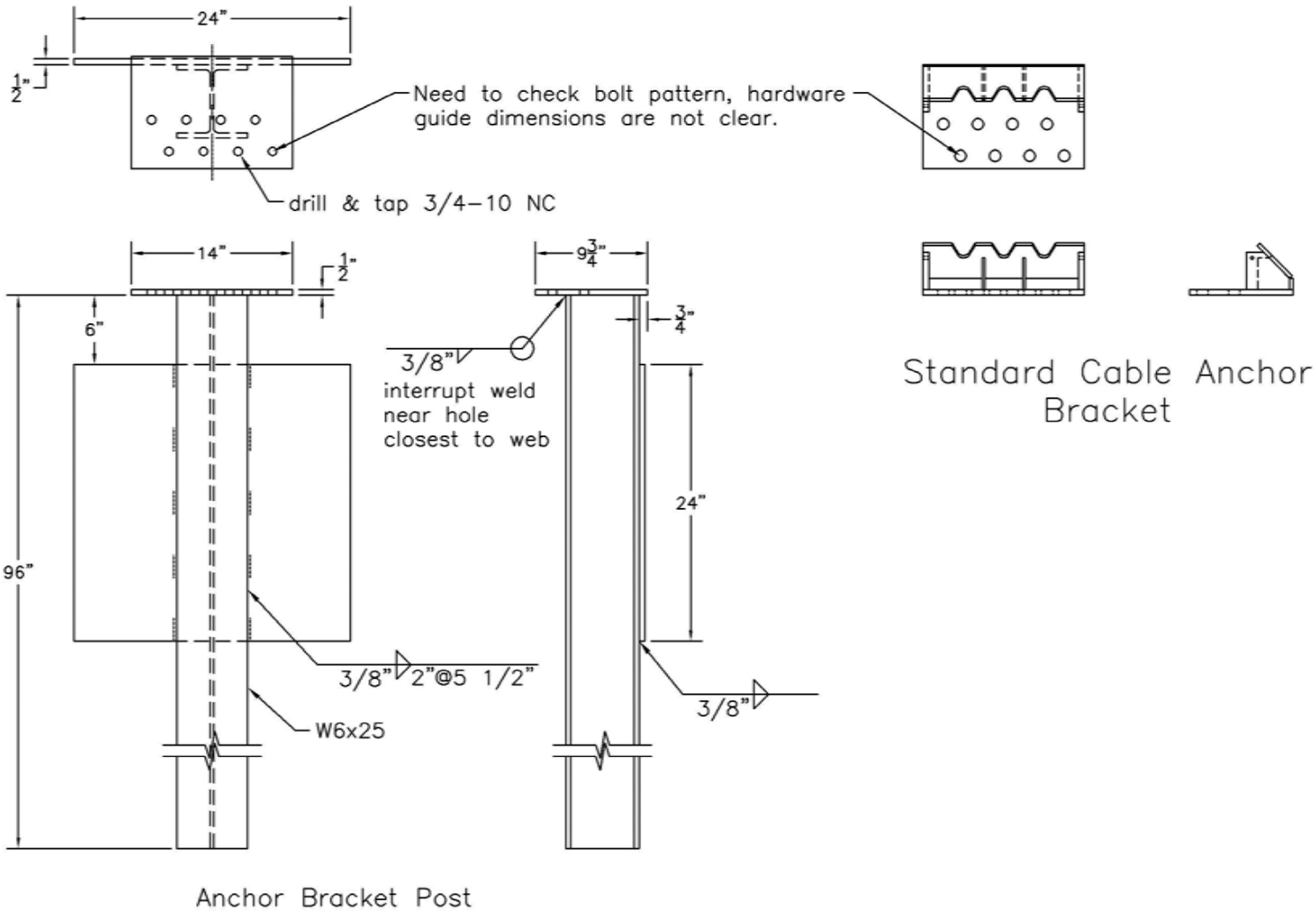

Figure D-4. End Anchor and Cable Bracket Details (English)

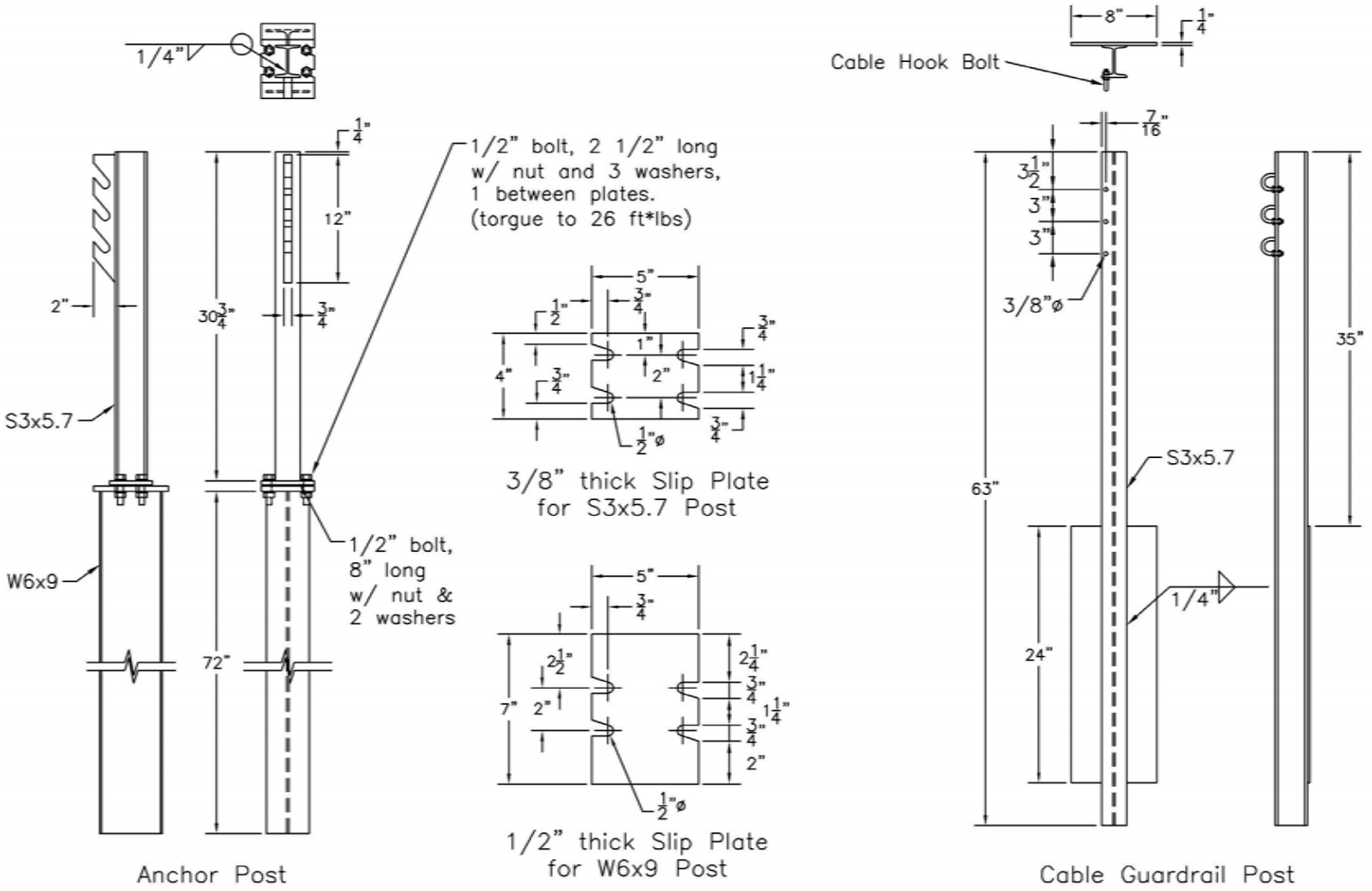

Figure D-5. Line and Slip-Base Post Details (English)

APPENDIX E

Test Summary Sheet in English Units

Figure E-1. Summary of Test Results and Sequential Photographs (English), Test CS-1

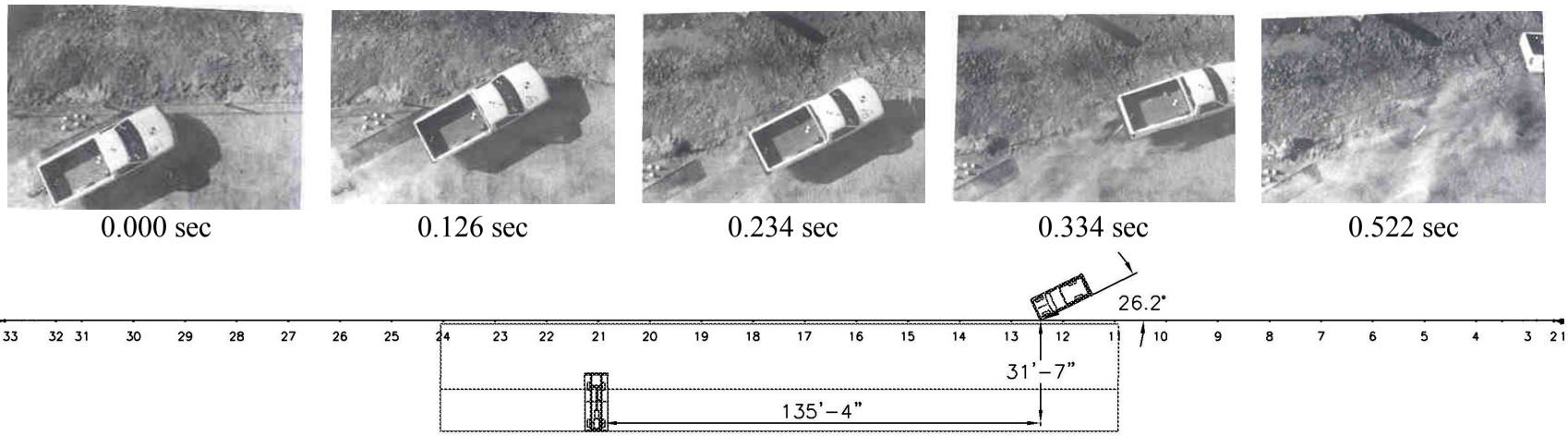

- Test Number CS-1
- Date 11/1/01
- Appurtenance ..... Three-cable guardrail installed adjacent to 1.5:1 slope
- Total Length ..... 485 ft
- Wire Rope
  - Diameter ..... ¾ in.
  - Top Mounting Height ..... 30 in.
  - Incremental Spacing ..... 3.0 in.
- Steel Posts
  - Post Nos. 1 and 34 ..... W6x25 by 96-in. long
  - Post Nos. 2 and 33 ..... S3x5.7 by 31¼-in. long with W6x9 by 72-in. long
  - Post Nos. 3 – 32 ..... S3x5.7 by 63-in. long
- Soil Type ..... Grading B – AASHTO M 147-65
- Vehicle Model ..... 1995 GMC 2500 ¾-ton pickup
  - Curb ..... 4,295 lbs
  - Test Inertial ..... 4,484 lbs
  - Gross Static ..... 4,484 lbs
- Vehicle Speed
  - Impact ..... 61.0 mph
  - Exit ..... NA
- Vehicle Angle
  - Impact ..... 26.2 deg
  - Exit ..... NA
- Vehicle Snagging ..... None
- Vehicle Pocketing ..... None
- Vehicle Stability ..... Unsatisfactory
- Occupant Ridedown Deceleration (10 msec avg.)
  - Longitudinal ..... 4.98 G's < 20 G's
  - Lateral (Not Required) ..... 15.19 G's
- Occupant Impact Velocity
  - Longitudinal ..... 4.27 ft/s < 39.37 ft/s
  - Lateral (Not Required) ..... 8.83 ft/s
- Vehicle Damage ..... Extensive
  - TAD[28] ..... NA
  - SAE[29] ..... NA
- Vehicle Stopping Distance ..... 135 ft-4 in. downstream Located at bottom of slope
- Barrier Damage ..... Moderate
- Maximum Rail Deflections
  - Permanent Set ..... NA
  - Dynamic ..... NA

Figure E-1. Summary of Test Results and Sequential Photographs, Test CS-1

APPENDIX F

Occupant Compartment Deformation Data, Test CS-1

Figure F-1. Occupant Compartment Deformation Data, Test CS-1

VEHICLE PRE/POST CRUSH INFO

TEST: CS-1
VEHICLE: 1995/GMC/2500/WHITE

POINT	X	Y	Z	X'	Y'	Z'	DEL X	DEL Y	DEL Z
1	-29.25	58	4.25				NA	NA	NA
2	-23.25	60.25	2.5				NA	NA	NA
3	-20.5	59	-0.25				NA	NA	NA
4	-14.75	58	-1.25				NA	NA	NA
5	-6.25	55.75	1.25				NA	NA	NA
6	1	54.25	3.25				NA	NA	NA
7	-29.75	55.25	-2.25				NA	NA	NA
8	-21.25	54.75	-3				NA	NA	NA
9	-13	54	-3.5				NA	NA	NA
10	-4.75	50.75	0				NA	NA	NA
11	-31.75	43.25	-6.375				NA	NA	NA
12	-22.75	43.5	-5.25				NA	NA	NA
13	-16	44.25	-6				NA	NA	NA
14	-8.25	43.75	-4.5				NA	NA	NA
15	-0.75	42.75	-0.625				NA	NA	NA
16	-29	34.5	-5.25				NA	NA	NA
17	-22.5	34.75	-5.25				NA	NA	NA
18	-15.5	34.25	-6				NA	NA	NA
19	-8.125	34.75	-4.75				NA	NA	NA
20	-2.5	34	-1.5				NA	NA	NA
21	-31.5	25.5	-6.375				NA	NA	NA
22	-15	26.75	-4.75				NA	NA	NA
23	-12	16.25	-4.75				NA	NA	NA
24	-32.75	28.5	-1				NA	NA	NA
25	-26.5	40.75	26.25				NA	NA	NA
26	-4	41	26.25				NA	NA	NA
27	3.25	40.75	25.5				NA	NA	NA
28							NA	NA	NA
29							NA	NA	NA
30							NA	NA	NA

ORIENTATION AND REFERENCE INFO

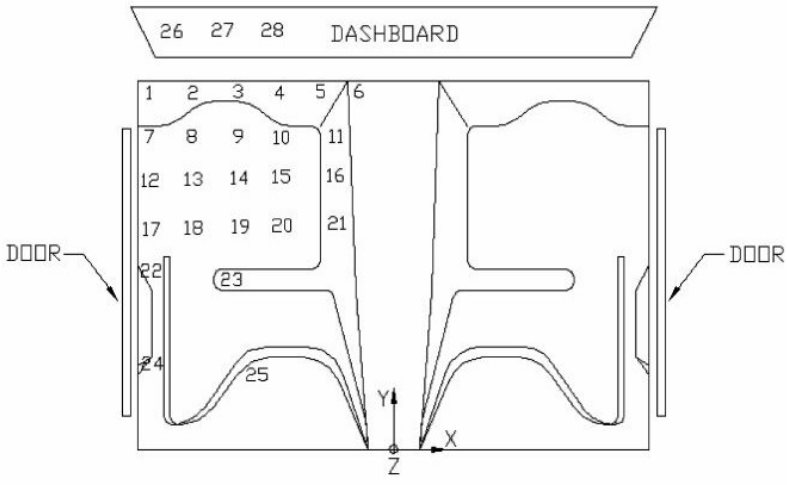

Figure F-1. Occupant Compartment Deformation Data, Test CS-1

APPENDIX G

Accelerometer and Rate Transducer Data Analysis, Test CS-1

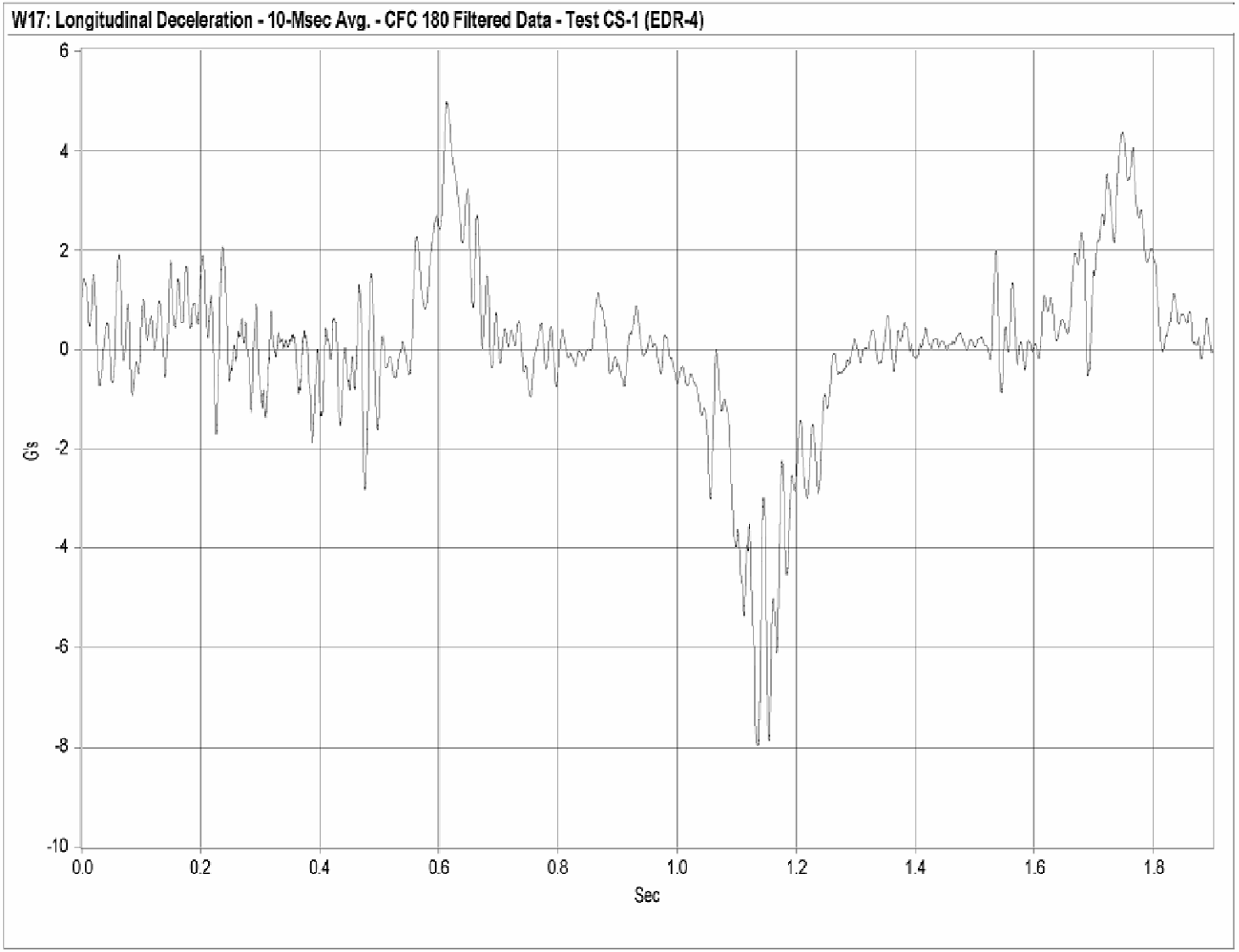

Figure G-1. Graph of Longitudinal Deceleration, Test CS-1

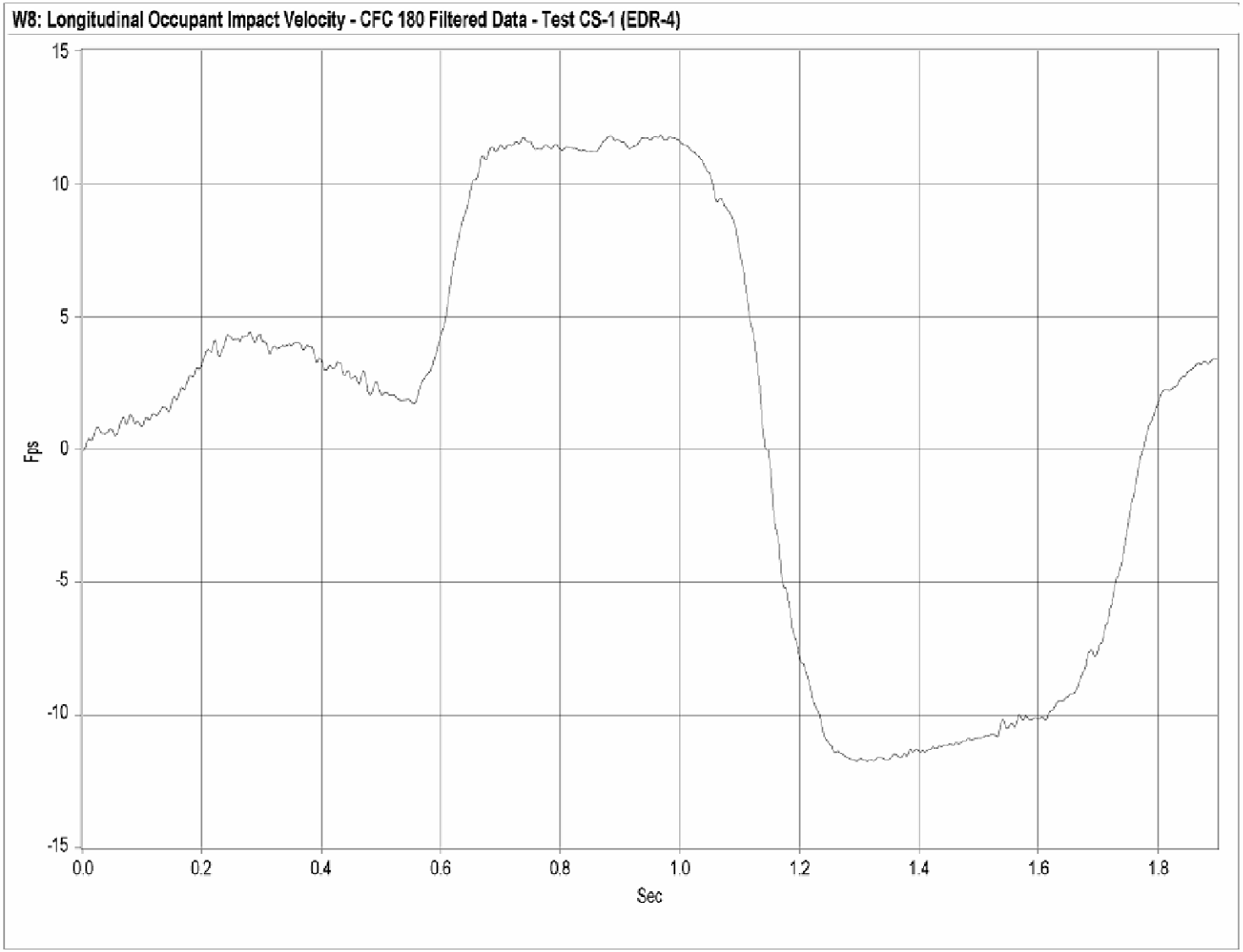

Figure G-2. Graph of Longitudinal Occupant Impact Velocity, Test CS-1

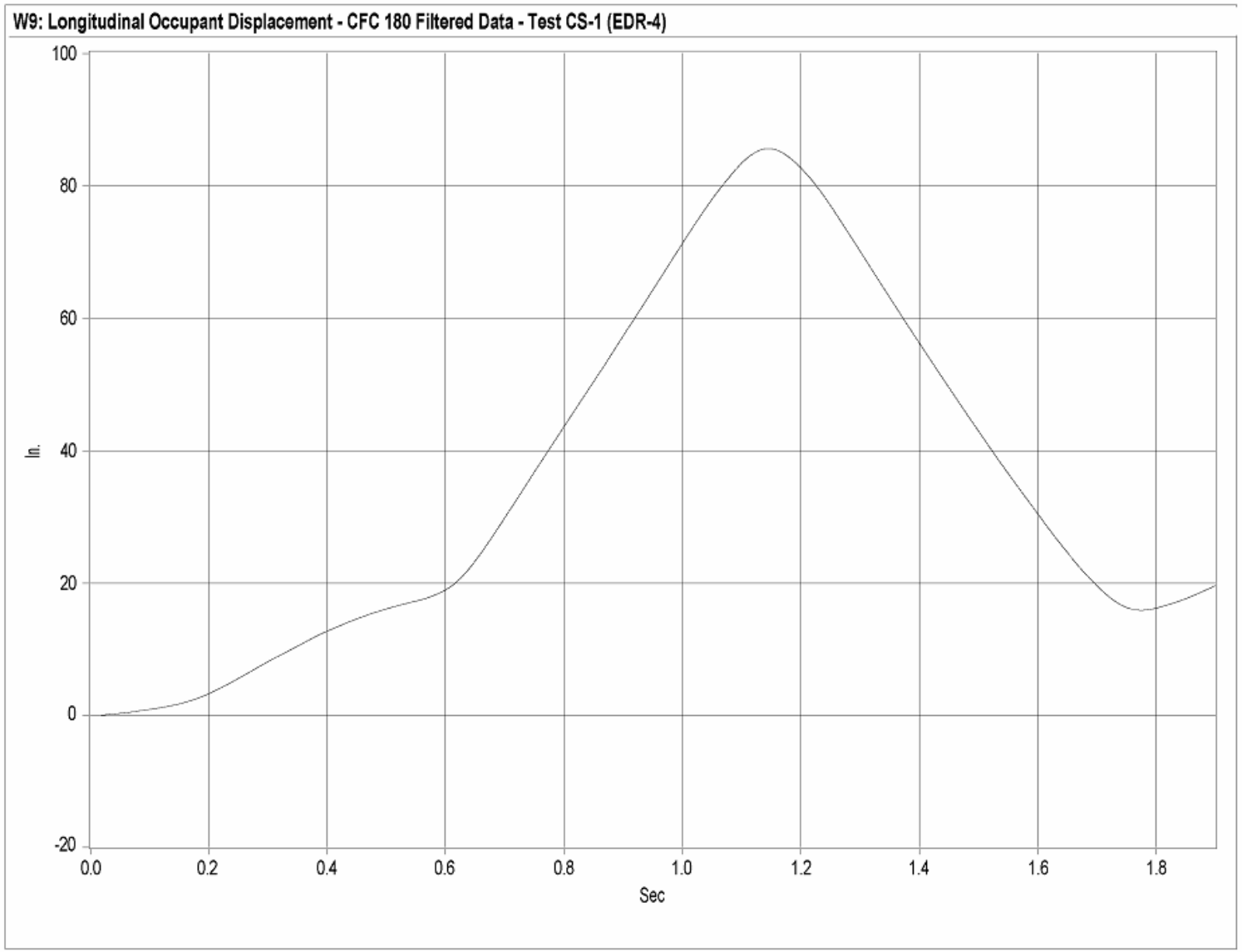

Figure G-3. Graph of Longitudinal Occupant Displacement, Test CS-1

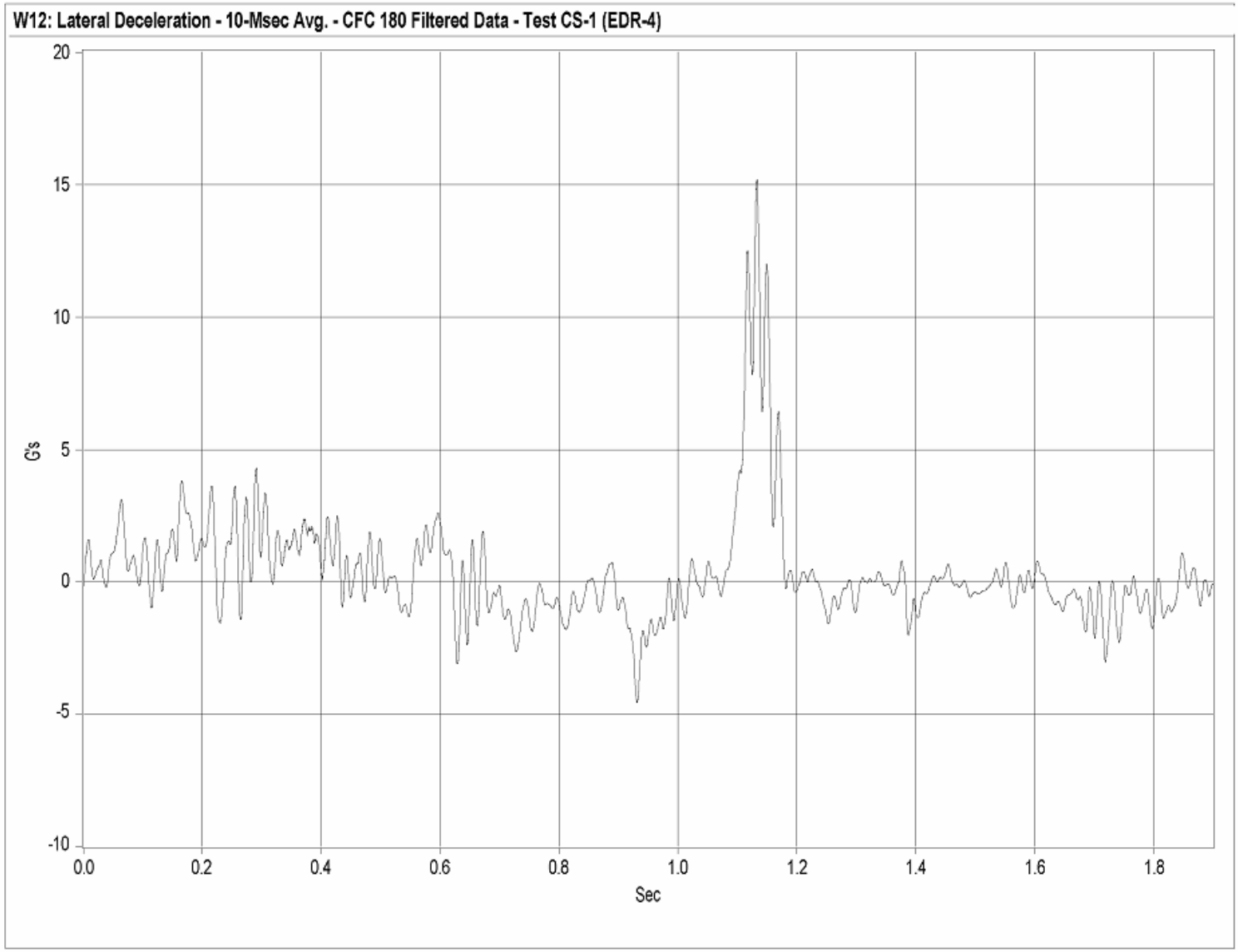

Figure G-4. Graph of Lateral Deceleration, Test CS-1

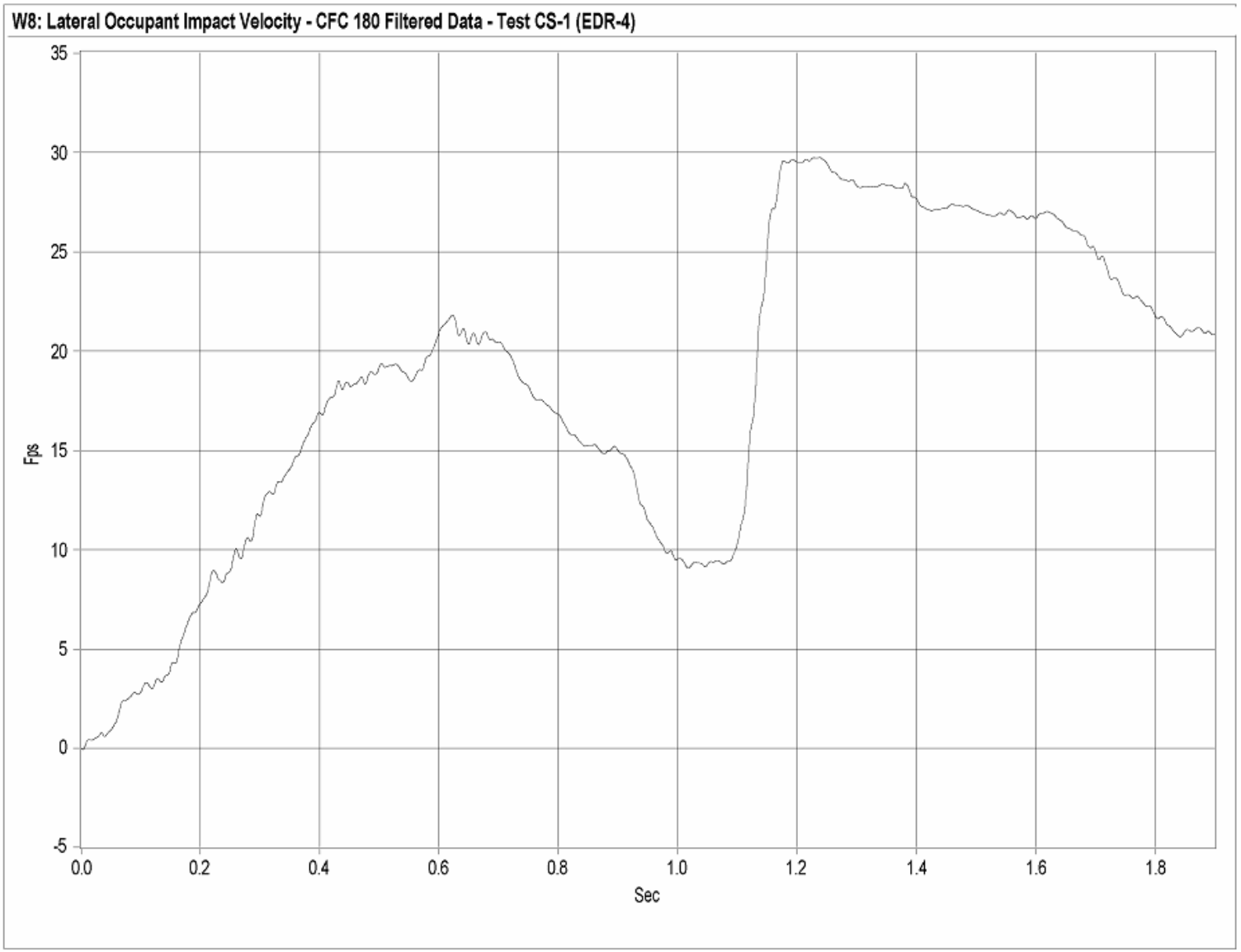

Figure G-5. Graph of Lateral Occupant Impact Velocity, Test CS-1

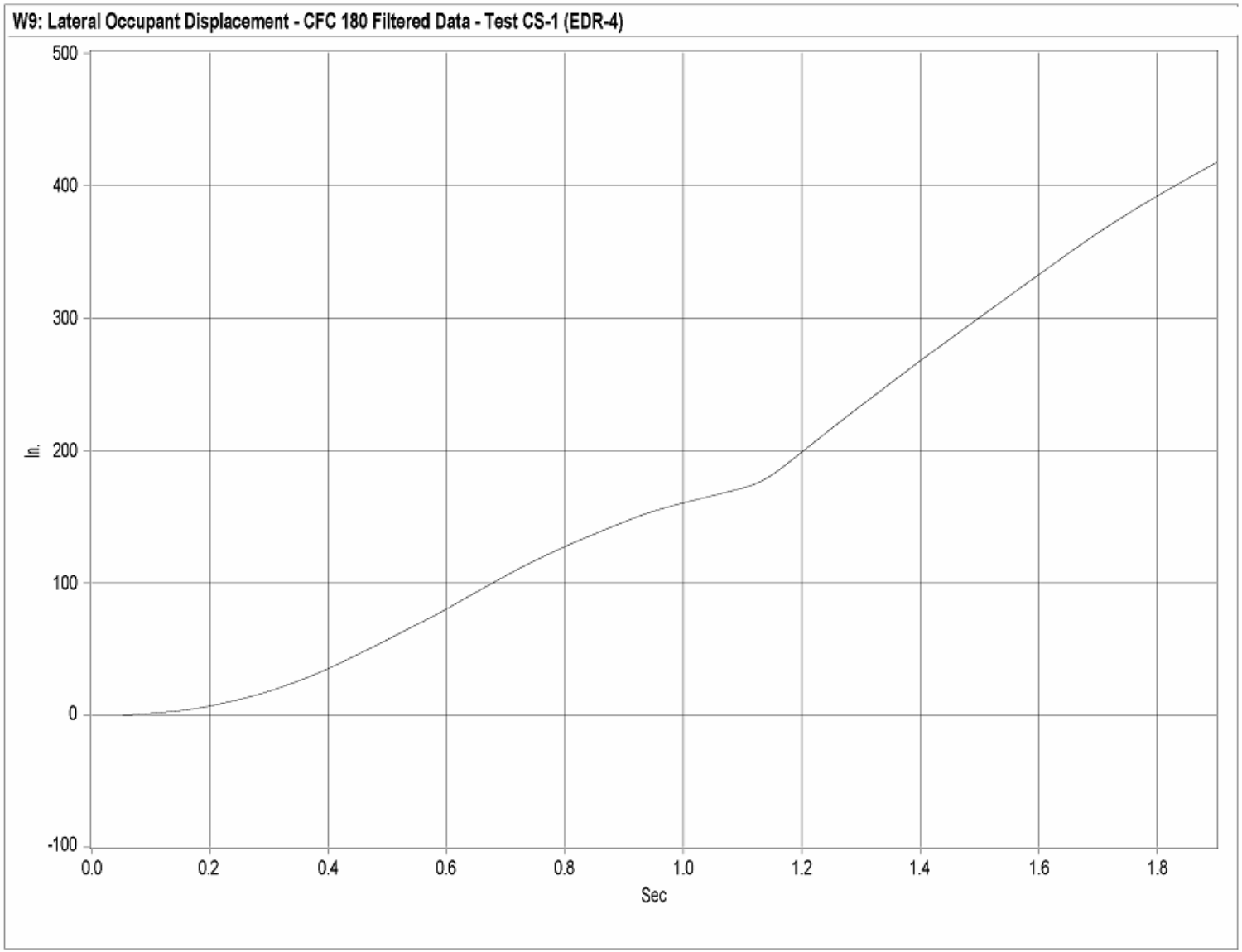

Figure G-6. Graph of Lateral Occupant Displacement, Test CS-1

Figure G-7. Graph of Yaw Angular Displacement, Test CS-1